DESIGN, OPERATION AND MAINTENANCE OF DIRECT AND INDIRECT EVAPORATIVE COOLING SYSTEMS IN DATA CENTER THERMAL MANAGEMENT

by

ASHWIN VENUGOPAL SIDDARTH

Presented to the Faculty of the Graduate School of

The University of Texas at Arlington in Partial Fulfillment

of the Requirements

for the Degree of

DOCTOR OF PHILOSOPHY

THE UNIVERSITY OF TEXAS AT ARLINGTON

August 2021

Acknowledgements

I would like to thank Dr. Dereje Agonafer for his encouragement and support during my time in University of Texas Arlington. I am forever indebted to his generosity and compassion towards me. I would also like to thank him for providing opportunities to work on industry-funded projects and advancing various networking possibilities through attending conferences.

I would like to thank Dr. Haji-Sheikh, Dr. Ameri, Dr. Amaya and Dr. Celik for serving on my thesis committee. I thank the Mechanical and Aerospace department staff for their patience and willingness to help. I thank Sally and Phil for their love and friendship. I have been fortunate to meet with incredible people in UTA, especially in the EMNSPC lab, I thank them all for their support, and friendship.

I would like to thank all the industry mentors in the Industry Advisory Board of the NSF funded consortium where I served as a graduate researcher. I thank Mark Seymour for his kind and encouraging words, critical feedback and for providing me an opportunity to work at Future Facilities. I thank Kourosh Nemati, most of all, for his friendship. I also thank John, Rick and Marianna for their concern and support. I would also like to thank Mestex, Facebook, CommScope, Future Facilities and NVIDIA for the opportunity to work with them over the years.

Most of all, I would like to thank my family and friends for their unconditional support. I thank my friends, Varun, Manasa, Abhishek, Rajesh, Rakesh, Janardhan, Vivekananda, Nayana and several others I was fortunate to know during my time at UTA. My mother (Pushpalatha) and my brother (Chinmaya) have always been there in my journey, providing enormous strength with their love and affection.

August 6, 2021

Abstract

DESIGN, OPERATION AND MAINTENANCE OF DIRECT AND

INDIRECT EVAPORATIVE COOLING SYSTEMS IN

DATA CENTER THERMAL MANAGEMENT

Ashwin Venugopal Siddarth, PhD

The University of Texas at Arlington, 2021

Supervising Professor: Dereje Agonafer

Evaporative cooling is an alternative data center cooling solution that presents significant energy cost savings in acquisition and operation when compared to conventional air conditioning and mechanical refrigeration systems. This research focuses on developing a deeper understanding in implementing, operating, and maintaining evaporative cooling systems integrated with air-side economization to realize the energy savings potential in data center cooling. An air handling unit (AHU) serves as a building block of any cooling equipment and houses the primary heat exchanger, air filters, air movers, a duct and damper system along with necessary electrical and control systems. The proposed approach systematically develops a comprehensive body of knowledge in evaporative cooling applicable to data center cooling. The territorial and climatic limitations of each evaporative cooling system integrated with air- and water-side economization for favorable ambient conditions is analyzed based on a psychrometric-based and data-driven modeling approach coupled with typical meteorological year data for various climate zones.

For direct evaporation cooling, three types of wet cooling media pads are experimentally characterized for the saturation effectiveness and system pressure drops. Analysis of the media pads based on experimentally validated CFD models establishes the criteria for media pad selection and sizing. The impact of calcium scaling due to continuous evaporation in the media pad is studied by designing and conducting an accelerated degradation test that determines the health monitoring parameter of the media pad and the maintenance interventions in the field. To achieve incremental humidification, a vertically split and staged media pad with discrete pumps for each stage is proposed to maximize water savings. The effectiveness is demonstrated by conducting characterization

testing on the air flow bench under controlled inlet air conditions. The mixing chamber in the AHU is comprehensively studied to eliminate the thermal stratification issue which can exacerbate the hot spots in the data center.

For indirect evaporative cooling, a separate AHU is designed, fabricated, and commissioned in Dallas, TX. The heat exchanger is an epoxy-coated Aluminum plate heat exchanger in the crossflow configuration with a water distribution system comprising spray nozzles/sprinklers. In these systems, the data center and outdoor air streams are segregated by the structure of the heat exchanger that still must affect efficient transfer of energy from the IT equipment exhaust into the outdoor air stream. In many cases the heat exchanger is wetted on the outdoor side to increase the range of ambient conditions (via adiabatic cooling) for which full free cooling can be realized. This addition of water not only changes the properties of the external air stream, but also the effectiveness of the heat exchanger. This research investigates how the effectiveness of an air-to-air heat exchanger changes as it is wetted, additionally identifying the off-exchanger conditions from a temperature perspective with the aim of producing a characteristic relationship that could be implemented by a simulation tool to give a reasonable approximation of heat transfer performance and used for analysis of the consequence of recirculated air affecting neighboring units. Two different types of water distributors are tested and at various heights from the top surface of the heat exchanger. A water collection grid is designed to map how well the spray system effectively distributes water within the heat exchanger passages. Heat exchanger performance is tested for fully wet, partially wet and flooded wetting configurations.

Table of Contents

Chapter 1

Introduction

1.1 OBJECTIVES

Evaporative cooling is an alternative data center cooling solution that presents significant energy cost savings in acquisition and operation when compared to conventional air conditioning and mechanical refrigeration systems. The added savings potential represented by air- and water-side economization for favorable ambient conditions based on psychrometric-based modeling approach coupled with Typical Meteorological Year data for various climate zones is well documented.

The development of theses systems is being driven in 2 ways:

- Large enterprises making onward development of their approach by refining it for each new data center, e.g. Facebook. These are often direct evaporative cooling systems
- Cooling equipment suppliers providing often large scale indirect evaporative solutions in proprietary form

For an end user or operator or other less-informed/less-well equipped organization there are a myriad of options with little unbiased guidance available. Many questions arise:

- Should I use direct or indirect?
- Should I use wet media or sprays?
- What media should I use?
- Do I need water purification?
- What maintenance is required?
- Can I collect and re-use water?
- When do I need secondary/top-up cooling systems?
- What configurations work with what systems?
- What controls do I need?
- When do I use outdoor ambient air and when do I recirculate?
- How do I ensure good mixing?

- What are the practical limits for humidity?
- What are the territory/climatic limitations?
- What are the primary considerations from a contaminant perspective (gaseous and particulate)?

The list is endless.

This research proposes a combination of literature search, experiment (where practicable) and simulation to produce a comprehensive guide to the pros and cons of different approaches. In addition, it will be useful to give/show examples of typical configurations that are being adopted and compare their relative merits (one system may be good for one climate or application while another is good for other climates/applications

1.2 PLAN AND APPROACH

To develop a comprehensive body of knowledge in evaporative cooling applicable to data center cooling, the following specific methods will be employed:

a) Cooling systems and component design: Literature search, experiments, and simulation
    i) Identifying territorial and climatic limitations
        (1) Psychrometric bin analysis to determine the climatic limitations on evaporative cooling system configurations
        (2) Territorial air quality data
        (3) Data on regional water inventory and water scarcity
    ii) Direct evaporative cooling (DEC) heat exchanger
        (1) Experimental characterization of wet cooling media pad performance
        (2) Studying the regional water quality and interaction with wet cooling media
        (3) Operational wet cooling media performance analysis
        (4) Evaluating impact of constant, variable and pulsated water flow over the wet cooling media on cooling performance, water quality and media pad life
        (5) Identify advantages or disadvantages in drying of wet cooling media
        (6) Staging of wet cooling media to facilitate segmented cooling
    iii) Indirect evaporative cooling (IEC) heat exchanger

(1) Experimental design of an air handling unit to characterize the IEC heat exchanger

(2) Experimental design of a water distribution system to study the water distribution effectiveness in the wet mode operation

b) Operations and maintenance: Literature search, experiments, and simulation

i) Calcium scaling of wet cooling media pad

(1) Design of an accelerated degradation test for evaluating the life of a media pad due to calcification

(2) Experimental testing of the wet cooling pad subjected to accelerated calcification conditions

ii) Dynamic scheduling of cooling control and evaluation of various cooling control strategies

Chapter 2

Cooling Systems and Component Design

2.1 Introduction

In this chapter, different components of the direct and indirect evaporative cooling units will be considered as well as the cooling unit as a system will be designed based on several factors.

2.2 Neural Network Based Bin Analysis for Indirect/Direct Evaporative Cooling of Modular Data Centers

Abhishek Walekar
University of Texas at Arlington
Arlington, TX, USA

Ashwin Siddarth
University of Texas at Arlington
Arlington, TX, USA

Abhishek Guhe
Mestex, A Division of Mestek Inc
Dallas, TX, USA

Nikita Sukthankar
University of Texas at Arlington
Arlington, TX, USA

Dereje Agonafer
University of Texas at Arlington
Arlington, TX, USA

2.2.1 ABSTRACT

With an increase in the need for energy efficient data centers, a lot of research is being done to maximize the use of Air Side Economizers (ASEs), Direct Evaporative Cooling (DEC), Indirect Evaporative Cooling (IEC) and multistage Indirect/Direct Evaporative Cooling (I/DEC). The selection of cooling configurations installed in modular cooling units is based on empirical/analytical studies and domain knowledge that fail to account for the nonlinearities present in an operational data center. In addition to the ambient conditions, the attainable cold aisle temperature and humidity is also a function of the control strategy and the cooling setpoints in the data center.

The primary objective of this study is to use Artificial Neural Network (ANN) modelling and Psychrometric bin analysis to assess the applicability of various cooling modes to a climatic condition. Training dataset for the ANN model is logged from the monitoring sensor array of a modular data center laboratory with an I/DEC module. The data-driven ANN model is utilized for predicting the cold aisle humidity and temperatures for different modes of cooling. Based on the predicted cold aisle temperature and humidity, cold aisle envelopes are represented on a psychrometric chart to evaluate the applicability of each cooling mode to the territorial climatic condition. Subsequently, outside air conditions favorable to each cooling mode in achieving cold aisle conditions, within the

ASHRAE recommended environmental envelope, is also visualized on a psychrometric chart. Control strategies and opportunities to optimize the cooling system are discussed.

2.2.2 NOMENCLATURE

ACU	Air Cooling Unit
AHU	Air Handling Unit
ANN	Artificial Neural Network
ASE	Air Side Economization
CA	Cold Aisle
DEC	Direct Evaporative Cooling
DC	Data Center
DP	Dew Point Temperature
IEC	Indirect Evaporative Cooling
OAH	Outside Air Relative Humidity (%)
OAT	Outside Air Temperature (F)
RH	Relative Humidity

2.2.3 INTRODUCTION

Data centers need to be maintained within a certain range of temperature and humidity for equipment reliability and energy efficiency. Evaporative cooling can be used in many guises to make data center cooling more efficient and enables elimination of chiller-based cooling entirely. In addition to that, evaporative cooling units along with air-side economization provides the data center industry a sure pathway to gain cooling efficiency. While disruptive cooling technologies such as liquid cooling [1] and immersion cooling [2] present energy saving benefits, the capital expenses in implementing evaporative cooling for an existing air-cooled data center is comparatively less.

Many studies show that majority of the energy used for data center cooling is utilized for direct expansion air conditioners (DX). Thus, to reduce the use of DX, other modes of cooling are being used. This includes air side economization (ASE), direct evaporative cooling (DEC), indirect evaporative cooling (IEC) and

multi-stage cooling (I/DEC). Use of these alternative modes of cooling reduces the power consumption of an ACU by over 70% as compared to the DX [3]. But the use of ASE is limited by the ambient air conditions such as temperature, humidity, and pollutants. The added savings potential represented by airside economization for favorable ambient conditions based on psychrometric-based modeling approach coupled with Typical Meteorological Year data for various climate zones is well documented. In this study, we set to investigate the applicability of ASE, IEC and IDEC cooling modes for a hot and humid climatic condition. More importantly, this study tests the feasibility of developing ANN models to account for the non-linearities inherent in data center cooling.

2.2.4 PSYCHROMETRIC BIN ANALYSIS

A psychrometric chart represents the thermodynamic properties of moist air, i.e. its graphical equation of state. The territorial weather data is readily available as typical meteorological year (TMY3) data for a specific location [4]. The hourly-bin TMY3 weather data for the Dallas-Love field weather station is shown in Figure 1a, visualized on a psychrometric chart. The ASHRAE recommended environmental envelope for ITE (Information Technology equipment) is considered in this study as a desired target envelope for data center cold aisle conditions. The recommended range is the guidance from ITE manufacturers for high reliability, minimal power consumption (of ITE) and maximum performance [5]. Figure 1b shows the ASHRAE recommended envelope on the psychrometric chart along with regions defined for categorization of territorial outside air conditions.

a)

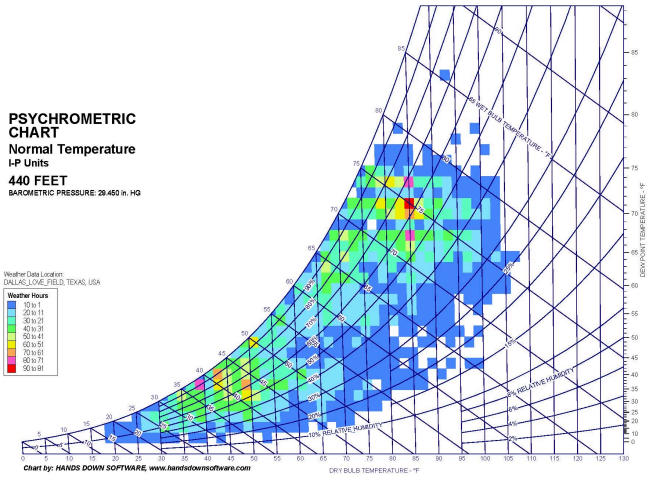

b)

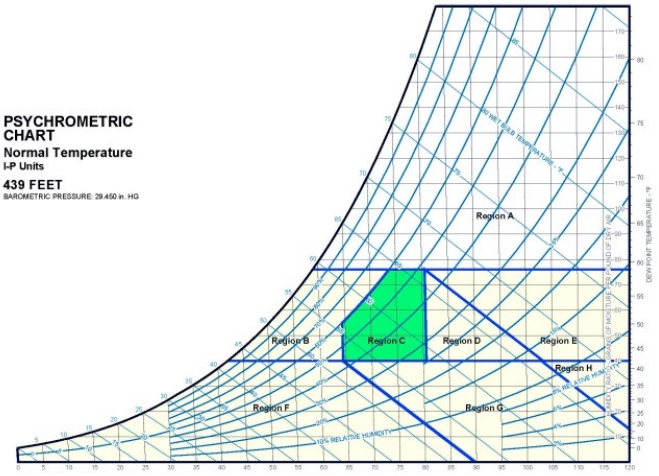

c)

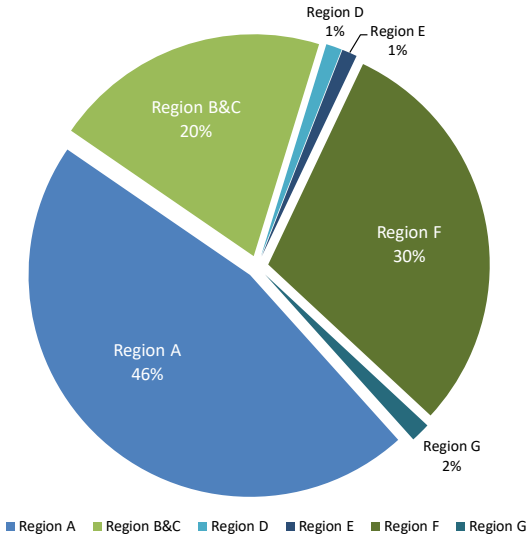

Figure 1: a) Dallas-Love Field TMY3 hourly weather bin-data plot;
b) ASHRAE recommended envelope for ITE along with regions A to H defined for categorization of territorial outside air conditions; **c)** Pie chart showing the percentage of weather bin-data distributed in terms of the outside air regions A to H

The regions A to H are defined by considering all possible thermodynamic processes for each cooling mode. The region C in Figure 1b is the targeted envelope for cold aisle conditions whereas the regions A to H are defined to categorize the outside air conditions over a typical year.

Table 1: ASHRAE Recommended Range for ITE

Recommended Envelope	
Low End Temperature	64^{o}F (18°C)
High End Temperature	81^{o}F (27°C)
Low End Moisture	41.9^{o}F DP (5.5°C)
High End Moisture	60% RH; 60^{o}F DP (15°C)

Previous studies have been able to use the regional weather data and estimate either the total number of hours available for air-side economization based on similar regions defined on a psychrometric chart or estimate the applicability of available modes of cooling by analyzing the underlying thermodynamic processes accompanying the various cooling modes [6,7]. As shown in Figure 1c, the 46% of outside air in region A depicts the percentage of outside air that requires dehumidification over a typical year to satisfy the targeted recommended range for cold aisle conditions. Similarly, the combined 50% of outside air from regions B, C and F can be considered as the total air-side economizer hours available. Furthermore, the upper and lower dew point temperature bounds, as per the ASHRAE recommended envelope, can be used as a reference for categorizing outside air conditions when evaporative cooling is to be implemented in addition to air-side economization. Figure 2 shows the percentage of total hours each month for Dallas-Love Field TMY3 data categorized based on the dew point temperature bounds. When the percentage of outside air for region A is considered month-wise in Figure 2, one can infer that the need for dehumidification is predominantly during the summer months. And the applicability of the direct and indirect evaporative cooling is evident for the rest of the months. However, such estimates of hours of applicability for air-side economization and evaporative cooling based on weather data and thermodynamic processes fail to account for the limitations due to operational control strategy and cooling system design.

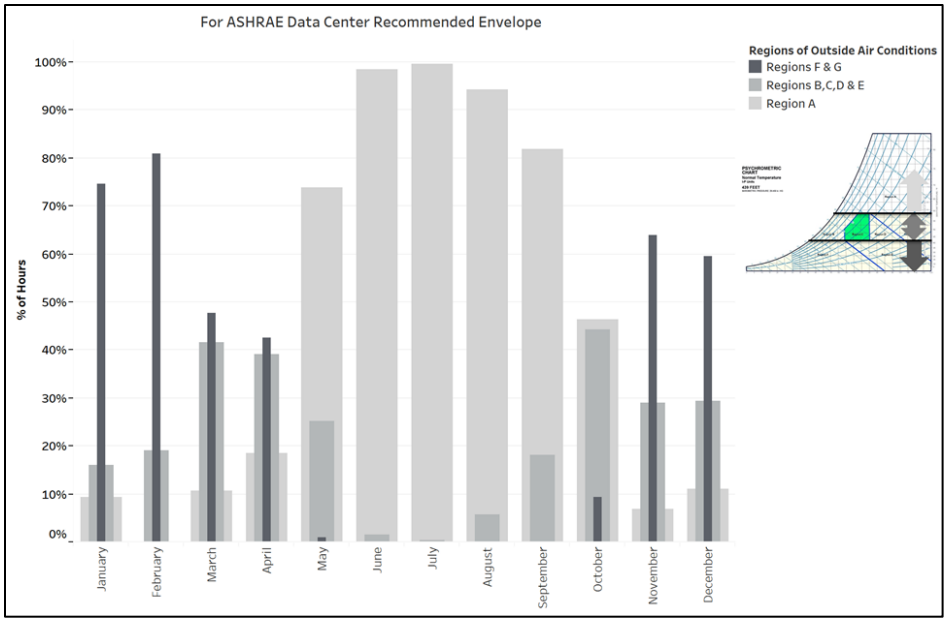

Figure 2: Monthly weather bins and percentage of total hours based on dew point temperature bounds

In this study, a test bed modular data center (MDC) with a cooling module consisting of three types of cooling configurations has been considered. These include the Air Side Economizer (ASE), Direct Evaporative cooling (DEC) and Indirect Evaporative Cooling (IEC). The MDC also consists of an IT module and ductwork for supply to the CA and return from the hot aisle. This MDC laboratory has been operating for several years and the cooling module is an Indirect/Direct evaporative cooling unit wherein air-side economization is also implemented.

An ANN model has been developed using the Levenberg-Marquardt algorithm function in MATLAB neural network toolbox. This model was trained using the logged data from a map of monitoring sensors for over a year from an operational data center [8,9]. Tableau software and a Python code was used for data pre-processing and cleaning. The trained network was then used to predict the PUE and cold aisle conditions for different modes of cooling. Using these predicted results, different bounds for cold aisle conditions for the cooling mode can be obtained. Further, the outside air conditions for which the predicted cold aisle conditions were within the ASHRAE recommended envelope were filtered out and new outside air regions for each cooling mode are defined. These results can be used to test the applicability of a cooling configuration for different weather zones while designing new data centers and for setting up control strategies in an existing data center implementing various cooling modes.

2.2.5 ANN MODELING AND TRAINING

ANN is a machine learning tool that can predict the results based on the learning data set. It uses the Levenberg-Marquardt algorithm to establish a relation between the input parameters with the outputs by assigning a set of values called as weights. These weights are updated with each iteration thus increasing the accuracy of the model. In this study, the curve fitting ANN tool in MATLAB has been used for defining, training, and testing of the model. The ANN model uses the Levenberg-Marquardt algorithm with 20 hidden neuros and a non-linear activation function for the hidden layers and a linear activation function for the output layer. The network uses seven input parameters and 3 output parameters. These include outside air temperature, humidity, IT load, temperature difference across the servers and the three types of cooling as the inputs and Power Usage Effectiveness (PUE) and the cold aisle temperature and relative humidity as the output. The network model is shown in Figure 3. The real time sensor data from the MDC laboratory in Dallas has been used for training and validation of the network. TMY 3 data for the Dallas Love-Field weather station has been used for testing and prediction.

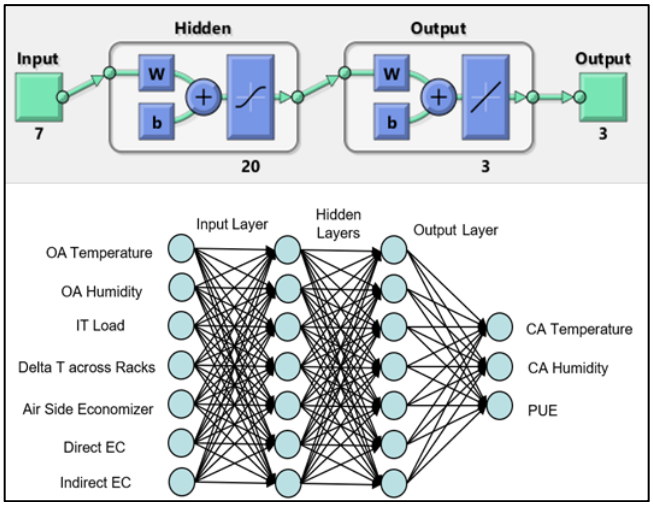

Figure 3: ANN model (top) and the network topology depicting input and output parameters (Bottom)

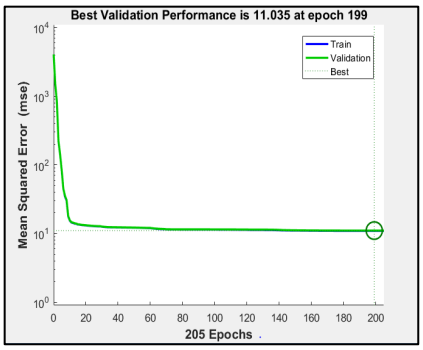

Figure 4: Performance Plot

Figure 4 shows the variation of the error with each iteration. It can be seen from the graph that the error starts at around 5000 and then decreases with each iteration. The training and validation stop when the MSE is stable at 11.035. This value represents the maximum MSE among all the validation errors and is called the best validation performance.

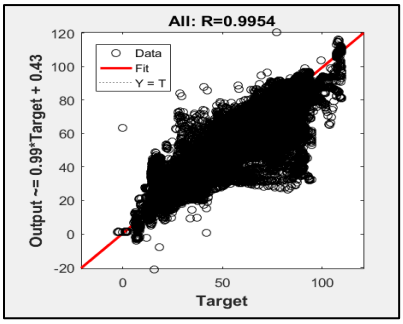

Figure 5: Regression Plot

Figure 5 represents the regression graph, in which the circles are the actual data points, and the line represents the best between the outputs and the targets. The average value for R is 0.9954 which is very close to 1 and it can be stated that the trained network predictions are acceptable. The training and validation errors is represented by the error histogram shown in Figure 6. It can be observed from the graph that the majority instances of the error lie between -3.5 and 2.8. The maximum validation error is 11.035 which is considered as the best performance achieved for the model.

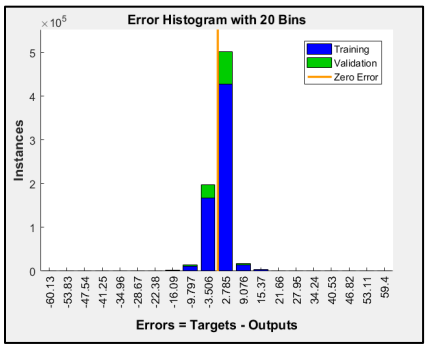

Figure 6: Error Histogram

2.2.6 RESULTS AND DISCUSSION

The TMY3 data from Dallas Love Field weather station was used as inputs to test the network. The IT load was kept constant at 15W and the rise in temperature across the servers was set to be 20. The type of cooling mode was parameterized for every run and the results were stored separately for each type of cooling mode. The predicted results were then analyzed to see how the cold aisle conditions varied over a typical year when the model was run on only one type of cooling. The output results from this ANN model are the predicted PUE, cold aisle temperature and relative humidity. The ANN model is used to predict the PUE of the data center for each type of stand-alone cooling mode when the data center is operated over a typical year. All the results are presented in this results and discussion section. Our findings are not generalizable beyond the subset of weather data examined and beyond the control logic and cooling mode settings considered in this study. However, the analysis framework and the results yielded in this study provide preliminary evidence to suggest that ANN models can be successfully used in place of traditional analysis methods.

2.2.6.1 Cold Aisle Envelopes Based on the Different Cooling Modes:

For ASE, the process of mixing OA and return air from the hot aisle is primarily dependent on the placement of the mixed air temperature sensor and the control algorithm of the damper system installed on OA and return air vents. Therefore, the training data obtained from the MDC laboratory must adequately capture this phenomenon when developing the ANN model and the predicted CA conditions will be representative of the control setpoints in the MDC laboratory. Figure 7 shows the predicted CA conditions plotted on the psychrometric chart if the DC operated on ASE for the whole year. We can see from Figure 7 that the dry bulb temperature is maintained between 64^{o}F and 81^{o}F for majority of time. The effectiveness of the mixing process, of recirculating

air with the OA, determines how efficiently the extreme cold and extreme hot outside conditions can be conditioned to the desired cooling setpoints in the CA. Therefore, the CA envelope obtained for ASE can be further improved by optimizing the mixing chamber of the cooling unit.

Figure 8 shows the predicted CA conditions plotted on the psychrometric chart if the DC operated in IEC mode. Here the air is cooled sensibly and hence there is not much rise in the humidity content of the cooled air. Hence, we can see that the relative humidity remains under 70%. Similarly, Figure 9 shows the predicted CA conditions plotted on the psychrometric chart if the DC operated on IDEC over a typical year.

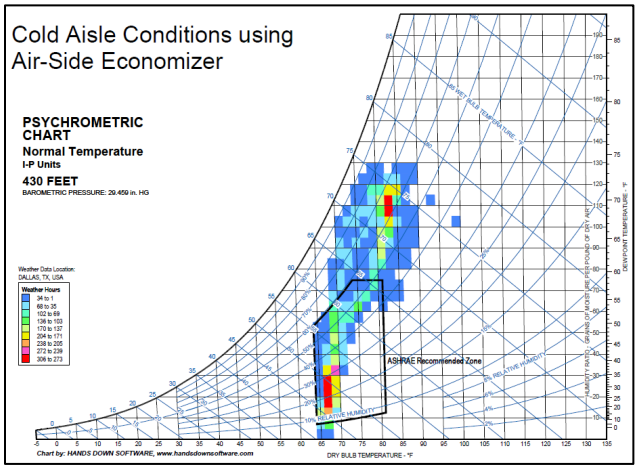

Figure 7: Predicted CA condition when operating the data center in ASE cooling mode throughout a typical year

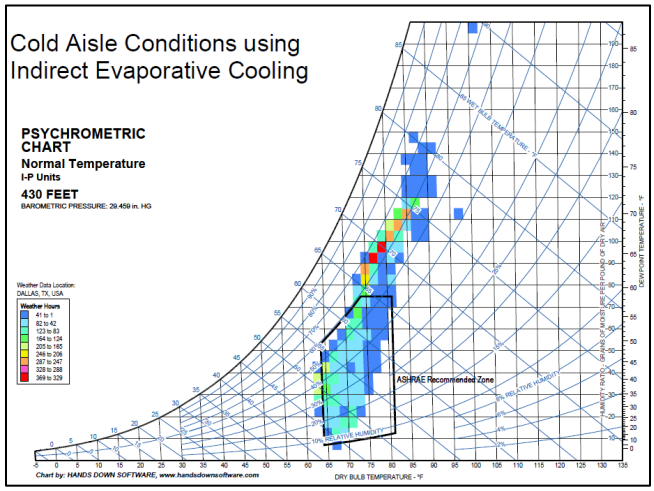

Figure 8: Predicted CA condition when operating the data center in IEC mode throughout a typical year

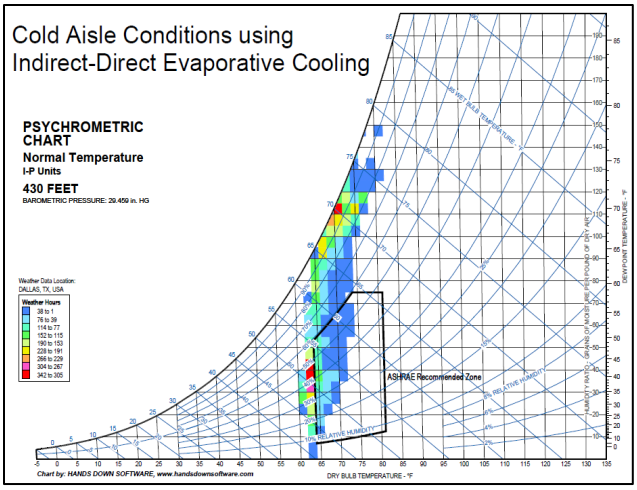

Figure 9: Predicted CA condition when operating the data center in I/DEC mode throughout a typical year

From Figure 9, we can see that the dew point temperature increases compared to the previous chart as there is humidification of the supply air due to DEC. The combined effect of both the direct and indirect evaporative coolers delivers an increased overall cooling effect. This can be easily inferred by comparing the lower dry bulb temperature bound of the CA envelopes plotted in Figure 7, 8 and 9. These Figures also suggest that humidity excursions are prevalent in the cold aisle regardless of the cooling configuration. The extent of humidification is a clear function of the operational saturation efficiency of the wet cooling media wall and the OAT. The validity of the data collection approach in the CA contributes to lower cooling setpoints [10] and thereby can also lead to in excessive humidification. Rapid changes in the OAT and stratification of inlet air can result in scenarios of excessive humidification [11]. Erroneous control strategy can lead to such high humidity (95% RH) conditions in the cold aisle, and this can be catastrophic due to condensation related ITE failures in the data center [12].

The box and whisker plot in Figure 10, 11 and 12 show variability of the CA temperature and humidity over each month for different but stand-alone cooling modes. For ASE and IEC modes, the monitoring sensor location, and the CA cooling setpoint is generally temperature-based and the variability in CA humidity is a function of OAT. Optimizing the mixing process of outside air and return air provides a possibility of reducing the variability in CA conditions. Control strategies to achieve incremental humidification in DEC is further explored in [11].

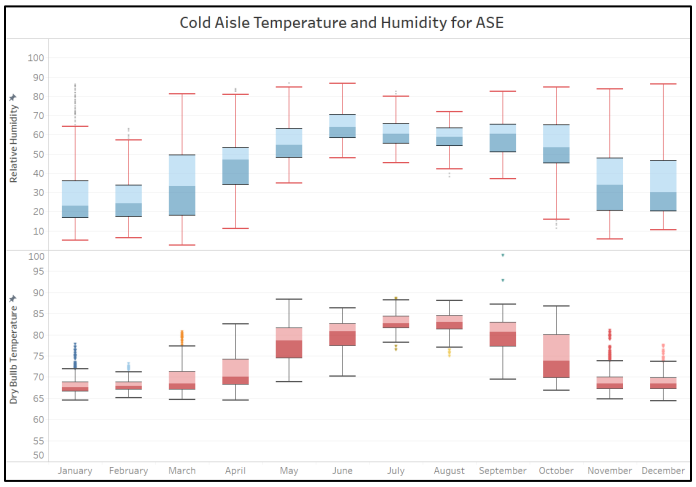

Figure 10: Variability of the CA condition when operating the data center in ASE mode throughout a typical year

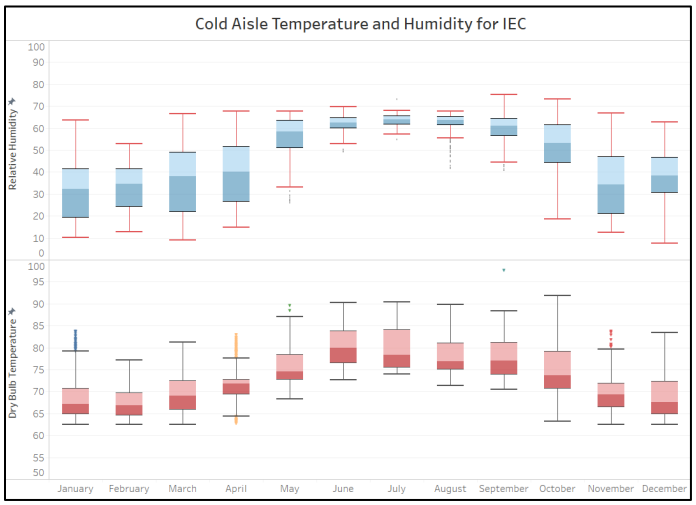

Figure 11: Variability of the CA condition when operating the data center in IEC mode throughout a typical year

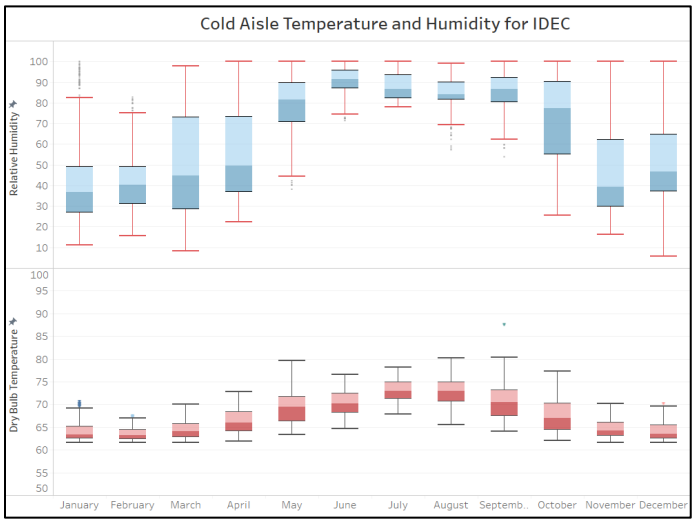

Figure 12: Variability of the CA condition when operating the data center in IDEC mode throughout a typical year

2.2.6.2 Outside Air Envelopes Based on Different Cooling Modes

The applicability of a cooling mode, for a specified location, is often reported in terms of the total OA hourly bins available for adequate cooling provisioning [6,7]. However, thermodynamic, and analytical models in previous studies assume an idealized airflow distribution and cooling control mechanism. In this study, such nonlinearities are inherent in the training data used for developing the ANN model. The predicted CA conditions from the ANN model yielded some interesting findings. By extracting the OA input conditions for which the predicted CA conditions satisfy the ASHRAE recommended envelope, OA envelopes can be visualized on a psychrometric chart. Using these results, the total effective hours of operation for a cooling mode over a typical year, as well as for each month, was obtained for all the cooling modes considered in this study. Figure 13 shows the OA plots for which ASE can be used to maintain the CA conditions within the ASHRAE recommended region. It can be observed that the high humidity and low temperature air was conditioned to be within the recommended bounds by mixing it with the hot and dry air from the hot aisle using ASE. But there are no points in the high humidity region once the temperature goes above 60^{o}F.

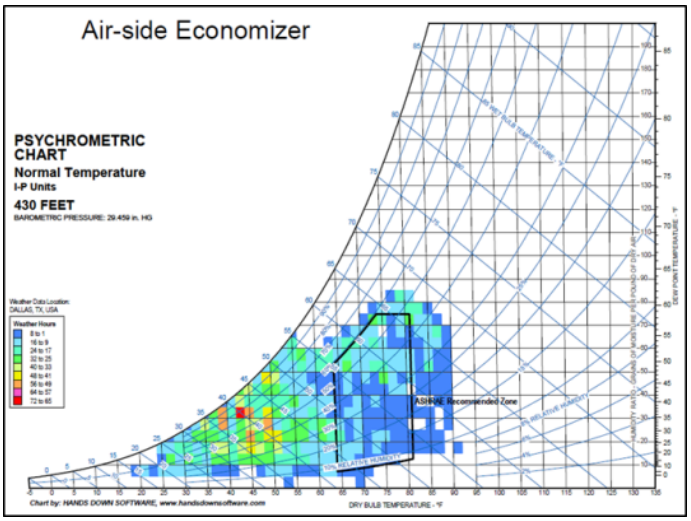

Figure 13: OA conditions when using ASE for achieving CA operating conditions in the ASHRAE Recommended Envelope

Also, depending on the effectiveness of the control algorithm, a large part the IEC utilizes return air for sensible cooling and adds no moisture to the supply air. This is evident in Figure 14, as the dataset used for training the ANN model was obtained from the MDC wherein the IEC operated by recirculating the return air when the outside air is hot and humid or just too humid. Thus, OA envelope for IEC in Figure 14 spans the high humidity region although much of the return air is recirculated for cooling purposes.

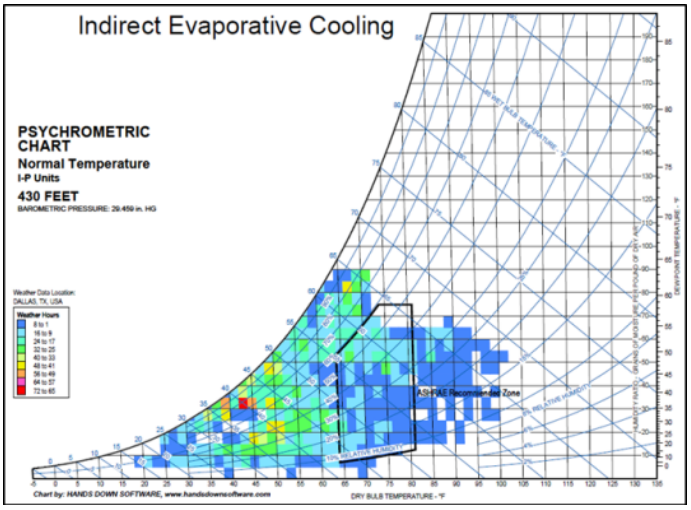

Figure 14: OA Envelope using IEC for achieving CA operating conditions in the ASHRAE Recommended Envelope

In the MDC laboratory, the control algorithm was setup in such a way as to always initiate IEC first and switch to IDEC only when additional cooling was required. During IDEC, the OA first undergoes sensible cooling with no moisture added. In the second stage, the pre-cooled air is then passed through the direct evaporative cooling pads further reducing its temperature. Also, a significant increase in seen in the humidity of the air during this second stage. As a result, the final supply air is cool and humid. Thus, I/DEC is mostly used for dry and very hot OA conditions. Again, erroneous control can lead to over-humidification of the pre-cooled air.

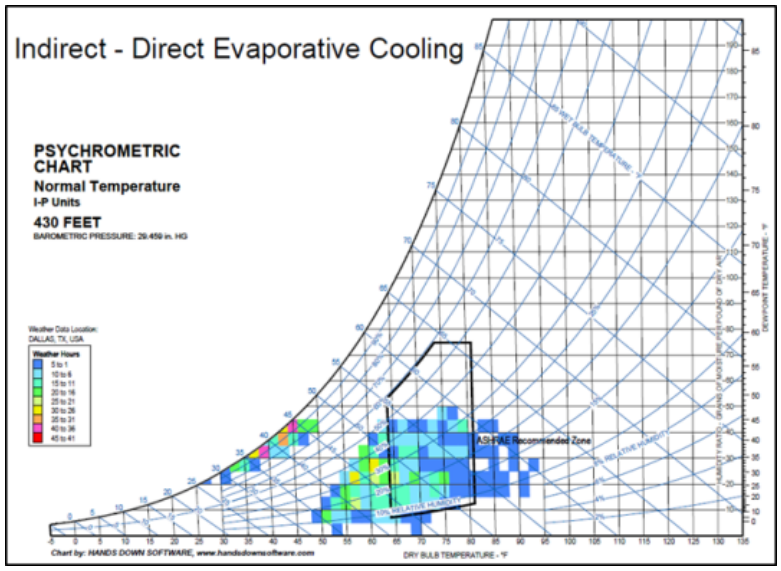

Figure 15: OA Envelope using IDEC for achieving CA operating conditions in the ASHRAE Recommended Envelope

Figure 16 shows the predicted month-wise usage of different type of cooling modes. It can be seen from the graph that the trend is similar for all types of cooling. The utilization is higher expect during the summer months. This is mainly because of the rise in the outside air temperature and humidity during the summer. It should be noted that the lack of utilization of any mode of cooling during the summer resulting in CA conditions within the ASHRAE recommended envelope is primarily due to the large fluctuations in humidity.

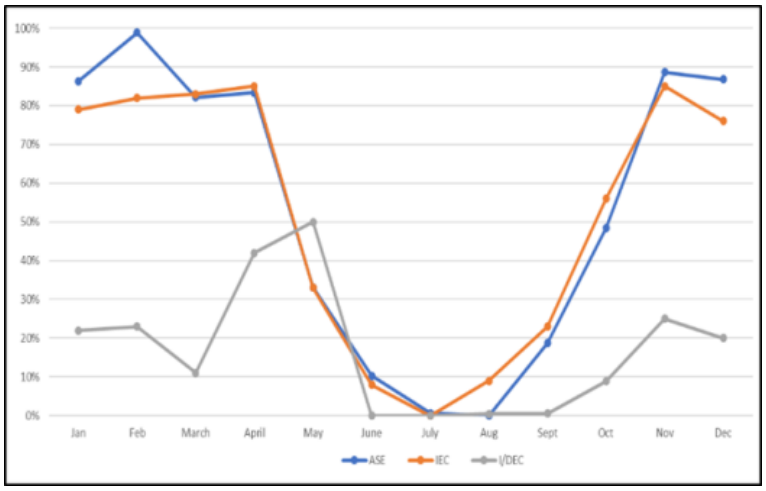

Figure 16: Month-wise %OA for different types of cooling satisfying ASHRAE Recommended Envelope

The cooling setpoints in data center cannot reliably consider humidity setpoints due to the lack of refined humidity control in evaporative cooled data centers without any dehumidification available. Even the humidification process due to the direct evaporative cooling lacks incremental humidification effect if the wet cooling media wall is not vertically staged with discrete pumps [11]. Therefore, alternative cooling such as direct expansion cooling or dehumidification of supply air must be used to maintain the server within the ASHRAE recommended zone during these months. Depending on the type of ITE populated in the data center, short humidity and temperature excursions can be safe and energy efficient. Taken altogether, the data presented here provide evidence that the three cooling modes i.e., ASE, IEC and IDEC can be used for cooling the outside air to the recommended envelope. From the OA envelopes, 53% of the outside air is compatible for ASE, 10% for IEC and 8% for IDEC when the targeted CA condition is the ASHRAE recommended envelope. Minimizing or accommodating the humidity excursions can further improve these figures. However, for total minimization of cooling power, controls must be set to first use ASE as it has the lowest PUE and thus minimizes the cost of cooling. Figure 17 represents the scenario when all the cooling modes are available, and the control algorithm mimics the controls set up on the MDC laboratory.

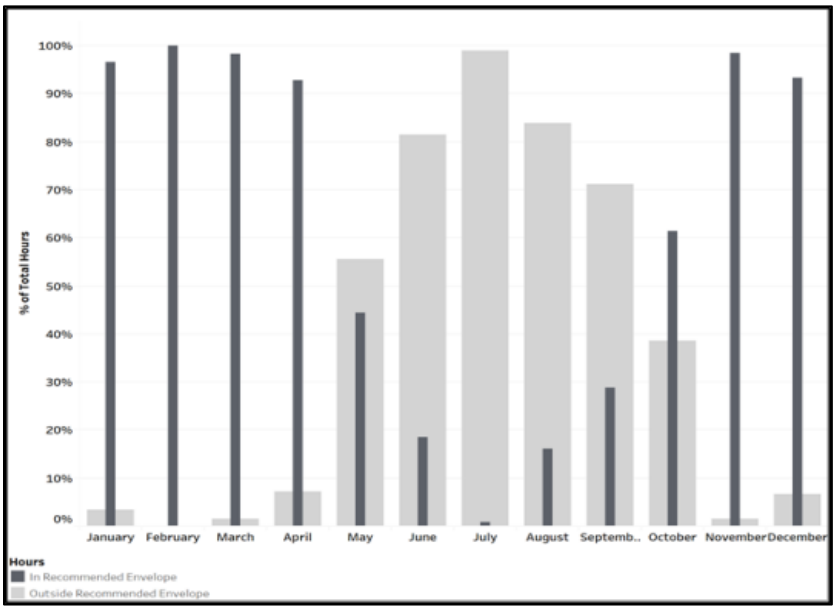

Figure 17: Month-wise Predicted Utilization for all cooling modes in tandem when targeting ASHRAE recommended CA conditions

There is a possibility of using data-driven ANN models to facilitate control strategies that can pro-actively minimize the operational cost. For the optimum sequence of operation and switching between cooling modes, further investigation is necessary. The transients involved in initiating a cooling mode and the temperature and humidity variations within the CA are all important operational features of the cooling system design that can be captured with an ANN model. The challenge in developing such models would primarily be in acquiring the right and enough training data set. Computational Fluid Dynamics models of data centers have been used to generate robust training data sets to predict the temperature and airflow distribution within a data center [13-15]. Future studies will have to continue to explore how the complex features of an operational data center can be extracted and adequately represented in a training dataset to develop better ANN models.

2.2.7 CONCLUSION

In this study, the logged field data from a modular data center was used to train the ANN model which was then used to predict the conditions inside the cold aisle. The results presented in this paper show that ANN can be utilized to predict the performance of the cooling systems which can be then used to set up control algorithms for the data centers. Firstly, the ANN model predicted the cold aisle conditions achieved when only one cooling mode is used over a typical year. For each cooling mode operated over a typical year, a CA envelope was visualized on a psychrometric chart. These results can be used to understand the variations in the cold aisle with respect to the cooling mode in different weather zones. Furthermore, OA envelopes were visualized on a psychrometric chart to determine the variability of the outside air conditions over which a cooling mode can be effectively used to attain ASHRAE recommended CA conditions. The ANN model accounts for the non-linearities developed in the data center due to the interdependence of mechanical, electrical and control systems and hence give a more realistic results compared to other analysis methods.

2.2.8 REFERENCES

[1] M. Sahini, U. Chowdary, A. Siddarth, T. Pradip, and D. Agonafer, “Comparative study of high ambient inlet temperature effects on the performance of air vs. liquid cooled IT equipment,” in In Thermal and Thermomechanical Phenomena in Electronic Systems, 2017, pp. 544–550.

[2] R. Eiland, J. Edward Fernandes, M. Vallejo, A. Siddarth, D. Agonafer, and V. Mulay, “Thermal Performance and Efficiency of a Mineral Oil Immersed Server Over Varied Environmental Operating Conditions,” J. Electron. Packag., vol. 139, no. 4, p. 41005, 2017.

[3] Larry Kinney, “Evaporative Cooling for a Growing Southwest: Technology, Markets, and Economics”

[4] Wilcox, S. and W. Marion. User's Manual for TMY3 Data Sets, NREL/TP-581-43156. April 2008. Golden, Colorado: National Renewable Energy Laboratory

[5] ASHRAE TC9.9, Data Center Networking Equipment – Issues and Best Practices Whitepaper prepared by ASHRAE Technical Committee (TC) 9.9 Mission Critical Facilities, Data Centers, Technology Spaces, and Electronic Equipment.

[6] Metzger, Ian, Otto VanGeet, Caleb Rockenbaugh, Jesse Dean, and Chuck Kurnik. "Psychrometric bin analysis for alternative cooling strategies in data centers." ASHRAE Trans 117 (2011): 254-261.

[7] M. Vallejo, “Energy and Water Impacts of Data Center Cooling Systems: A Triple Bottom Line Assessment for Facility Design,” University of Texas at Arlington, PhD Dissertation, 2015.

[8] Gebrehiwot, Betsegaw Kebede. "Maximizing Use of Air-Side Economization, Direct and Indirect Evaporative Cooling for Energy Efficient Data Centers." University of Texas Arlington, PhD diss., 2016.

[9] Guhe, Abhishek. "Control Strategies for Air-Side Economization, Direct and Indirect Evaporative Cooling and Artificial Neural Networks Applications for Energy Efficient Data Centers." ." University of Texas Arlington, Master’s Thesis., 2016.

[10] Tradat MM, Khalili SS, Sammakia BB, et al. Comparison and Evaluation of Different Monitoring Methods in a Data Center Environment. ASME. International Electronic Packaging Technical Conference and Exhibition, ASME 2017 International Technical Conference and Exhibition on Packaging and Integration of Electronic and Photonic Microsystems (): V001T02A019. doi:10.1115/IPACK2017-74105.

[11] A. Al Khazraji, A.Siddarth, M. Varadharasan, A. Guhe, D. Agonafer, J. Hoverson and M. Kaler, “Experimental Characterization of Vertically Split Distribution Wet- Cooling Media Used in the Direct Evaporative Cooling of Data Centers”, IEEE Itherm Conference, San Diego, CA, USA, (2018)

[12] Mulay, V. “Humidity Excursions in Facebook Prineville Data Center”, electronics-cooling.com, December 10, 2012; URL:https://www.electronics-cooling.com/2012/12/humidity-excursions-in-facebook-prineville-data-center/

[13] Song Z, Murray BT, Sammakia B. Multivariate Prediction of Airflow and Temperature Distributions Using Artificial Neural Networks. ASME. International Electronic Packaging Technical Conference and Exhibition, ASME 2011 Pacific Rim Technical Conference and Exhibition on Packaging and Integration of Electronic and Photonic Systems, MEMS and NEMS: Volume 2 ():595-604. doi:10.1115/IPACK2011-52167.

[14] Zhihang Song, Bruce T. Murray, Bahgat Sammakia, Airflow and temperature distribution optimization in data centers using artificial neural networks, International Journal of Heat and Mass Transfer, Volume 64, 2013, Pages 80-90, ISSN 0017-9310, https://doi.org/10.1016/j.ijheatmasstransfer.2013.04.017.

[15] J. Athavale, Y. Joshi and M. Yoda, "Artificial Neural Network Based Prediction of Temperature and Flow Profile in Data Centers," 2018 17th IEEE Intersociety Conference on Thermal and Thermomechanical Phenomena in Electronic Systems (ITherm), San Diego, CA, 2018, pp. 871-880.
doi: 10.1109/ITHERM.2018.8419607

[16] Gao, Jim, and Ratnesh Jamidar. "Machine learning applications for data center optimization." Google White Paper (2014).

[17] Walekar Abhishek, “Psychrometric Bin Analysis for Data Center Cooling Modes Using Artificial Neural Networks” MS Thesis, Proquest, 2018.

[18] F. Adejokun, A. Siddarth, A. Guhe and D. Agonafer, “Weather Analysis using Neural Networks for Modular Data Centers” Proceedings of the ASME 2018 International Technical Conference and Exhibition on Packaging and Integration of Electronic and Photonic Microsystems, San Francisco, CA, USA, IPACK2018-8253, (2018).

[19] Shrivastava, Saurabh K., James W. VanGilder, and Bahgat G. Sammakia. "Data center cooling prediction using artificial neural network." In ASME 2007 InterPACK Conference collocated with the ASME/JSME 2007 Thermal Engineering Heat Transfer Summer Conference, pp. 765-771. American Society of Mechanical Engineers, 2007.

2.3 Generic Methods for the Thermal Design of Evaporative Cooled Data Centers

2.3.1 ABSTRACT

With the increasing load on the servers, the cost and energy required to cool a data center has been on the rise. This has kept the researchers to explore more efficient and economical cooling technologies for data centers. One such technology is evaporative cooling. The evaporative cooling systems are one of the most effective methods available for cooling the data centers. So, developing the generic methods for the thermal design of data centers is of utmost importance. This research aims to identify, develop, and validate the thermal model for Direct Evaporative Cooling and Indirect Evaporative Cooling. By taking the environmental data of each location and

server rack specifications as inputs, the performance and cost analysis are done. Strategies to cope with system component failures have also been considered by the model. A tool, that works on the identified methods has been developed. The tool gives the performance results, the cost analysis, and a comparison between direct and indirect evaporative cooling, allowing the user to make decisions on the type of cooling that can be used for specific environmental conditions.

2.3.2 INTRODUCTION

2.3.2.1 Data Centers – An Overview

Data Centers are facilities that house IT equipment used to perform functions like data processing, storage, transmission and enabling swift access to the data. The IT equipment responsible for performing these operations are known as servers, which are the core for the Internet of Things. These servers are stacked on top of each other in the form of server racks. A data center can occupy anywhere from one room to a whole level of a building. The servers are stacked in several racks arranged in single rows forming aisles. Figure 1 shows a modular data center. Modular Data Centers are the modern systems of data center deployment that can be placed anywhere. Modular data center systems consist of purpose-engineered modules and components to offer scalable data center capacity with multiple power and cooling options [1]. Now, as the data centers are run continuously all

the year, a large amount of heat is generated. To keep the servers operating and maintain their life, this heat needs to be removed quickly. Therefore, the cooling of data centers is of utmost importance.

Figure 1: Modular Data Center

There are various techniques that can be used to cool down the data centers. Firstly, there is liquid cooling in which water or other liquids are sent to the critical components through tubes. This is a highly effective method due to water's high heat transfer capacity. But this method is very complex and dangerous. Then we have immersion cooling, where the servers are submerged in a thermally conductive dielectric medium. The dielectric medium is usually oil. Although this method is a potential solution for green data centers [3], there are a lot of changes that should be made to the existing server designs and components. The following figure shows how the oil immersion cooling works.

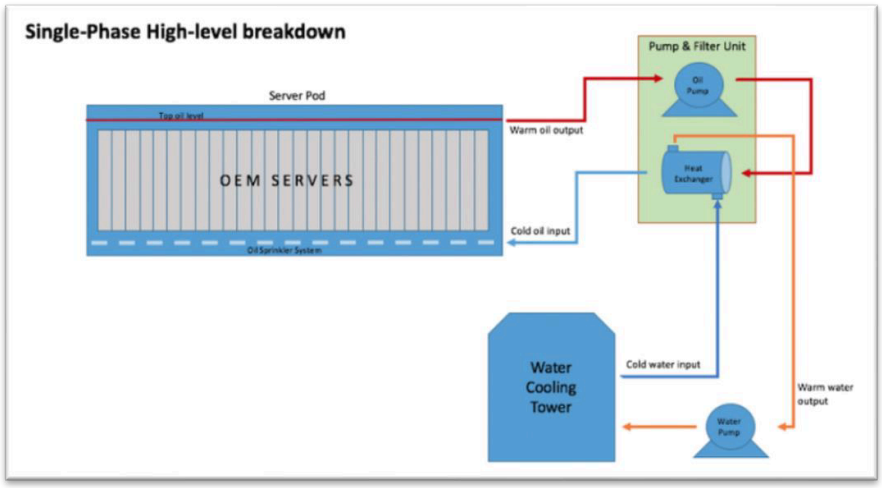

Figure 2: Schematic of an oil immersion cooled data center

Air Cooling is the most popular and widely used technique, due to its simplicity and flexibility. Air cooling is further divided into different methods. Computer Room Air Conditioning (CRAC): This is a traditional method to cool down the data center. CRAC unit is a device that monitors and maintains the temperature, humidity, and air flow distribution inside the data center. The CRAC units work on the refrigeration cycle, and most of the power is consumed by the compressor. The hot exhaust air is sent to the CRAC units where the liquid refrigerant takes up the heat from the hot exhaust air. It is then compressed inside a compressor. The compressed evaporated refrigerant is condensed in the cooling tower and is sent back to the CRAC unit. The water inside the cooling tower takes up the heat from the refrigerant and ejects it into the atmosphere. These units are expensive and are not highly efficient. The following figure shows the working of a CRAC system.

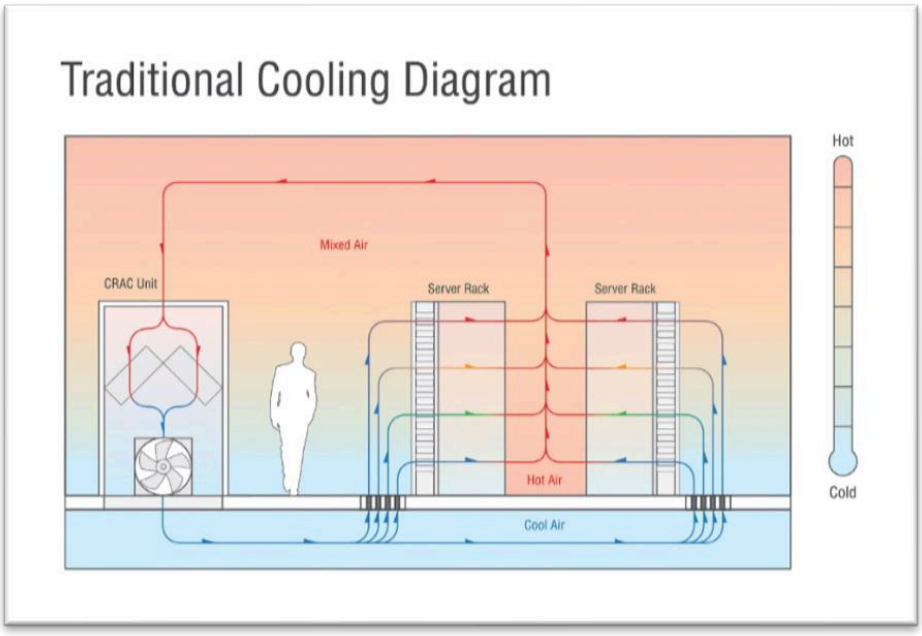

Figure 3: CRAC System and the typical airflow management in a raised floor data center

Air Side Economization (ASE): Air side economization is being currently used in most of the data centers for being economical and highly efficient. In this method, whenever the ambient air conditions like dry bulb temperature and relative humidity are favorable, the outside air is directly used to cool down the IT room. Mechanical systems like fans could be used when some heating of the outside air is required. One of the drawbacks of this method is the introduction of contaminants present in air to the IT equipment. This will cause the equipment to fail and could lead to shut down. The working if an ASE is explained in the following figure.

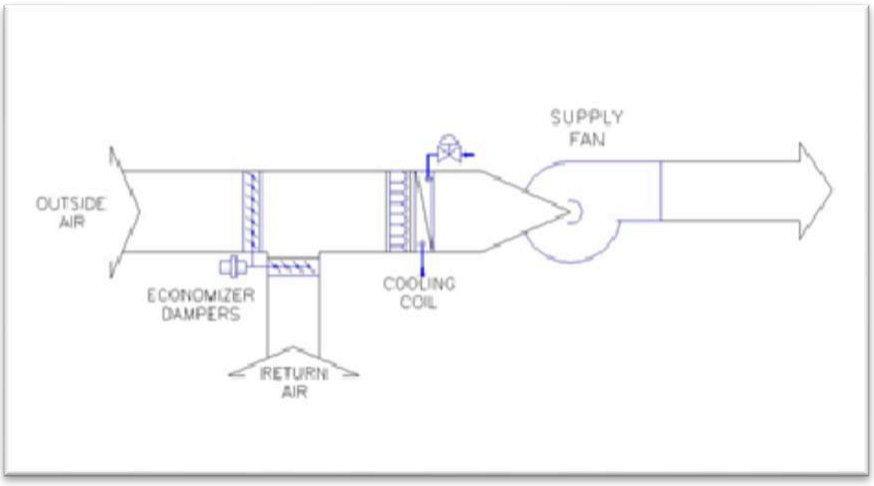

Figure 4: Air-side Economizer

Evaporative Cooling: In this technique, cooling is achieved by evaporation of water. The hot outside air used as inlet to the data center, is introduced to a wet media pad or pipe where the water gets evaporated by taking the heat from the incoming air. This air is then sent to the IT room to cool down the servers. The air at the inlet of the IT room although being low in temperature has high moisture content. This moisture content could lead to the contamination of the equipment, so counter measures must be taken to reduce the risk. There are two types of evaporative cooling: direct and indirect. A comprehensive study about these is shown in the upcoming chapters. The following figure shows the basic principle of evaporative cooling.

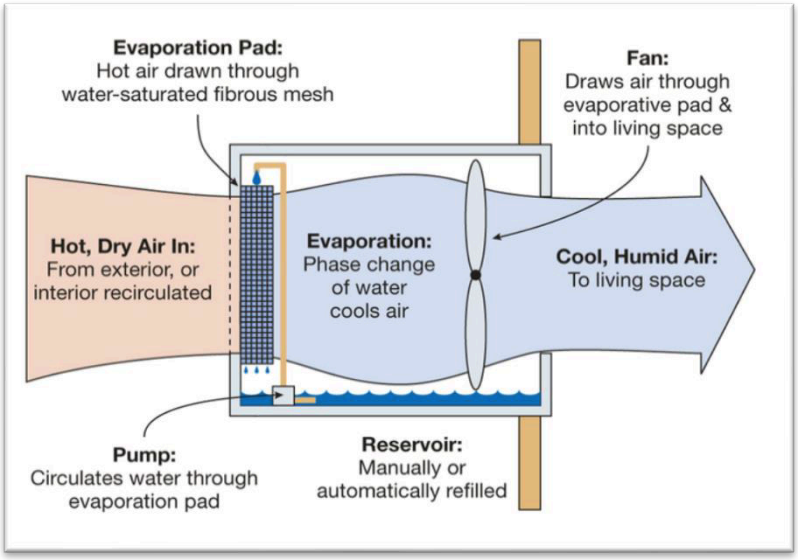

Figure 5: Evaporative Cooling [6]

2.3.2.2 Psychrometry

The definitions have been re The definitions have been restated from [18] and [19].

- Dry Bulb Temperature (DBT): The temperature of air around us, measured with a normal dry thermometer. It is one of the most important parameters. It indicates the heat content and is depicted by the horizontal axis of the psychrometric chart.
- Relative Humidity (ϕ): It gives the amount of moisture content present in the air. It is the ratio of vapor pressure of moisture to the saturation pressure at the dry bulb temperature.
- Wet Bulb Temperature (WBT): It is the temperature measured by wrapping a wet cloth around the thermometer wick and introducing it to air flow. It is represented by the slanted lines on the psychrometric chart.
- Dew Point Temperature (DPT): It is the temperature at which the condensation of moisture begins, when the air is cooled at constant pressure.

- Humidity Ratio (ω): It is the ratio of mass of water vapor to the mass of air in any given volume of mixture. On the psychrometric chart, it is represented by the vertical axis.
- Degree of Saturation (μ): It is the ratio of air humidity ratio to humidity ratio of saturated moist air at same temperature and pressure.

The psychrometric chart represents the physical and thermodynamic properties of moist air, graphically. A psychrometric chart is plotted for a particular temperature. If the dry bulb temperature and relative humidity are known for a particular pressure, all the remaining properties can be found out from the chart. The psychrometric chart with the allowable regions and recommended zones was shown in figure 1-7. So, depending upon the outside air temperature if it's in the allowable regions, we can decide whether we need to cool down the air, or heat it, or humidify it or dehumidify it or sometimes a combination of two processes to bring the air into the recommended zone. The following figure shows the processes we can do on the outside air to bring it into the recommended zone.

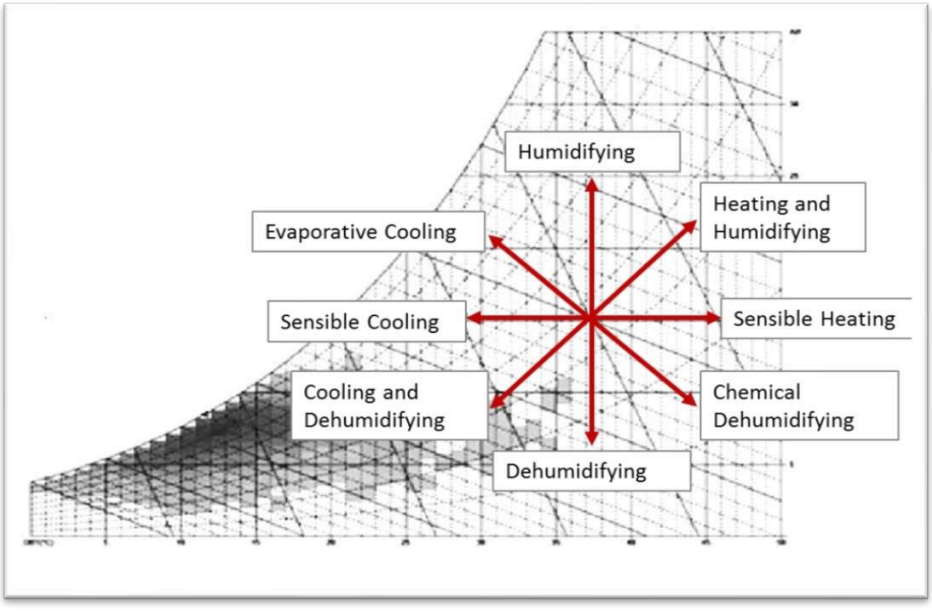

Figure 6: Psychrometric processes [20]

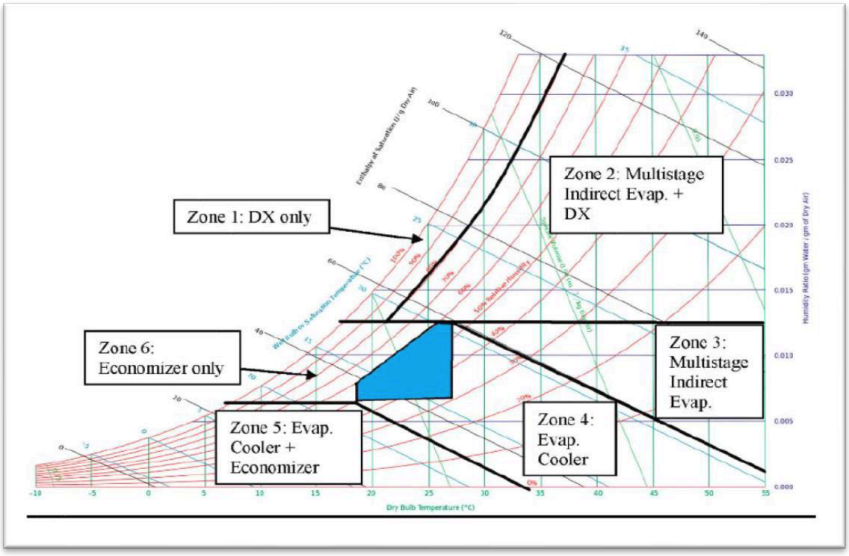

Figure 7: Cooling processes

According to psychrometric bin analysis performed by [21], using evaporative cooling using evaporative cooling will give better results than CRAC and Direct Expansion Cooling.

2.3.3 SCOPE OF THE WORK

2.3.3.1 Literature Review & Motivation

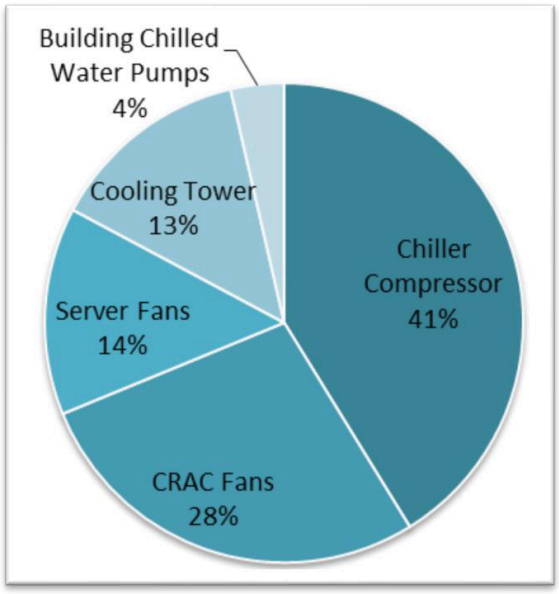

Figure 8: Energy Consumption Breakdown

With the increase in web-based services and cloud computing there has been a drastic increase in the demand for data centers. With increase in demand the cost of acquisition and leasing of data center facility and servers from vendors has increased. This made organizations and researchers to develop models and strategies that will assist in building their own data center facilities. So, in the recent years, a lot of research has been going on in the field of evaporative cooling. Several thermal models have been presented by numerous authors and organizations. One of first organizations to design their own data center was Facebook [8] in 2011. For this thermal design Facebook followed the black- state approach and assumed everything will be working at maximum efficiency. They custom designed the model so that it could run on Air Side Economization throughout the year as the weather conditions were favorable at Prineville, Oregon. The thermal models developed were delivered as a part of the Open Compute Project [9]. Thermal models for Direct and Indirect Evaporative cooling were developed and presented as pre-design and design tools by [10]. The pre-design tools give the first estimation of cooling potential and hours of discomfort. More detailed thermal models that go from the chip inside the server to the cooling tower have been developed and presented in [11], [12], [13], [14]. In all these papers, highly detailed

models from the chip level to server level to rack level till the cooling tower level have been discussed. Along with the thermal models, influence of server inlet temperatures has been discussed in [11]. Many other factors that have an impact on cooling have been discussed in the other three papers.

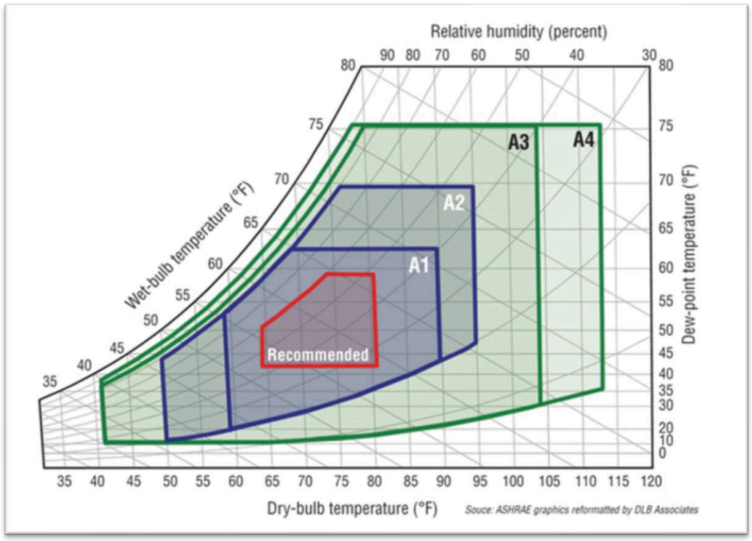

Figure 9: Thermal Guidelines as per ASHRAE Technical Committee 9.9

Holistic thermodynamic models were developed using system and component physics so that the energy consumption and heat transfer phenomenon inside the data center can be predicted by [15]. These holistic models helped technologists to understand and identify the amount of energy used for cooling purposes among others. All these thermodynamic models till now discuss only about the heat transfers, energy consumption and effectiveness by the data center. One of the important resources that has not been considered is water consumption. Some light was thrown into this direction by [16], where heat transfer models were prepared to validate the performance of the evaporative cooling pad. After a couple of years in 2015, [17] developed models that consider water consumption as an important factor while calculating the operational costs for the data center. All the thermodynamic models discussed till now, account for almost all the major components of the data center. These models are specific, or custom made by the researchers and organizations to serve their purposes. This work seeks

to identify, develop, and establish the general methods to be followed for the thermal design of a data center based on evaporative cooling. All these models will be used to develop a tool that provides performance and cost analysis for each type of evaporative cooling for each geographic location, making it easier for the customer to make executive decisions.

2.3.3.2 Objectives

- Identifying and establishing the general methods for the thermal design of a data center while accounting for water consumption.
- Adding redundancy to the existing models.
- Developing a tool (an application) that gives performance and cost analysis.

2.3.4 METHODOLOGY FOR THERMODYNAMIC MODELING

A thermodynamic model has been developed for both Direct and Indirect Evaporative Cooling. Each model is derived based on the first law of Thermodynamics. Each sub-model has been considered as a black-box model and only heat and mass transfer has been considered. The thermodynamic cost model that accounts for the energy and water consumption costs have been calculated on annual basis. The boundary conditions are assumed to be the same for both the cooling strategies. Quasi - steady state conditions are assumed to exist at the operating points. The weather data for each city has been taken from the TMY3 data [22]. The commercial utility rates for water and electricity have been taken from the available data for each city. It is also assumed that the all the servers are running at the same performance level and at maximum loading conditions. All the fans are equally efficient, and all the pumps are running at their maximum speed. Now that all the assumptions being made have been listed, thermodynamic model for each cooling strategy will be developed.

2.3.4.1 Direct Evaporative Cooling

In DEC, the water comes into direct contact with the supply air stream through a water spray or wetted cooling media. The fan shown in figure 10 draws the air from outside through the wet media pad and sends the cool air to IT room. A pump is used to keep the media pad always wet. The water absorbs the heat from the air and evaporates thereby cooling the air stream.

In DEC, the dry bulb temperature decreases, and humidity increases while the wet bulb temperature remains the same due to adiabatic cooling. The following figures shows the working of a direct evaporative cooling system and the process diagram on the psychrometric chart.

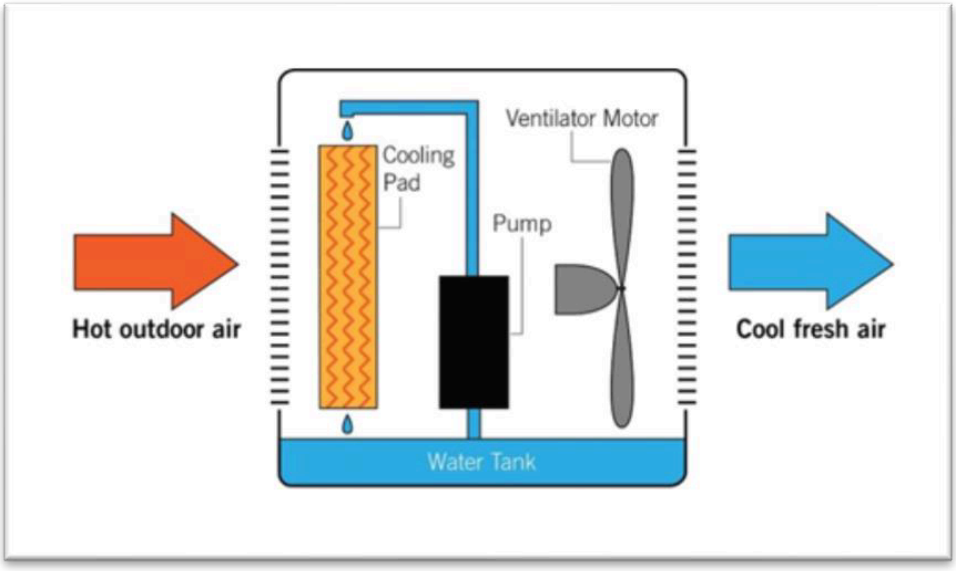

Figure 10: Direct evaporative cooling [23]

IT room model: The heat generated inside the IT room will be due to the servers and inefficiencies of the server fans.

$$Q_{\text{serv}} = P_{\text{serv}} - P_{Sf} \quad (1)$$

As a rack is composed of several servers, assuming each rack has the same number of servers, the heat dissipated by " Q_{rack} " from each rack will be the same. If the temperature rise between the rack is given by " ΔT_{rack} ", then the mass flow rate of air through the rack can be calculated by

$$m_a = \frac{Q_{\text{rack}}}{C_{p^*\Delta T_{\text{rack}}}} \tag{2}$$

The inefficiency of the server fans can be determined through fan laws. As this model concentrates to provide the general methods, the server fan inefficiencies are assumed to be minimal, enabling us to consider that the heat generated in the IT room to be the heat generated by the servers alone. This means the total heat generated can be equated to the IT compute power.

$$Q_{\text{room}} = P_{IT} \tag{3}$$

Equation (1) can also be used to calculate the rack and IT heat load but as this research aims to give cooling solutions to those who want to setup a data center based on evaporative cooling, exact values for the variables will not be available.

Pump model: The power requirement for the water pump can be determined by using the pressure drop in the circulating water loop, flow rate required and pump efficiency.

$$P_{wp} = \left(\Delta p_{wp} * v_{wp}\right)/\eta_{wp} \tag{4}$$

It can also be calculated using the following equation

$$P_{wp} = P_{\text{ref}} \times (V_w/V_{\text{ref}})^3 \tag{5}$$

P_{ref} and V_{ref} can be obtained from the manufacturer's data is the required flow.

Supply fan model: For the supply fan/blower, redundancy has been introduced. This is to make sure the system keeps working in case of any contingencies. The power required by the supply fan depends on the flowrate that needs to be delivered. According to the fan laws and data from manufacturer, the power for the supply fan is calculated using

$$P_{\text{Sfan}} = n * P_{\text{ref}} \times (V_{\text{SfanAir}} / V_{S\,\text{fref}})^3 \quad (6)$$

Water consumption model: the water consumed to cool down the inlet air is calculated using the mass balance equation. The outside air temperature and relative humidity are taken from the TMY3 data. The minimum air exit temperature that can be obtained through the media pad is given by [24] as

$$t_{min} = t_d - \left(SE_{\text{media}} * (t_d - t_w)\right) \quad (7)$$

Here “is the saturation effectiveness of the media pad being used. It depends on the material being used varies from 60%-93%. “” is the wet bulb temperature of outside air. The exit air temperature from the cooling pad is taken as the supply air temperature for the IT room and hence it should be within the operating conditions. The rate of evaporation is given by product of mass flow rate of air and the difference between the humidity ratio of air before and after the wet media pad.

$$m_{\text{evap}} = m_a\left(\omega_{a,e} - \omega_{a,i}\right) \quad (8)$$

Power Usage Effectiveness (PUE): PUE is a measure of performance of the cooling system. The total power consumed in Direct Evaporative Cooling is given by

$$P_{\text{total}} = P_{\text{Sfan}} + P_{wp} + Q_{\text{room}} \quad (9)$$

Now, PUE is calculated using equation (1-1),

$$PUE = \frac{P_{\text{total}}}{Q_{\text{room}}} \tag{10}$$

Cost model: The cost of water consumption is determined by calculating the water consumed for the whole year and then multiplying it with the commercial rate of water and adding the base charge for the particular city.

$$C_{\text{water}} = C_{\text{base}} + (U_{\text{water}} * \text{Rate}) \tag{11}$$

Here, “” is the units of water consumed in gallons per year.

The cost of energy consumption is also calculated in a similar manner. The energy rates vary widely through the state. For validation of the case study, commercial rates have been taken for each city.

2.3.4.2 Indirect Evaporative Cooling

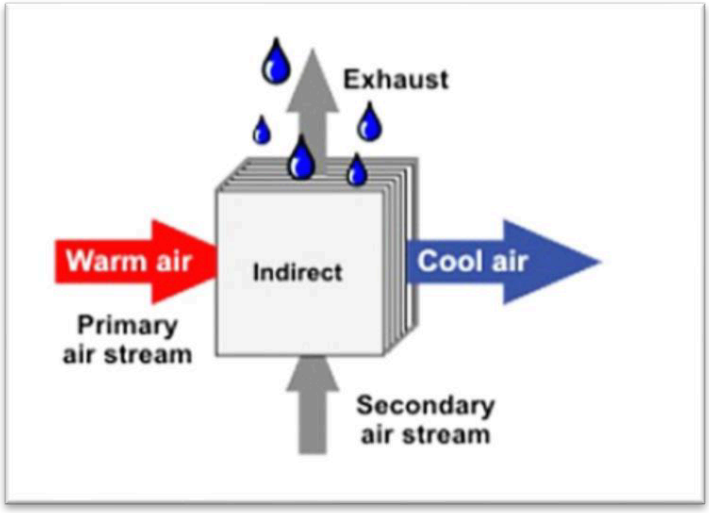

Figure 11: Indirect evaporative cooling [25]

Principle & Working: In IEC, the water doesn't come in direct contact with the air stream. A heat exchanger is used to lower the temperature of the inlet air stream. Inside the heat exchanger, a secondary air stream cools down the primary inlet air stream. The secondary air stream is cooled down by the water stream. In this type of cooling, both the dry bulb and wet bulb temperatures of the inlet air get decreased, while the humidity of the air remains the same. This thermodynamic process is known as sensible cooling. In IEC, the return air is mixed with the inlet air to achieve the target inlet temperatures. Although this method does not increase the humidity of the primary air stream, which is beneficial. But when compared to DEC, it costs more and is less efficient. The main components of an indirect evaporative cooling are supply fan that brings the primary air into the system, a cooling tower that acts as the heat exchanger and the IT room. The following figure shows the working of IEC.

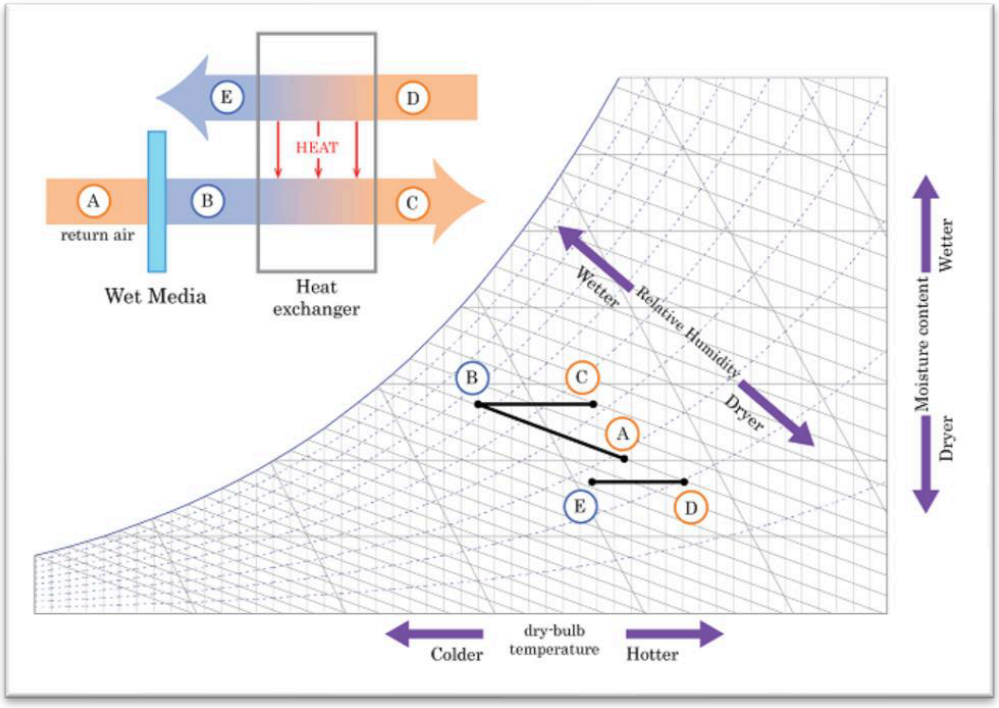

Figure 12: Thermodynamic process [26]

IT Room Model: The IT room model for indirect evaporative cooling is similar to that of direct evaporative cooling as there will be no change in the setup of the IT room.

Hence, the heat load of the IT room is equal to the power requirement of the IT room.

$$Q_{\text{room}} = P_{IT} \tag{12}$$

Supply fan model: The model for the supply fan for primary air will be similar to the model used in direct evaporative cooling. Redundancy is again introduced here and the equation for power consumed by the supply fan is

$$P_{\text{Sfan}} = n * P_{\text{ref}} \times (V_{\text{SfanAir}} / V_{S\,\text{fref}})^3 \tag{13}$$

Cooling Tower Model: The cooling tower is the main component of IEC that differentiates it from DEC. The cooling tower acts as a heat exchanger. IT consists of a water pump that regulates the water flow, fan that regulates the air flow inside the cooling tower and a wet media that cools down the secondary air stream. The heat load on the cooling tower is calculated as,

$$Q_{CT} = Q_{\text{room}} + \eta_{wp} * P_{wp} + \eta_{sf2} * P_{sf2} \tag{14}$$

Power required for running the water pump and supply fan depend on the mass flow rate of air calculated from the heat load. These can be calculated in a similar as shown previously for DEC.

Water Consumption Model: The water consumed inside the cooling tower depends on the effectiveness of the wet media. Its effectiveness depends on the material being used and it varies from 60% to 90%. The amount of water being consumed is found out by multiplying the mass flow rate of air with the increase in the humidity ratio of secondary air.

$$m_{\text{evap}} = m_a(\omega_{a,e} - \omega_{a,i}) \tag{15}$$

PUE: The total power consumed by the Indirect Evaporative Cooling System is

$$P_{\text{total}} = P_{\text{Sfan}} + P_{wp} + Q_{\text{room}} \tag{16}$$

Thus,

$$PUE = \frac{P_{\text{total}}}{Q_{\text{room}}} \tag{17}$$

Cost Model: The cost model for IEC is exactly similar to that of DEC and the same set of equations will be used to do the cost analysis.

2.3.5 THE DESIGN TOOL

Now, after the general methods for thermal design of a data center that will be operating on evaporative cooling systems have been identified, developed & established and have been nicely documented in one place as a single body, it is time to put the face onto that body. The tool "ECT" stands for "Evaporative Cooling Tool" and should not be confused with "Electroconvulsive Therapy" formerly known as electroshock therapy. The tool was developed using MATLAB's "App Designer". The functionality of the tool is based on the models mentioned till last chapter. All the models were coded using MATLAB, so that the cumbersome analytical equations can be avoided, and the computation time could be reduced. The tool developed can be exported as a standalone application with a ".exe" extension and the user can install the application from the setup.

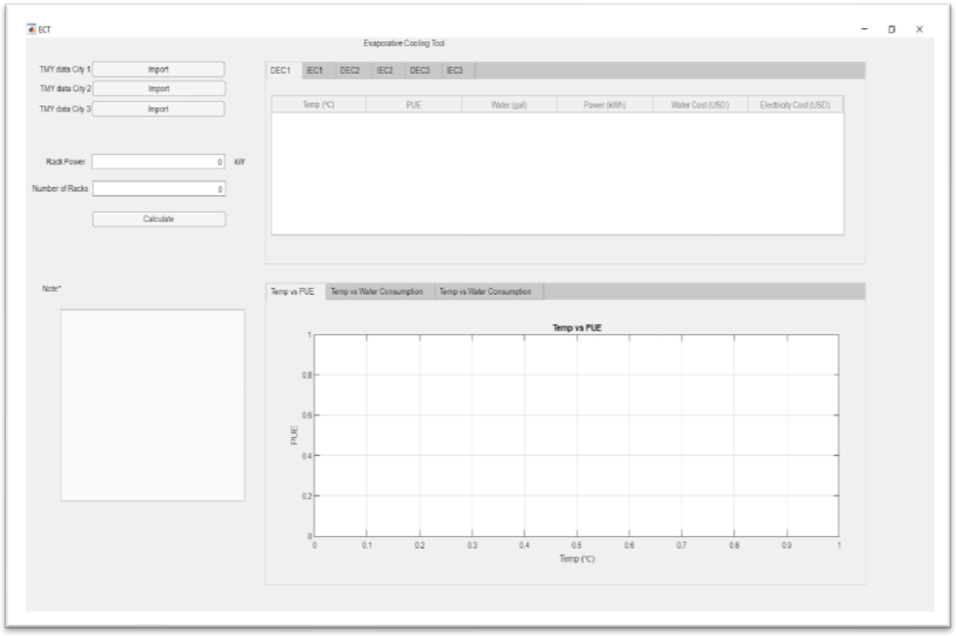

Figure 13: Tool layout- initial

Figure 13 shows how the tool looks once opened. The tool can keep up to three TMY3 dara files of an ".xlsx" format as inputs. It also gives the option for the user to input the power required for each rack and the number of racks. After hitting the calculate button, the tool does the performance and cost analysis for DEC and IEC for each city. The results are displaced in the form of tables and some comparison analyses are shown in graphs.

The text on the bottom left gives the assumptions made in the models, so that the user s aware of the data that has been considered while doing the calculations. From the results obtained, a user can make effective decisions on whether they should implement evaporative cooling system or not based on the performance and cost analysis, water, and energy consumptions as they are bound by the economical and geographical conditions.

2.3.6 RESULTS AND DISCUSSION

After the development of the tool, the models have to be validated. For this, a scenario has been considered where a customer plans to migrate to evaporative cooling. Three locations have been chosen for this

study. First is Dallas Fort Worth, which is hot and moist. Second is Portland, which has a cold and marine climate and Minneapolis has a cold and humid climate as per [27]. It is being assumed that the user will have 5 racks each of 5kW power requirement. For this case study, the IT room inlet temperatures and the temperature rise across the racks have been taken from previous experimental data performed for CRAH units by [28]. The server used in the experimental setup was 1.5 RU Open Compute Servers. The fans are assumed to be running at 100% efficiency, and 100% outside air is being used in case of DEC. Using the TMY3 data for the 3 cities and the rack inlet temperatures and the temperature rise across the rack, all the other required parameters were calculated by the tool. The performance and cost analysis for the three cities was done using the tool and comparisons on water consumptions in each area for DEC and IEC shown in graphs.

Table 1: Inlet temperature and ΔT

Rack inlet temperature **°C**	**ΔT** **°C**
15	17.5
20	17
25	17.5
30	10.75
35	7.62
40	4.85
45	4

Before the results are displayed, the TMY3 data for DFW is shown as an example to let the reader know how the TMY3 data looks like, All the unnecessary columns have been hidden.

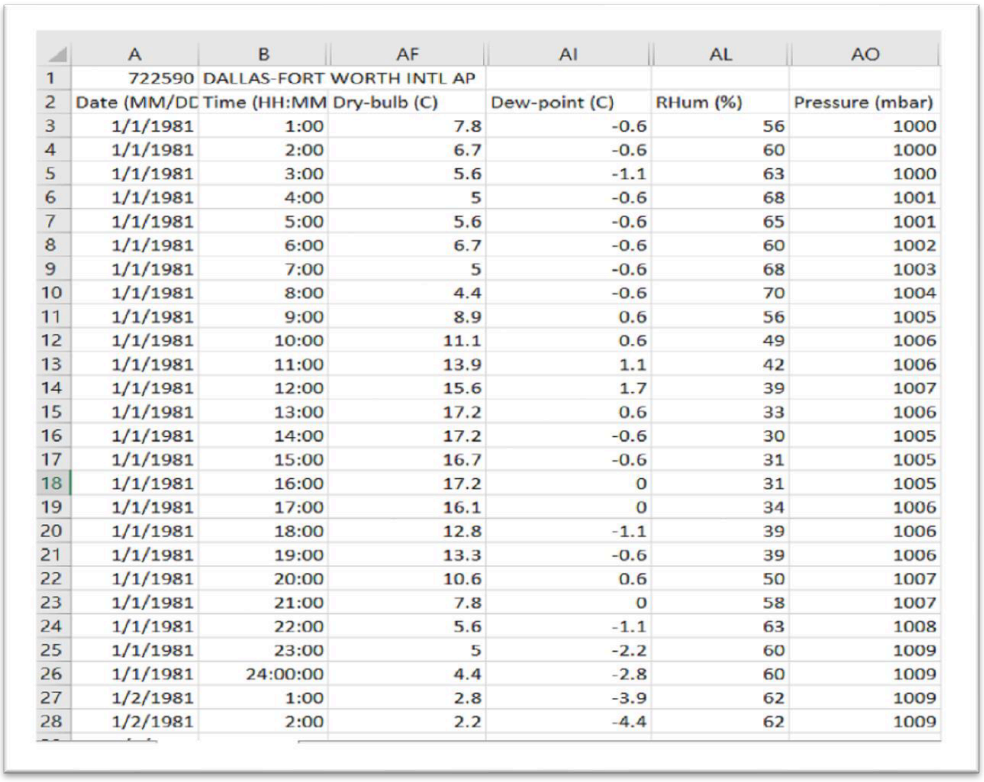

	A	B	AF	AI	AL	AO
1	722590	DALLAS-FORT WORTH INTL AP				
2	Date (MM/DD	Time (HH:MM	Dry-bulb (C)	Dew-point (C)	RHum (%)	Pressure (mbar)
3	1/1/1981	1:00	7.8	-0.6	56	1000
4	1/1/1981	2:00	6.7	-0.6	60	1000
5	1/1/1981	3:00	5.6	-1.1	63	1000
6	1/1/1981	4:00	5	-0.6	68	1001
7	1/1/1981	5:00	5.6	-0.6	65	1001
8	1/1/1981	6:00	6.7	-0.6	60	1002
9	1/1/1981	7:00	5	-0.6	68	1003
10	1/1/1981	8:00	4.4	-0.6	70	1004
11	1/1/1981	9:00	8.9	0.6	56	1005
12	1/1/1981	10:00	11.1	0.6	49	1006
13	1/1/1981	11:00	13.9	1.1	42	1006
14	1/1/1981	12:00	15.6	1.7	39	1007
15	1/1/1981	13:00	17.2	0.6	33	1006
16	1/1/1981	14:00	17.2	-0.6	30	1005
17	1/1/1981	15:00	16.7	-0.6	31	1005
18	1/1/1981	16:00	17.2	0	31	1005
19	1/1/1981	17:00	16.1	0	34	1006
20	1/1/1981	18:00	12.8	-1.1	39	1006
21	1/1/1981	19:00	13.3	-0.6	39	1006
22	1/1/1981	20:00	10.6	0.6	50	1007
23	1/1/1981	21:00	7.8	0	58	1007
24	1/1/1981	22:00	5.6	-1.1	63	1008
25	1/1/1981	23:00	5	-2.2	60	1009
26	1/1/1981	24:00:00	4.4	-2.8	60	1009
27	1/2/1981	1:00	2.8	-3.9	62	1009
28	1/2/1981	2:00	2.2	-4.4	62	1009

Figure 14: TMY3 data for Dallas Fort Worth weather station [22]

The dry bulb, relative humidity, dew point and pressure values are taken from the TMY3 data for the whole year.

Table 2: Results for DEC- DFW weather

Temp °C	PUE	Water 'gal'	Power 'kWH'	Water Cost '$'	Electricity Cost '$'
15	1.0323	48463	226060	229.14	10173
20	1.0322	47743	226060	225.91	10173

25	1.0323	49147	226070	232.21	10173
30	1.0333	83550	226290	386.33	10183
35	1.0358	119360	226840	546.74	10208
40	1.0424	167100	228290	760.63	10273
45	1.0523	208870	230460	947.78	10371

The above table shows the results as obtained in the tool for Dallas Fort Worth Area when DEC system is used for the whole year. The table shows the PUE, amount of water consumed, and the energy consumed and their respective costs. The PUE is close to 1, thereby stating that the models pretty accurate. Another major trend that must be considered is that, as the rack inlet temperature increases, the mass flow rate required to cool down the data center also increases. This leads to an increase in the energy and water consumption and their respective costs.

The table shown below is for DFW area when Indirect Evaporative Cooling is used throughout the year. This also follows a similar trend of increased power consumption with increase in the rack inlet temperatures. The water consumption remains almost the same for all rack inlet temperatures. It can be observed that the PUE in case of IEC is more than PUE of DEC, thus proving the rule of thumb that DEC is more efficient than IEC.

Table 3: Results for IEC – DFW weather station

Temp °C	**PUE**	**Water 'gal'**	**Power 'kWH'**	**Water Cost '$'**	**Electricity Cost '$'**
15	1.0329	282510	226210	127.7	10180

20	1.0329	282510	226210	127.7	10179
25	1.0329	282510	226210	127.7	10180
30	1.0340	282510	226440	127.7	10190
35	1.0365	282510	226990	127.7	10214
40	1.0431	282510	228440	127.7	10280
45	1.0530	282510	230610	127.7	10378

In the following table, a similar trend as that of Table 2 can be seen. As the rack inlet temperature increases, the water consumption and power required to cool the data center increase.

Table 4: Results for DEC - Portland

Temp °C	PUE	Water 'gal'	Power 'kWH'	Water Cost '$'	Electricity Cost '$'
15	1.0554	20740	231130	104.94	10401
20	1.0552	20432	231130	103.56	10399
25	1.0555	21033	231160	106.25	10402
30	1.0693	35756	234180	172021	10538
35	1.1024	51081	241440	240.87	10865
40	1.1904	71513	260700	332.40	11732

45	1.3224	89391	289600	412.50	13032

Table 5 shows the results for Minneapolis when Direct Evaporative Cooling is run throughout the year. The trend is again same as in case of other DEC systems.

Table 5: Results for DEC – Minneapolis

Temp ℃	PUE	Water 'gal'	Power 'kWH'	Water Cost '$'	Electricity Cost '$'
15	1.0554	22641	231130	113.45	10401
20	1.0552	22304	231100	111.95	10399
25	1.0555	22960	231160	114.89	10402
30	1.0693	39032	234180	186.89	10538
35	1.1024	55760	241440	261.83	10865
40	1.1904	78064	260700	361.75	11732
45	1.3224	97581	289600	449.19	13032

Similar trend can be observed in the other IEC systems as evident from the following table.

Table 6: Results for IEC – Minneapolis

Temp ℃	PUE	Water 'gal'	Power 'kWH'	Water Cost '$'	Electricity Cost '$'

15	1.0639	62192	233000	290.65	10485
20	1.0637	62192	232960	290.65	10483
25	1.0641	62192	233030	290.65	10486
30	1.0796	62192	236430	290.65	10639
35	1.1169	62192	244590	290.65	11007
40	1.2158	62192	266270	290.65	11982
45	1.3643	62192	298770	290.65	13445

Also, shown below are the results displayed in the tool. The tabs named DEC1, IEC1 etc. stand for DFW, Portland and Minneapolis.

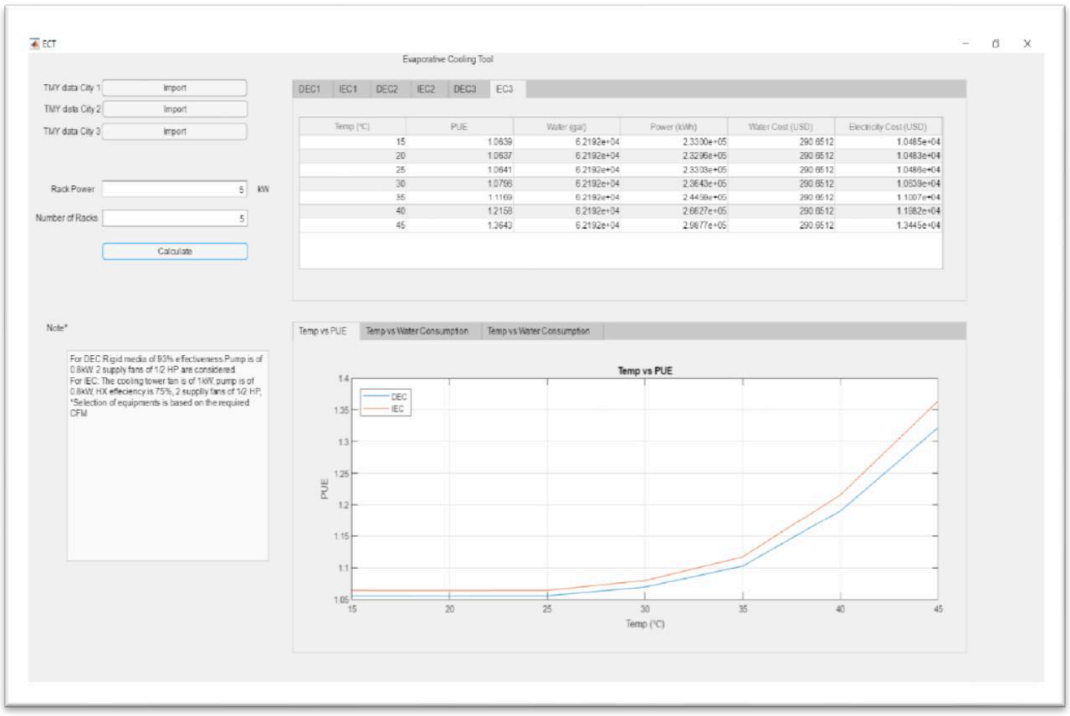

Figure 15: Results displayed in the Design Tool

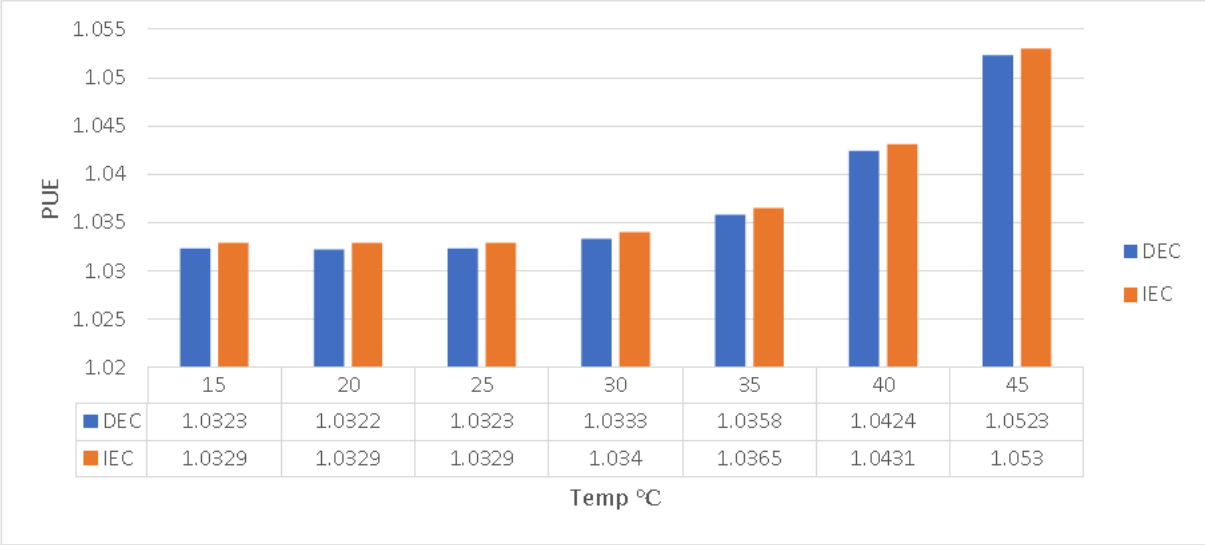

Figure 16: PUE comparison between DEC and IEC

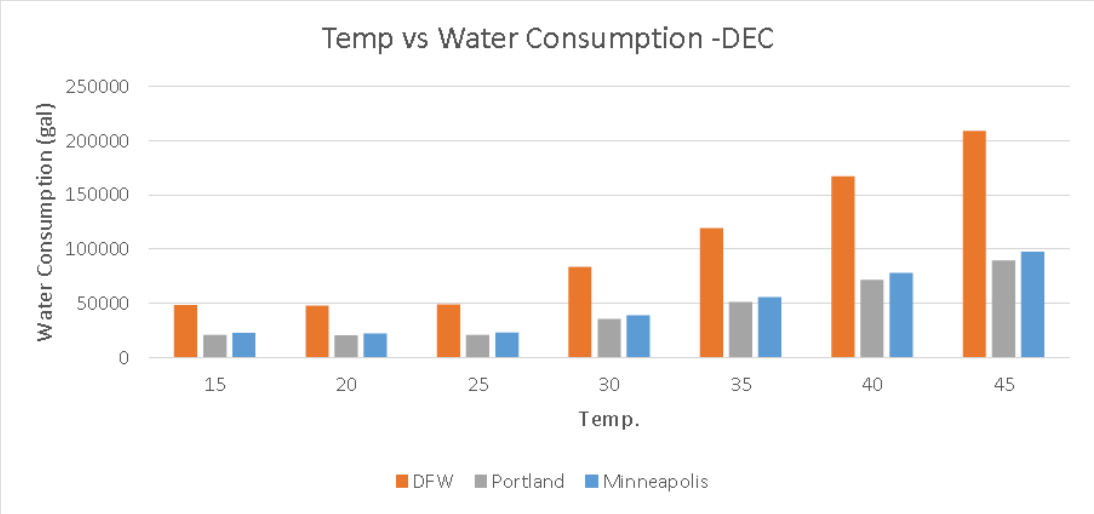

Figure 17: Comparing water consumption for DEC

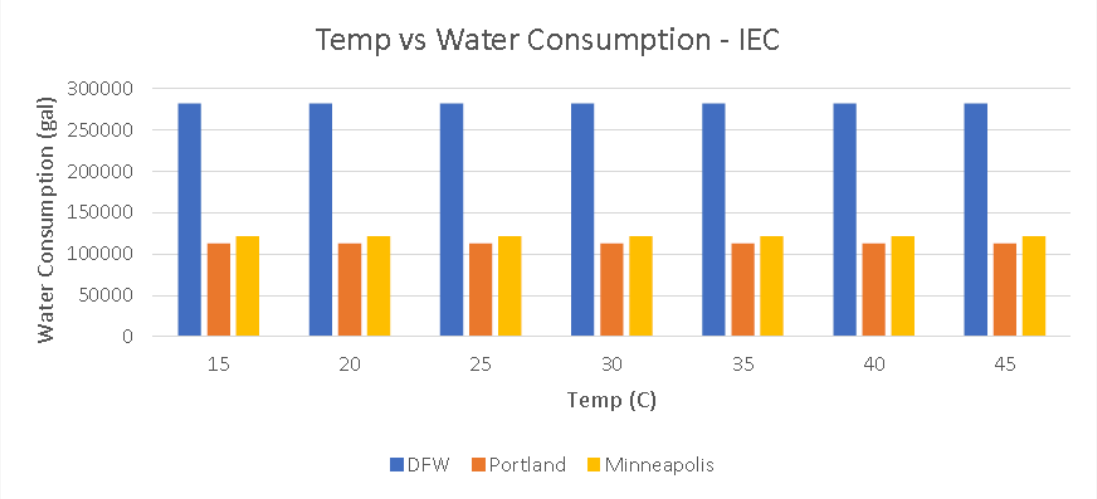

Figure 18: Comparing water consumption for IEC

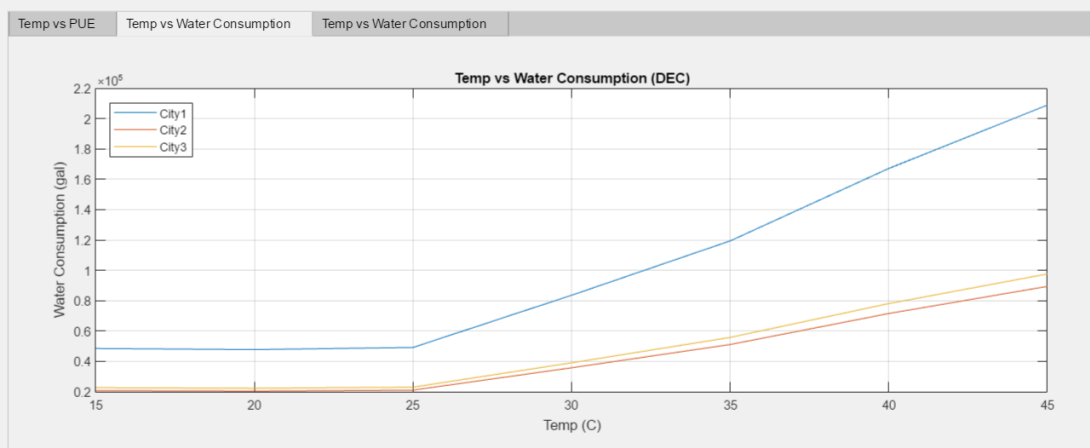

Figure 19: Temperature and water consumption – DEC

2.3.7 CONCLUSION

The general methods for the thermal design that have been identified developed and established are reliable and have been validated as shown in the results. It was observed that with increase in the inlet temperatures, the water and power consumption increased. The water consumption model developed here is complete and useful for evaluating water usage effectiveness

The tool that has been developed here is ready to be shipped as a standalone application. As observed from results, the PUE is best at 20℃ for both the cooling systems for each city. This temperature is well within the ASHRAE recommended region.

Finally, it can be concluded that the tool which is based on the established methods gives reliable results and it was observed that DEC is more efficient than IEC, which is exactly how it should be.

In the future, these methods can be improved by researching the following areas:

- Models for air flow systems cab be accounted for in the IT rooms
- Analytical models at server levels can be introduced

- Models for thermal mixing of ambient and data center return air in the evaporative air handling unit

2.3.8 REFERENCES

[1] J. Rath, "DCK Guide To Modular Data Centers: Why Modular?," 20 Oct. 2011. http://www.datacenterknowledge.com/archives/2011/10/20/dck-guide-to-modular-datacenters-why-modular/.

[2] http://e.huawei.com/en/products/network-energy/dc-facilities/ids2000.

[3] R. Gates, "Eight emerging data center trends to follow in 2016," 15 December 2015.

[4] submer, https://submer.com/what-is-immersion-cooling/.

[5] J. Sasser, "A Look at Data Center Cooling Technologies," https://journal.uptimeinstitute.com/a-look-at-data-center-cooling-technologies/.

[6] https://www.homepower.com/articles/home-efficiency/equipment-products/when-passivestrategies-arent-enough/page/0/1?v=print.

[7] ASHRAE TC 9.9, "Thermal Guidelines for Data Processing Environments–Expanded Data Center Classes and Usage Guidance," 2016.

[8] Frachtenberg et.al., "Thermal design in the open compute datacenter," 13th IEEE ITherm Conference, 2012.

[9] "Open Compute Project," http://www.opencompute.org/.

[10] Stabat et.al., "Pre-Design and Design Tools for Evaporative Cooling," ASHRAE Winter Meeting CD, Technical and Symposium Papers. 107. 643-652, 2001.

[11] Breen et.al., "From chip to cooling tower data center modeling: Part I Influence of server inlet temperature and temperature rise across cabinet," in 12th IEEE, Itherm Conference, Las Vegas, NV, 2010.

[12] Walsh et.al., "From chip to cooling tower data center modeling: Part II Influence of chip temperature control philosophy," in 12th IEEE Itehrm Conference, Las Vegas, NV, 2010.

[13] Breen et.al., "From Chip to Cooling Tower Data Center Modeling: Influence of Air-Stream Containment on Operating Efficiency," in ASME/JSME Thermal Engineering Joint Conference, Honolulu, 2011.

[14] Breen et.al., "From Chip to Cooling Tower Data Center Modeling: Chip Leakage Power and Its Impact on Cooling Infrastructure Energy Efficiency," ASME. J. Electron. Packag. , vol. 134, no. 4, 2012.

[15] Iyengar et.al., "Thermodynamics of information technology data centers," IBM Journal of Research and Development, vol. 53, no. 3, pp. 9:1-9:15, 2009.

[16] S. M. O. O. I. O. MC Ndukwu, "Mathematical Model for Direct Evaporative Space Cooling Systems," Nigerian Journal of Technology, vol. 32, no. 3, pp. 403-409, 2013.

[17] Vallejo, "ENERGY AND WATER IMPACTS OF DATA CENTER COOLING SYSTEMS: A TRIPLE BOTTOM LINE ASSESSMENT FOR FACILITY DESIGN," 2015.

[18] ASHRAE, HVAC Fundamentals Handbook, ASHRAE, 2016.

[19] B. A, "HVAC Made Easy - Overview of Psychrometrics," 2012.: https://pdhonline.com/courses/m135/m135content.pdf.

[20] "Psychrometric Processes," http://printablepsychrometric.me/201703/psychrometric-chartcooling-and-dehumidification/12/627/.

[21] I. Metzger, O. VanGeet, C. Rockenbaugh, J. Dean and C. Kurnik, "Psychrometric Bin Analysis for Alternative Cooling Strategies in Data Centers," ASHRAE Transactions, 2011.

[22] National Solar Radiation Data Base, http://rredc.nrel.gov/solar/old_data/nsrdb/1991-2005/tmy3/.

[23] http://www.kyf-aircooler.com/product/kyf-180y-industrial-portable-air-coolers.

[24] M. Vallejo, "ENERGY AND WATER IMPACTS OF DATA CENTER COOLING SYSTEMS: A TRIPLE BOTTOM LINE ASSESSMENT FOR FACILITY DESIGN," 2015.

[25] http://www.airhandlers.net/.

[26] S. Kaam, "Tom Hootman. Net zero energy design. A guide for commercial architecture. John Wiley & Sons.," 2013. https://commons.wikimedia.org/wiki/File:The_process_of_indirect_evaporative_cooling.png.

[27] http://reca-codes.org/about-iecc.php.

[28] J. E. Fernandes, "Minimizing power consumption at module, server, and rack levels within a data center through design and energy efficient operation of dynamic cooling solutions," ProQuest Dissertations and Theses, 2015.

[29] http://www.wikiwand.com/en/Evaporative_cooler.

2.4 Experimental Characterization of Vertically Split Distribution Wet- Cooling Media Used in the Direct Evaporative Cooling of Data Centers

Ahmed Al Khazraji[1], Ashwin Siddarth[1], Mullaivendhan Varadharasan[1], Abhishek Guhe[2], Dereje Agonafer[1], James Hoverson[2] and Mike Kaler[2]

[1]University of Texas at Arlington
P.O. Box 19023
Arlington, TX, United States, 76019
[2]Mestex, a Division of Mestek Inc,
4830 Transport Drive,
Dallas, TX 75247, USA

2.4.1 ABSTRACT

When operating in direct evaporative cooling (DEC) mode, the amount of moisture added to a system can be controlled by frequently modulating water supply to the wet cooling media. Though many challenges arise due to geographical and site conditions, this concept can be applied to data centers to serve as a cost-effective alternative for maintaining the operating temperature of the facility at any weather condition. However, this method results in scale and mineral build up on the media because of an irregular water distribution. To prevent the scale formation, the operators allow the water supply continuously on the cooling media ultimately leading towards the high consumption of facility water and significantly deteriorating the Wet cooling media life. This challenge has been addressed for the first time by experimentally characterizing the vertically split distribution wet cooling media. These systems allow some section of the media to be wetted while other sections remain dry. Various configuration of vertically staged media may be achieved by dividing the full width of the media into two, three, four or more number of equal and unequal sections and providing individually controlled water distribution headers. To increase the number of stages and provide smooth transition from one stage to the other, a MATLAB code is written to find width of DEC media sections for known total width of the media and number of sections. Here, an experimental design to characterize the performance characteristics of a vertically split wet cooling media which has separate water distribution setup has been presented. Apart from relative humidity and temperature, other parameters of interests like pressure drop across the media and saturation efficiency of the rigid media are

presented. In the unequal configuration, the media was tested for 0%, 33%, 66%, and 100%. This research provides a potential solution towards the limitation of direct evaporative cooling in terms of energy savings, facility water, reliability, and contaminants.

2.4.2 Introduction

Evaporative cooling process remains one of the least expensive techniques which provides an optimum cooling with minimum energy usage [1 , 2] especially, in data centers, where the information technology (IT) equipment such as servers and network switches are housed. All these equipment and other necessary electronic units consume large electricity power and dissipates heat energy at the same time [1 , 3] . In data center, cooling requirement changes according to the IT load and outside environment (e.g. diurnal and seasonal changes). Also, IT and electronic components must be maintained at certain temperature and humidity so that they operate reliably for their expected lifetime.

Data center equipment are surrounded by air that contains a combination of gasses which include nitrogen (78%), oxygen (21%), carbon dioxide (0.3%), and water vapor. The water vapor in air is known as humidity, and this water vapor needs to be maintained in a proper amount in the air surrounding IT equipment so that the IT equipment can be protected from dangerous static electrical discharge. Also, too much or too little amount of vapor can be harmful to the internal electronic components and lead to failure and downtime [4] . To overcome the challenge of excess humidification, the technique called as staging of DEC media has been proposed through this research, where the DEC media is divided into multiple vertical sections or staking two or more sections together by providing separate water distribution headers to control each section. This staging of DEC media provides incremental control over humidity and temperature and enables reduction of electricity and water consumption [5] . In this experimental study, the wet cooling media has been given a vertical split into two unequal sections and tested for 0%, 33.3%, 66.7% and 100% wetting stages at any given time. These types of

wetting stages have been tested and investigated for incremental effect on relative humidity (RH) as well as temperature of discharge air.

2.4.3 EXPERIMENTAL SETUP

The experimental set up consists of an air-flow bench, Variable Exhaust System (Blower), and the test duct for the evaporative cooling test (Figure 1). Air-flow bench is a device which can be used for testing the thermal resistance of the test sample, testing for fan performance curve and to calculate the airflow rate. It consists of a blast-gate that controls the opening and closing of the chamber for air entry, flow straighteners to channelize the air flow path and nozzles with different diameter sizes to achieve the desired flow rate (Figure 2).

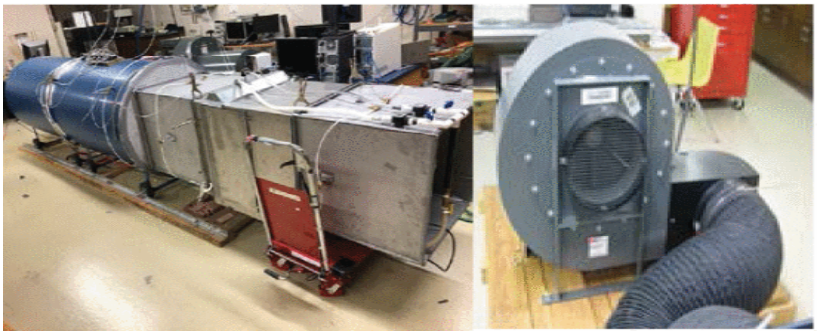

Figure 1: The air-flow bench and the air blower

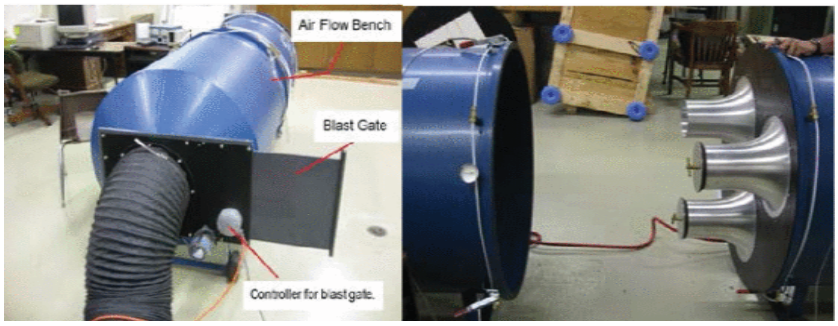

Figure 2: Blast gate and the nozzle plate

The DEC pad is sitting inside the middle zone of the test duct. The duct was initially modeled in modeling software, PRO-E and then fabricated for the experimental testing. The three duct segments were 0.6m X 0.6m in dimensions and 1.8m long. It was attached to the downstream end of the airflow bench with the cooling pad fitted approximately 0.7m away from the downstream [1] .

Eight Dwyer A-302F-A pressure taps were fitted on the upstream and downstream ends of the duct to measure the static pressure across the DEC media. Eighteen RF Code R155 humidity-temperature tags were mounted such that one tag covers one-ninth of the cross-sectional area of the duct on two plastic egg crates light diffusers where the sensors were placed at 24 inches before and after the wet cooling media to measure the RH and Temperature for the inlet and outlet (Figure 3).

Figure 3: RF Code R115 Humidity-Temperature Sensors

The middle section of the duct is shown in figure 5 where the DEC media, water reservoir, water pump, water, distribution header, and water level regulator are placed (Figure 4).

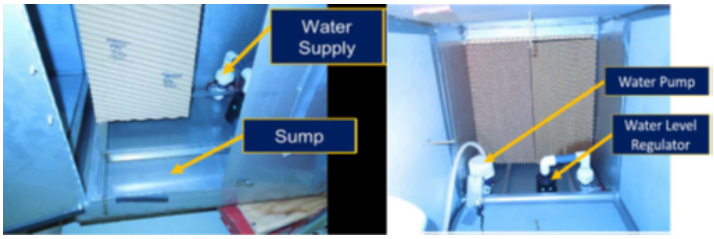

Figure 4: Water level regulators, water pump, and the sump downstream of the duct

Figure 5: Digital water flow meter on each water supply and Fantech Dehumidifier

To prevent the air and water leaks during the test, duct tapes and water-resistant foams (R-Matte-rigid insulating water-resistant material) were used (Figure 6).

2.4.4 TEST PROCEDURE AND RESULTS

KUUL 12'' cellulose DEC media was partitioned into two un-equal sections 33.3% and 66.6% and tested for four wetting stages. Figure 7 and Table 1 show the splitting and the water pumping state of the staging of the DEC media.

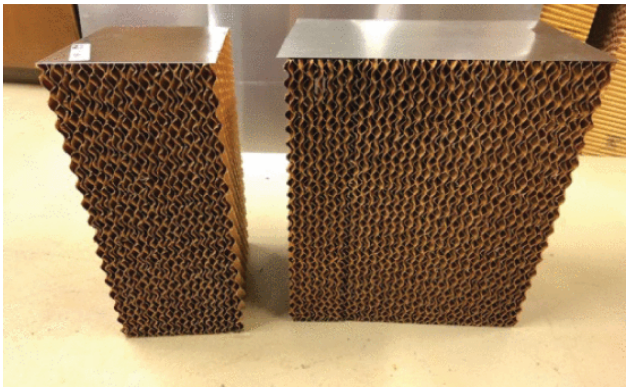

Figure 7: The un-equal splitting of DEC media

Table 1: Two Sectioned Media Showing Pump On/Off State [3]

Stage	Section width (1 = on & 0=OFF)		% of media that's wet
	8 inch	16 inch	
1	0	0	0
2	1	0	33.3
3	0	1	66.7
4	1	1	100

The two sections of the DEC media were tightly kept inside the middle segment of the duct with water distribution taps on the top of each section and was split by aluminum metal sheet to prevent the water crossing from the wet section to the dry section during the test. The two sections of the DEC media were supplied water by separate water distribution headers and all possible gaps were tightly sealed (Figure 8).

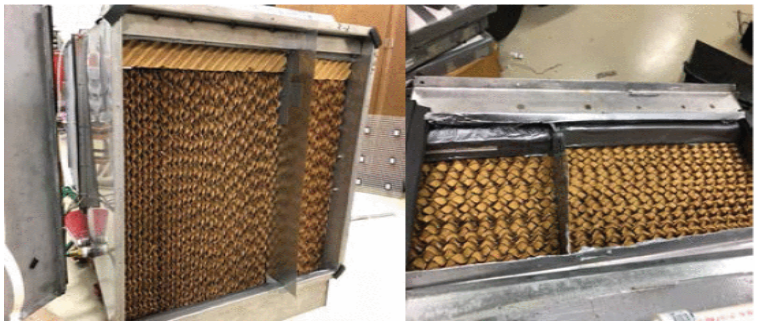

Figure 8: Side and Top view of the DEC pad fitted inside the middle duct

2.4.4.1 Stage one of the tests:

In the stage the DEC media was tested with 0% wet which is a dry test, the test was conducted under room temperature 73 F and varying air velocity starting from 613 FPM to 233 FPM to calculate the pressure drop across the DEC media. It has been observed that at 613 FPM the pressure drop across the DEC media was about 0.25 Inch of H_2O. Comparing with the manufacturer data for the same FPM air velocity, the pressure drop was found about 0.24 in of H_2O. This proves that the results are in good agreement with the manufacturer data [1]. (Figure 9)

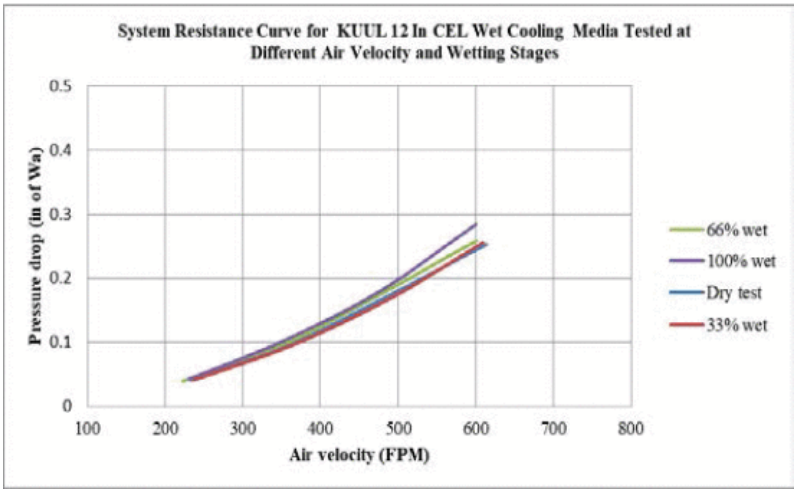

Figure 9: Pressure drop curve for KUUL 12in cellulose at different air velocity and wetting stages

2.4.4.2 Stage two of the tests:

The second stage of the test was for 33% wet DEC media; the test was conducted at higher inlet temperature (Figure 10). To achieve the high upstream air temperature, two ProFusion Heat Industrial Fan-Forced Heaters (Model HA22-48M) (Figure 11) were placed at the inlet of the airflow bench blower. And the water flow rate was kept constant during the test (1gpm). In this wetting stage, the variation of RH, temperature and Pressure drop across the DEC media were tested. Pressure drop was found about 0.2554 inH^2O at 609 FPM and 91° F. (Figure 9).

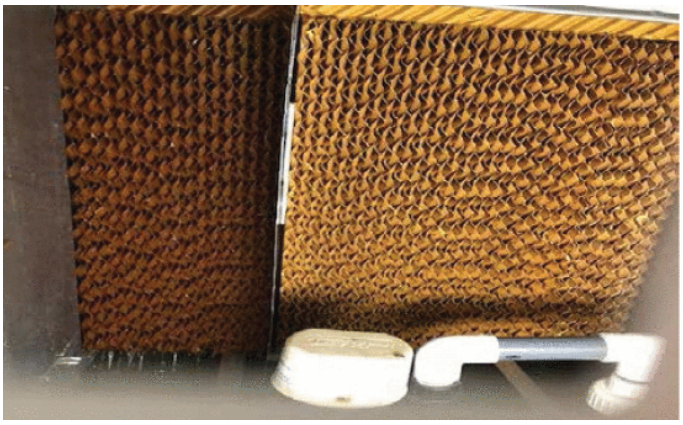

Figure 10: Showing 33% of the cooling media under test

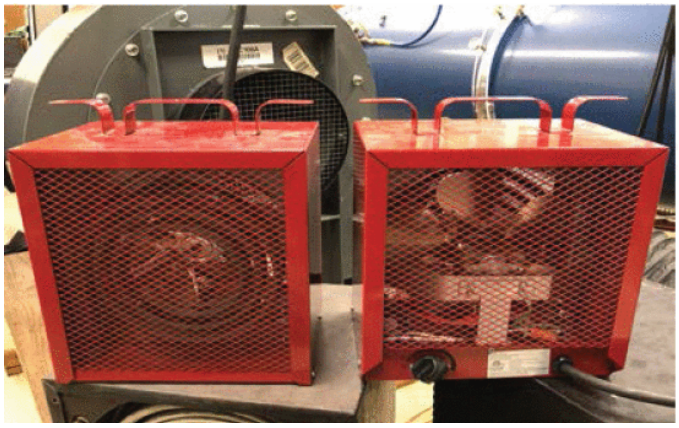

Figure 11: ProFusion Heaters

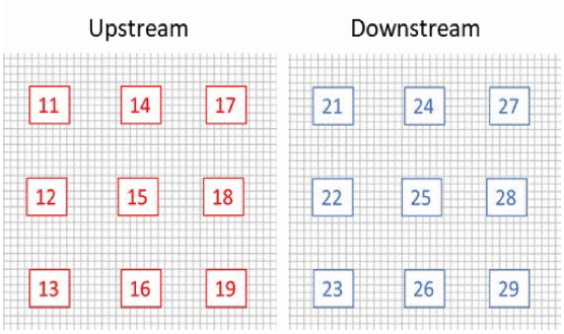

Figure 12: Location of upstream and downstream temperature and relative humidity sensors with respective sensor ID numbers

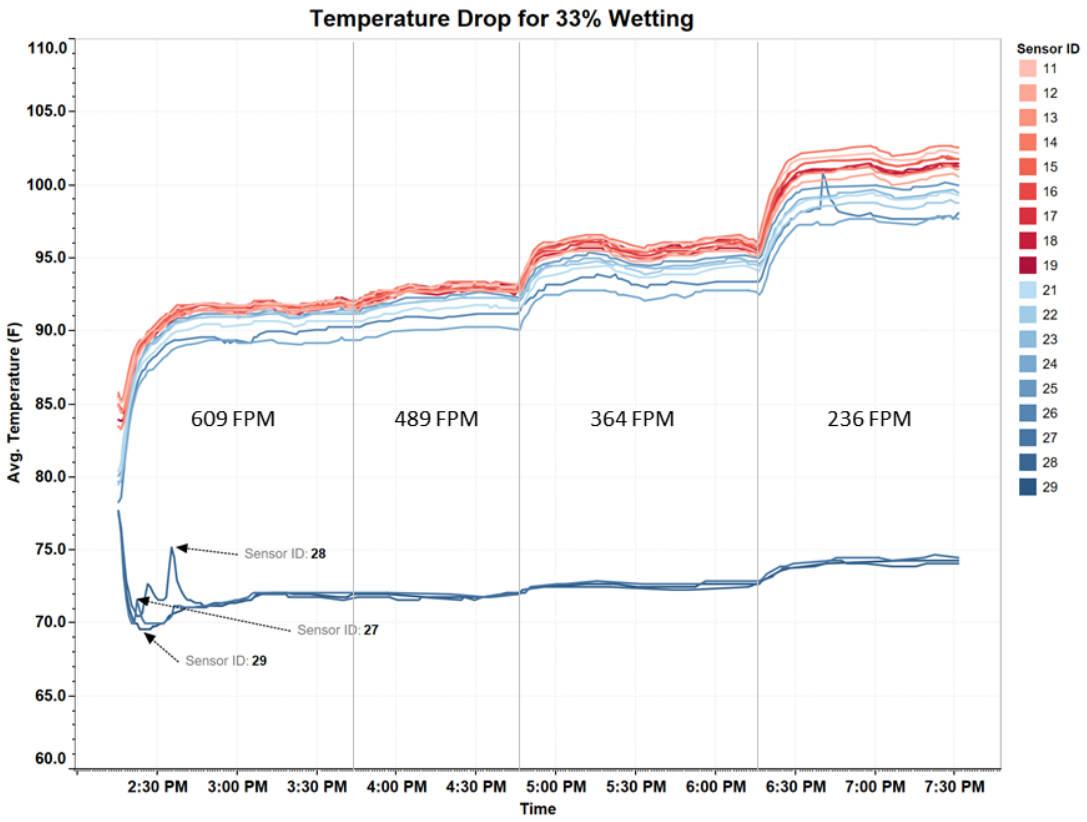

Figure 13: Upstream and downstream temperature during 33% wetting for different face velocities of inlet air

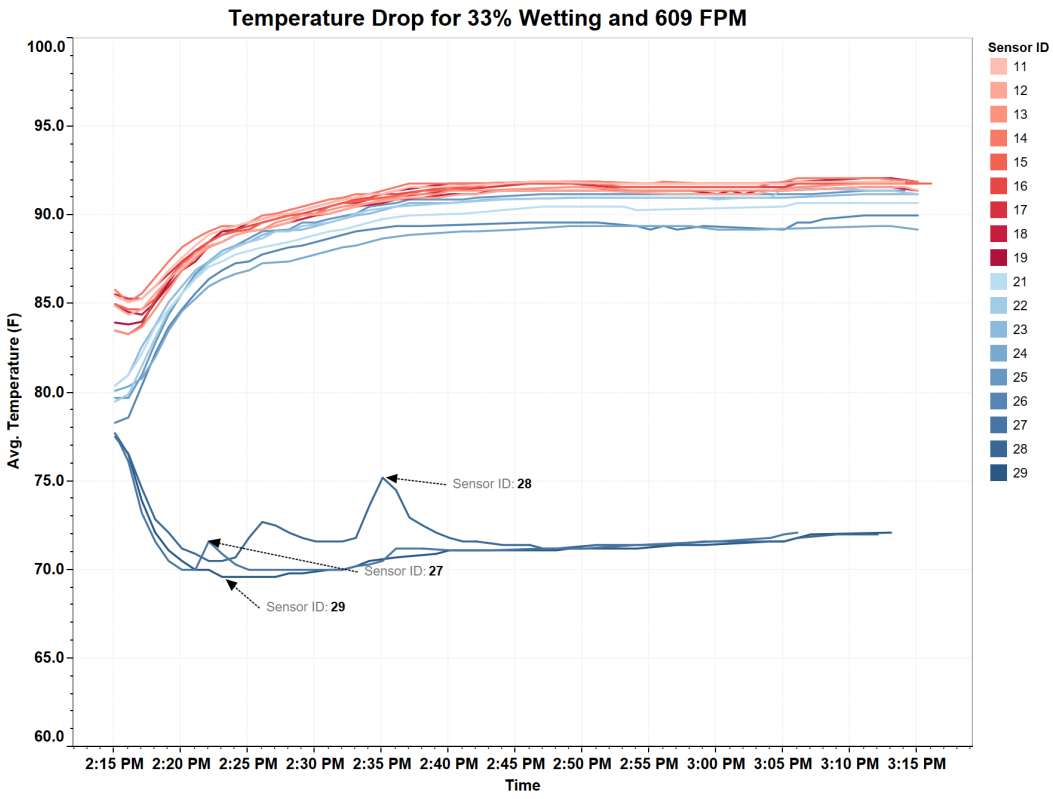

Figure 14: Temperature drop across the 33% wet media pad with 609 FPM inlet air face velocity

Figure 13 shows the temperature variations of the RF code sensors upstream and downstream with different air velocities starting from 609 FPM till 236 FPM for 33% wet media test to calculate the pressure drop across the wet cooling media. Figure 14 shows the readings of each sensors during 609 FPM, it was observed that the downstream temperature sensors readings for the wet side (27, 28, and 29) were decreased all way till 68°F from 77 °F and it took about 30 minutes until reached the steady stated of 72 F°. While the other 6 sensors for the downstream dry side (21, 22,23,24,25, and 26) went all way up with the upstream sensors. The upstream temperature rose all way up to 92°F from 84°F.

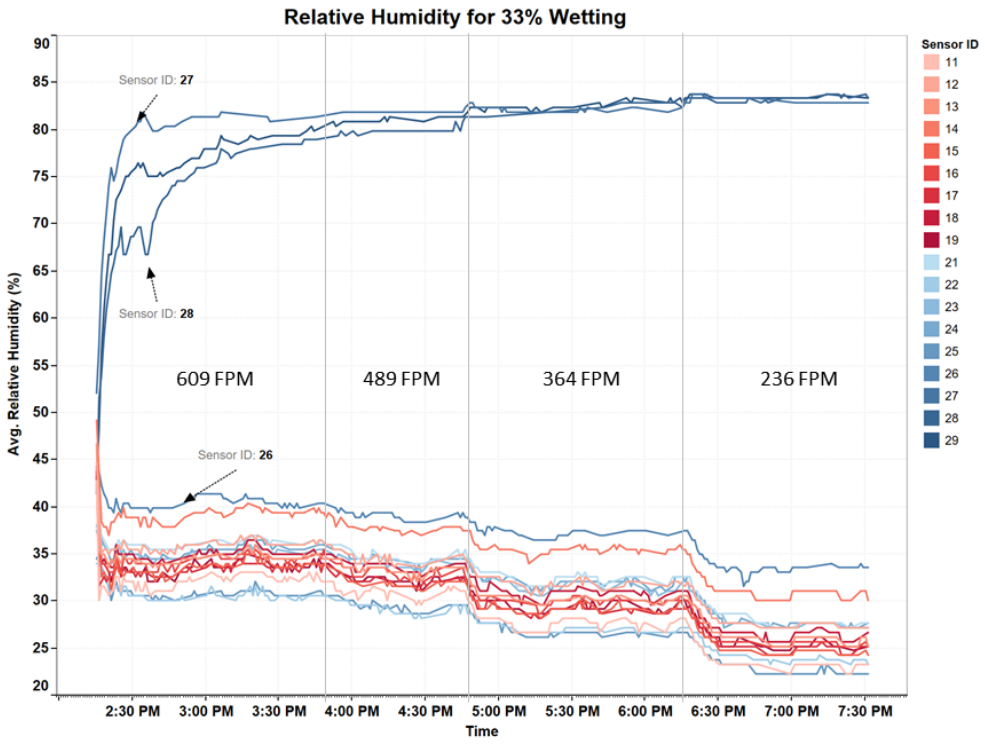

Figure 15: Upstream and downstream RH during 33% wetting for different face velocities of inlet air

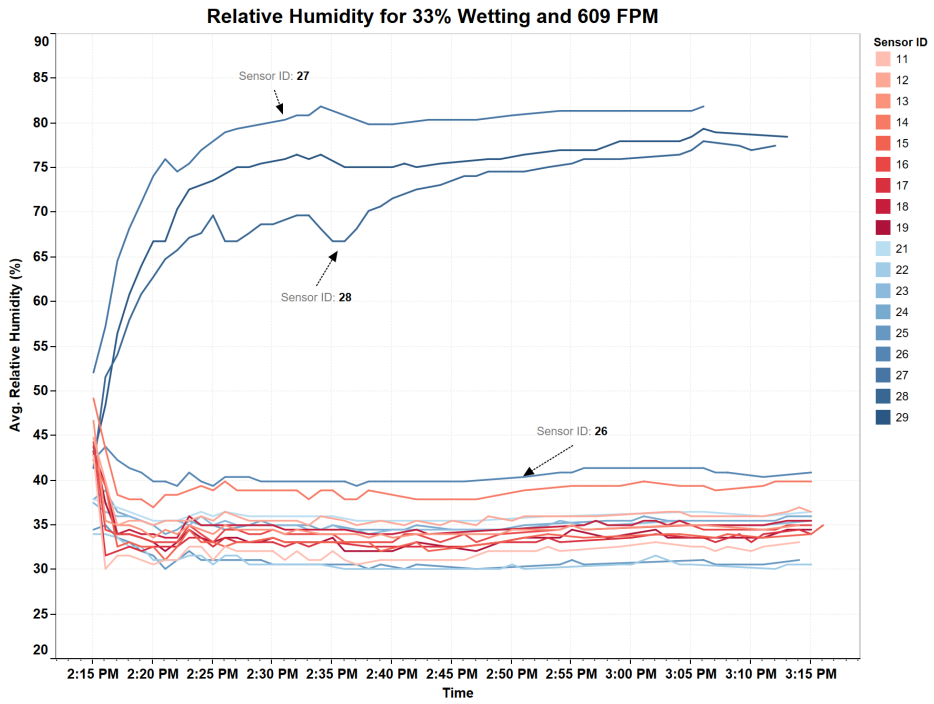

Figure 16: Relative Humidity variation across the 33% wet media pad with 609 FPM inlet air face velocity

Figure 15 shows the variation in RH between downstream and upstream with different air velocity whereas Figure 16 shows the RH readings of each sensors during 609 FPM. It was observed that the RH for the downstream wet side sensors went all way up to 82 % from 42 %, and the sensors for the dry side were decreased with upstream sensors to 30% - 40% during a constant air velocity of 609 FPM.

2.4.4.3 Third stage of the tests:

the third stage was for 66% wet of DEC media, where the 33% part kept fully dry, and the 66% part was fully wet.

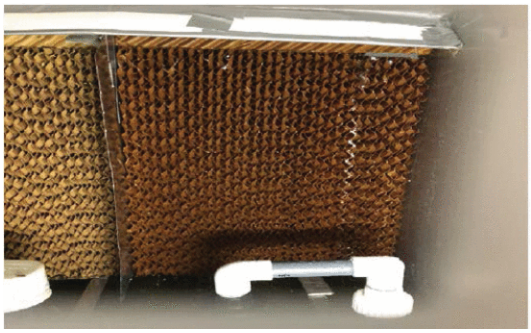

Figure 17: Showing 66% DEC Cooling Media Under Test

The test was carried out at higher inlet air temperature 90°F by operating both the heater with varying air velocity from 601 FPM to 222 FPM to calculate the pressure drop during the wetting test. The pressure drop was found about 0.258 inch of H_2O at 601 FPM. (Figure 9).

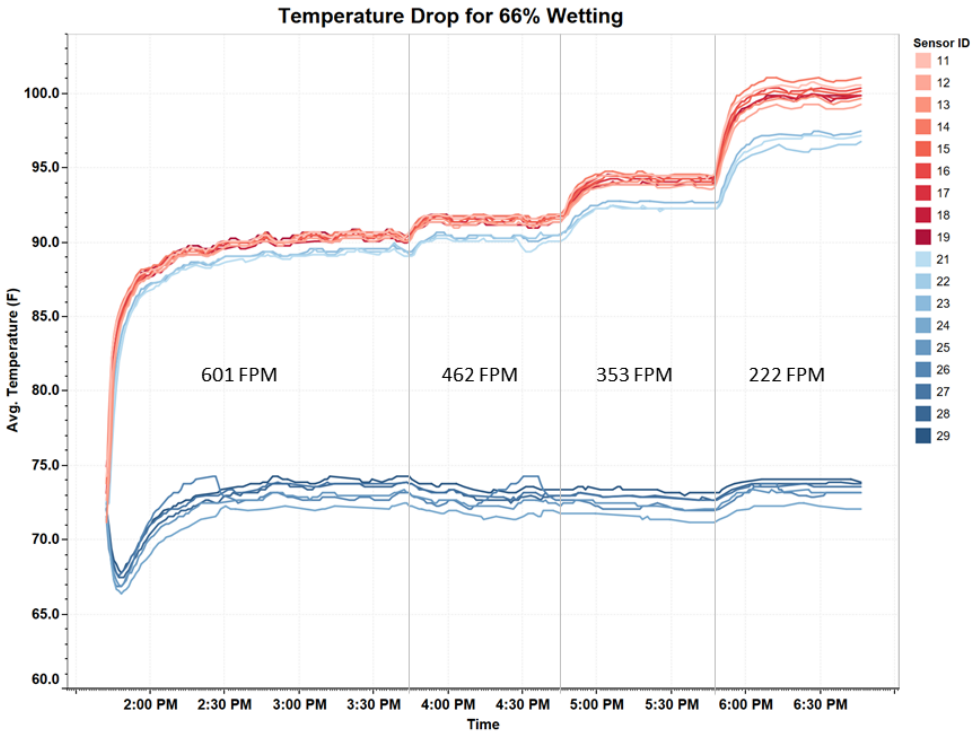

Figure 18: Upstream and downstream temperature during 66% wetting for different face velocities of inlet air

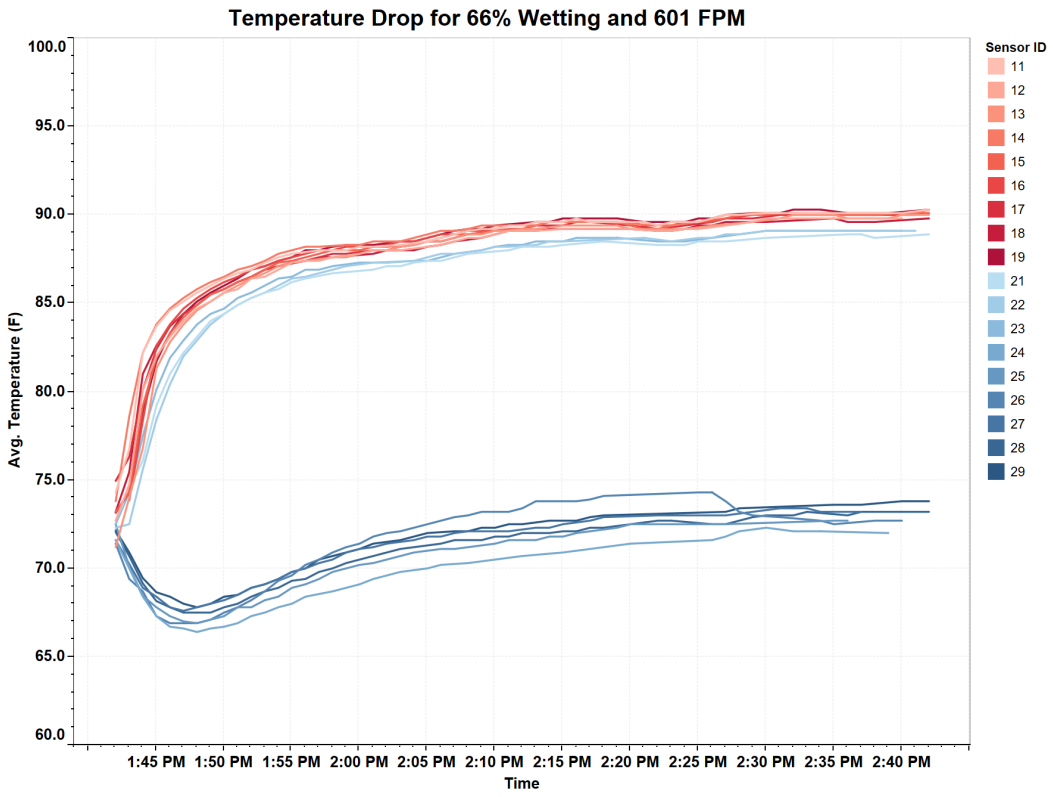

Figure 19: Temperature drop across the 66 % wet media pad with 601 FPM inlet air face velocity.

Figure 18 shows the temperature variation during the test. It was observed that the upstream temperature rose all way up to 100 °F from 72 °F while the downstream temperature increased from 65 °F and remain about 70 °F during different air velocity. Figure 19 shows the temperature readings of each sensors during 601 FPM. It was observed that the downstream temperature sensors readings for the wet side (24, 25, 26, 27, 28, and 29) were decreased all way till 66°F from 72 °F and it took about 50 minutes until reached the steady stated of 72 F°. While the other 3 sensors for the downstream dry side (21, 22, 23, and 24) went all way up with the upstream sensors. The upstream temperature rose all way up to 90°F from 75°F.

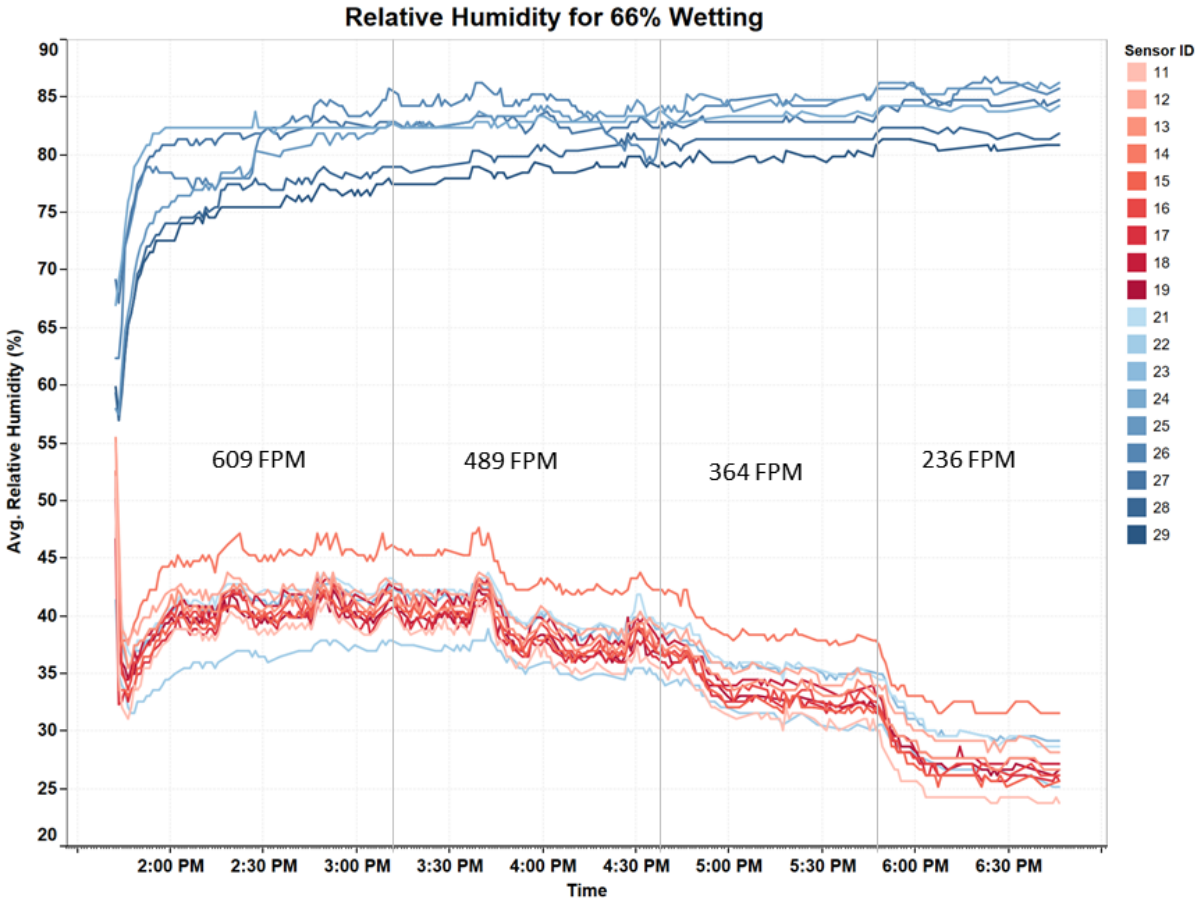

Figure 20: Upstream and downstream RH during 66% wetting for different face velocities of inlet air

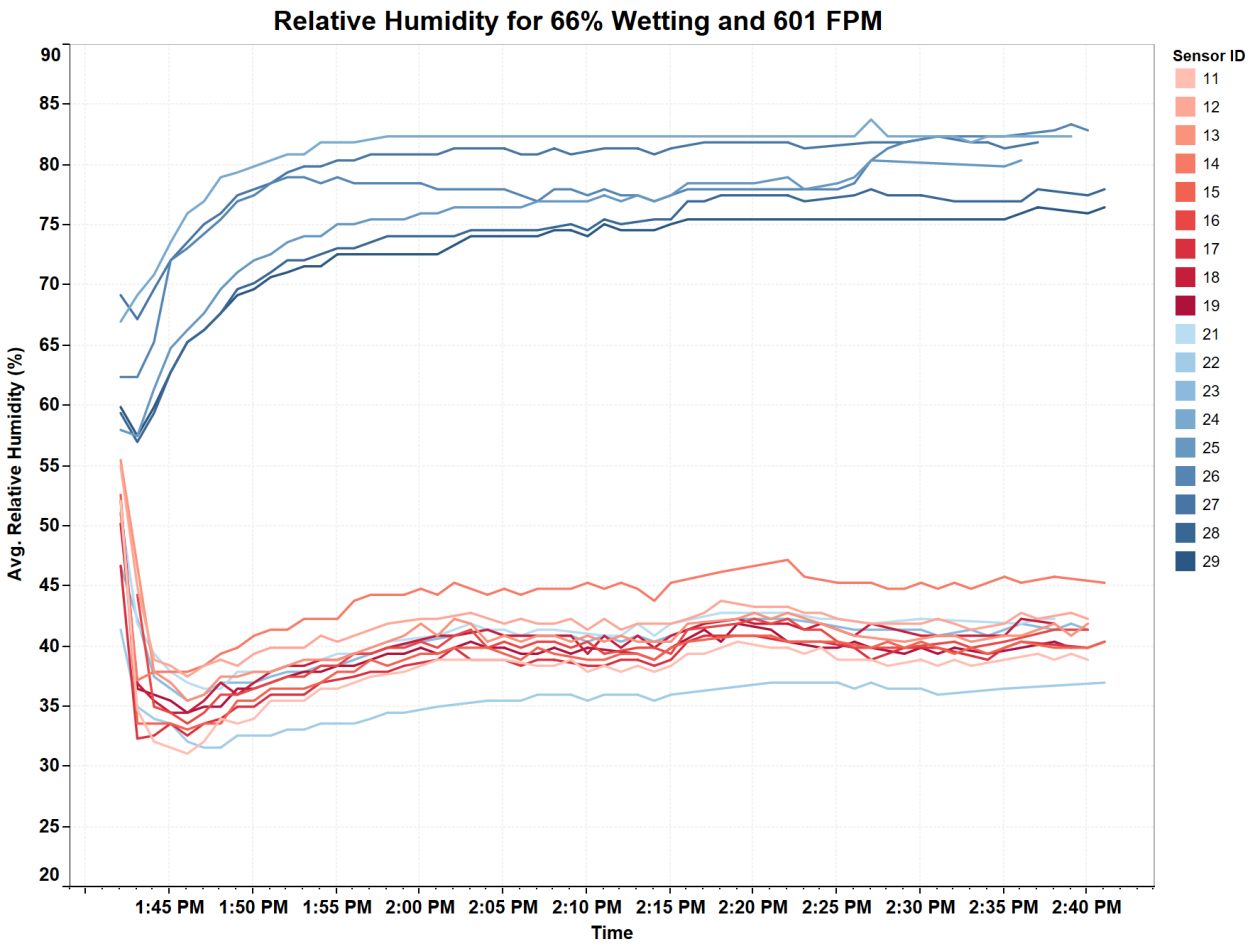

Figure 21: Relative Humidity variation across the 66 % wet media pad with 601 FPM inlet air face velocity

Figure 20 shows the variation in the RH between Downstream and upstream during different air velocity. In figure 21 shows the RH readings of each sensors during 601 FPM, it was observed that the RF code sensors for RH of the wet side downstream went all way up between 74% – 84% from 58%, while the sensors on the dry side downstream remain below 40%. The upstream RH rose from 35 % and remains about 42% during the initial air velocity 601FPM as shown in Figure 21.

2.4.4.4 Fourth stage of the tests:

In this stage, both sections of the DEC media tested as 100% wet. The test was carried out with both heaters on to achieve the higher inlet temperature and varying air velocity start from 600 FPM to 231 FPM to calculate the pressure drop for the wet DEC media. The pressure drop was found 0.28 in of H_2O (Figure 9).

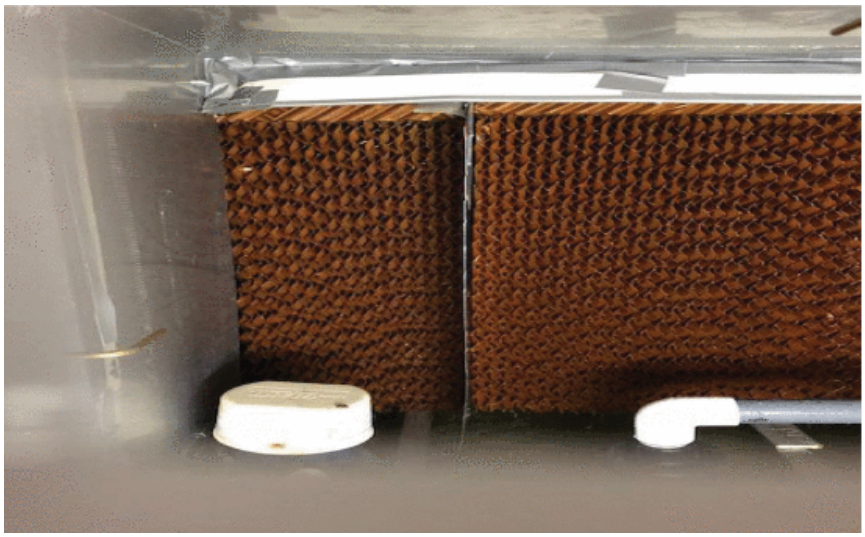

Figure 22: showing the 100% wet DEC media under test

Figure 19 shows the temperature variations of the RF code sensors upstream and downstream with different air velocity. It was observed that the upstream temperature rose all the way up to 102°F from 73°F. The downstream temperature readings decreased from 78°F to 70 and it took about 30 minutes to reach the steady state of 73 and remains constant during with different air velocity.

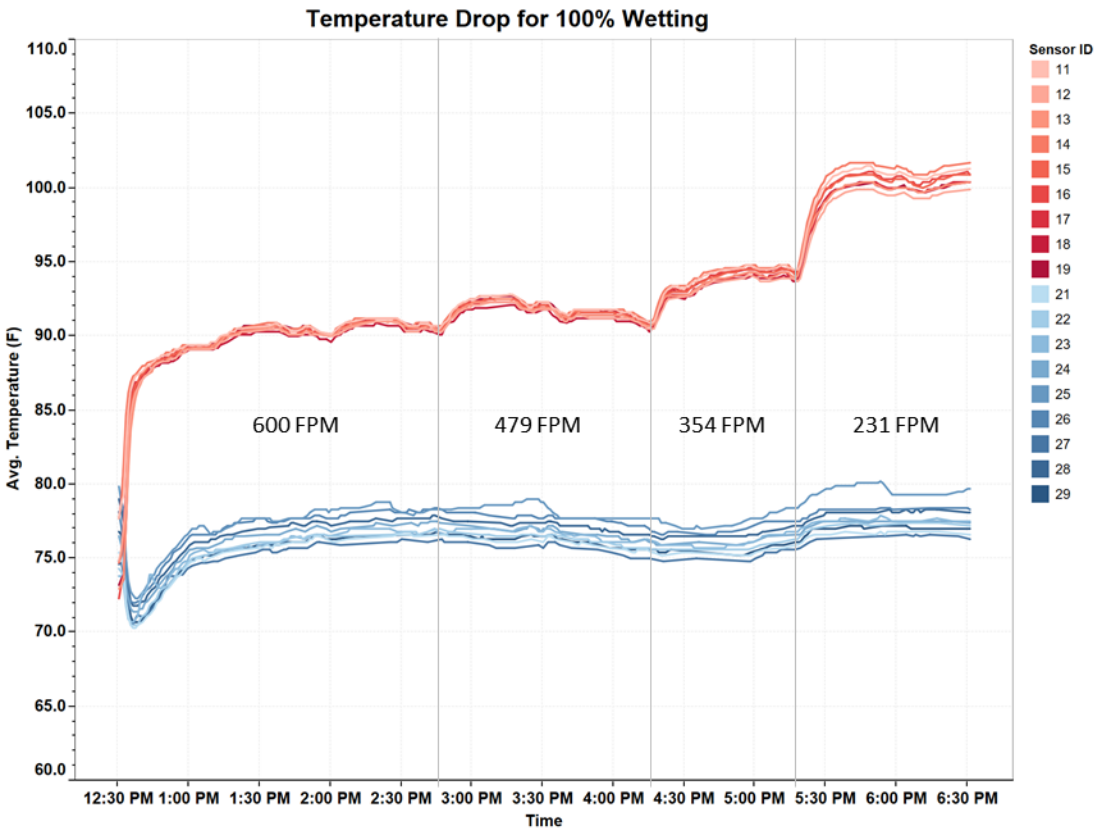

Figure 23: Upstream and downstream temperature during 100% wetting for different face velocities of inlet air

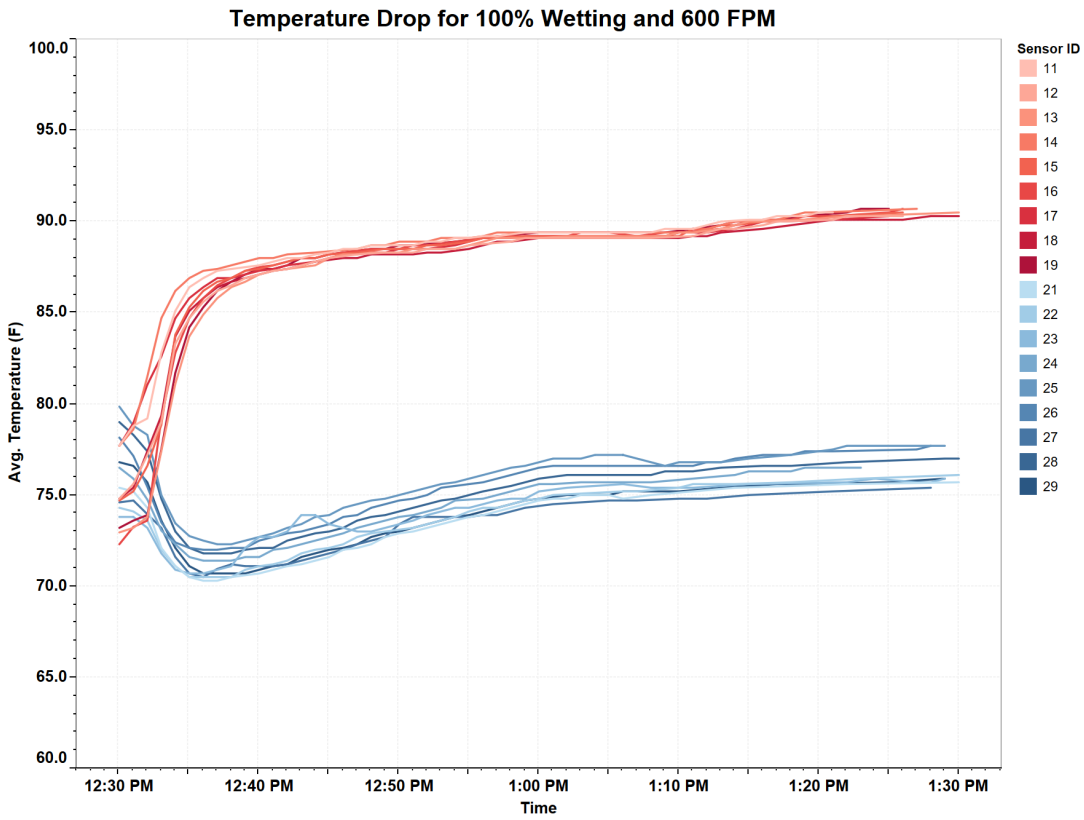

Figure 24: Temperature drop across the 100 % wet media pad with 600 FPM inlet air face velocity.

The below figure shows the humidity variations of the RF code sensors upstream and downstream during the 100% wet media testing. It was observed that the downstream humidity went all way up between 70% - 82% from 55%. The upstream humidity readings increased from 40% to 48 % during the wetting phase (constant air velocity) and then decreased back to 30% for the varying air velocity test.

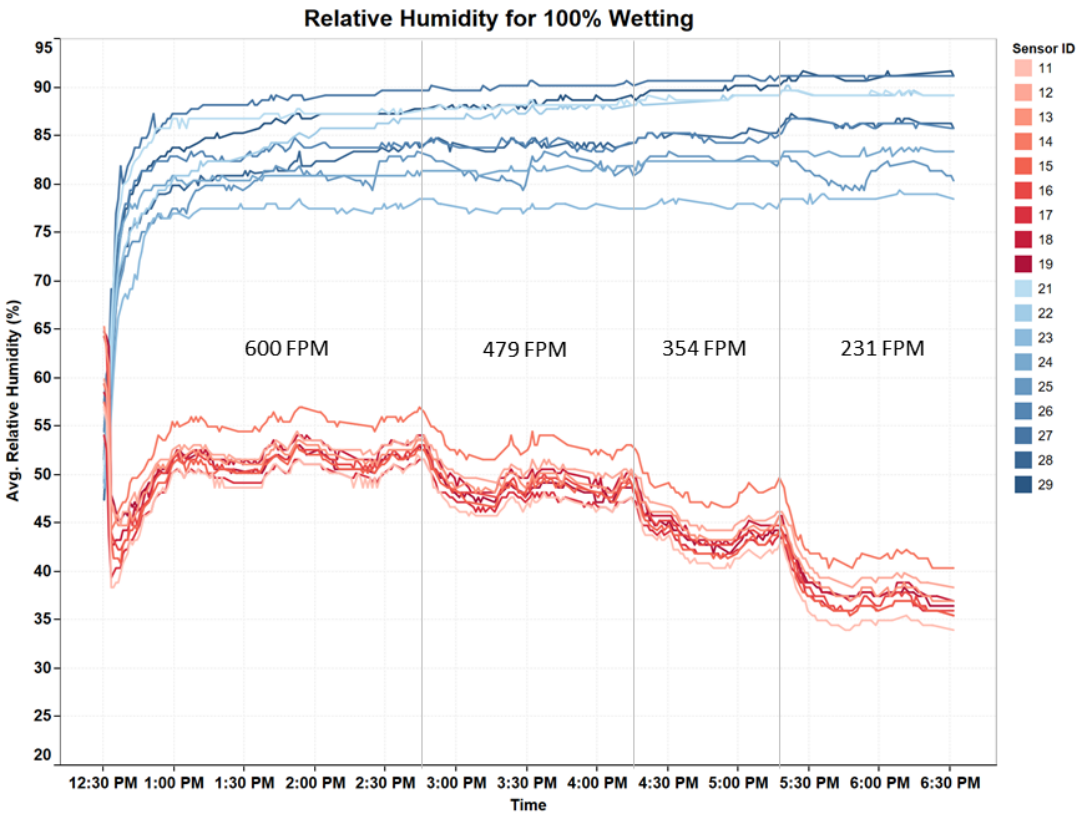

Figure 25: Upstream and downstream RH during 100% wetting for different face velocities of inlet air

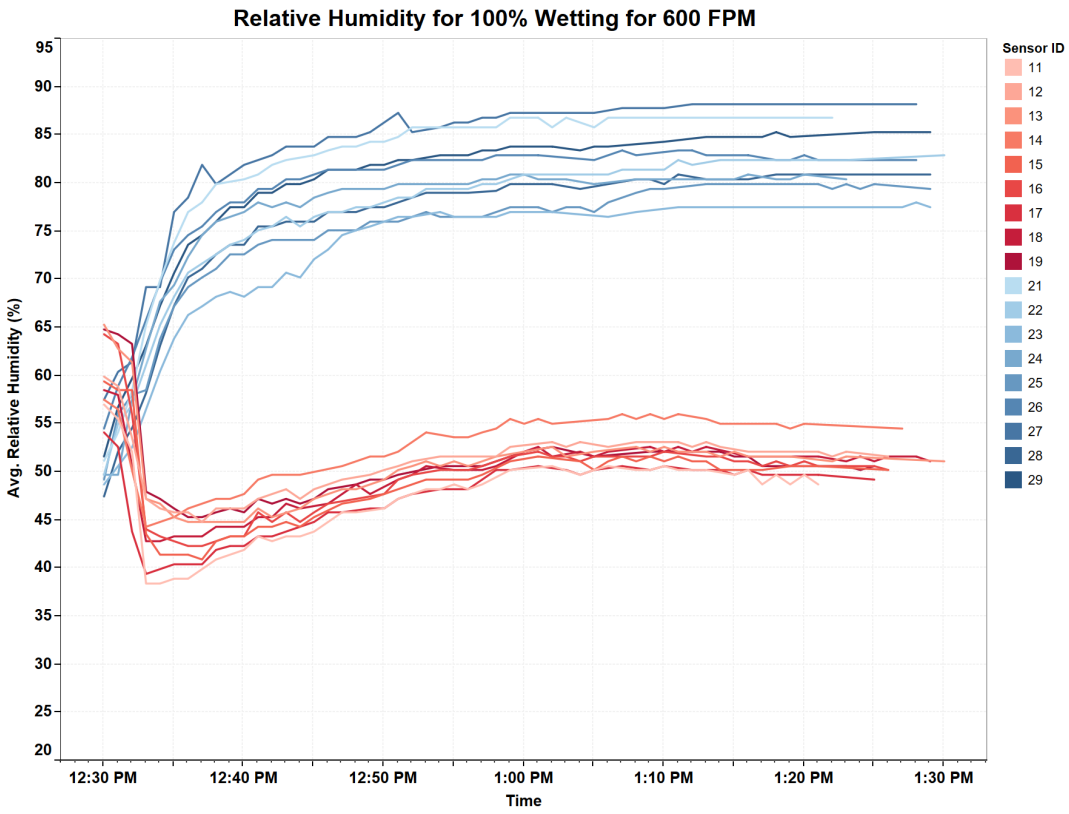

Figure 26: Relative Humidity variation across the 100 % wet media pad with 600 FPM inlet air face velocity

2.4.5 THEORETICAL ANALYSIS: ADIABATIC MIXING OF AIR STREAM

The staging of DEC media has a simple configuration (Fig.27a and 27b) where downstream air leaving the staged DEC media has different temperature and humidity (ssaturated air and dry air). At adiabatic saturation conditions [7] , the saturated air leaving the wet section can be mixed adiabatically with the dry air that leaving the dry section.

The properties such as (h, ω and *v*) of each section can be determined from the psychometric chart depending on the experimental results of the downstream temperature and relative humidity of each section.

As we know, this is a steady- flow mixing, so the mass flow rate ($\dot{m}$) in each stream are:

Energy and Mass conservation:

(V_1, V_2) are known in the experiment as flow rate (FPM).

And

(v_1,v_2) are a Specific volume (m^3/ kg dry air). From the psychometric chart.

The enthalpy and the specific humidity of the mixture can be determined from below Eq. (3, 4)

Now from these two properties, we can determine the temperature and relative humidity of the mixed air from the psychometric chart (See figure 28).

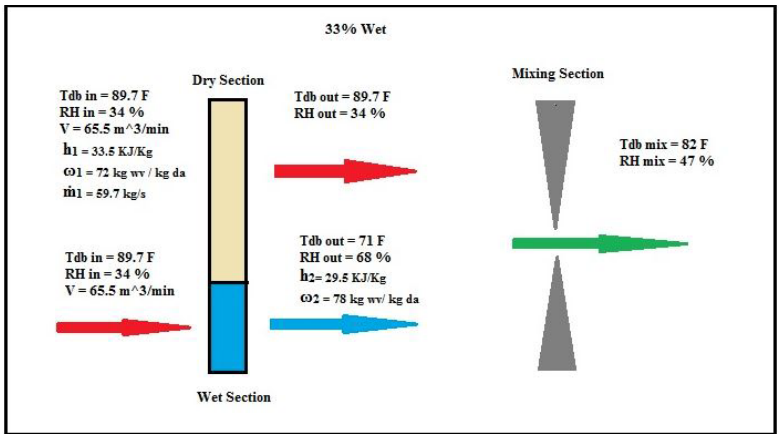

Figure 27a: 33% wet section of the DEC media

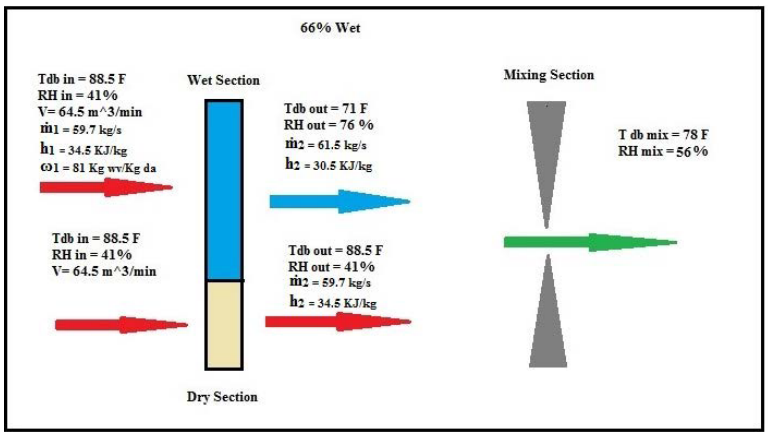

Figure 27b: 66% wet section of the DEC media

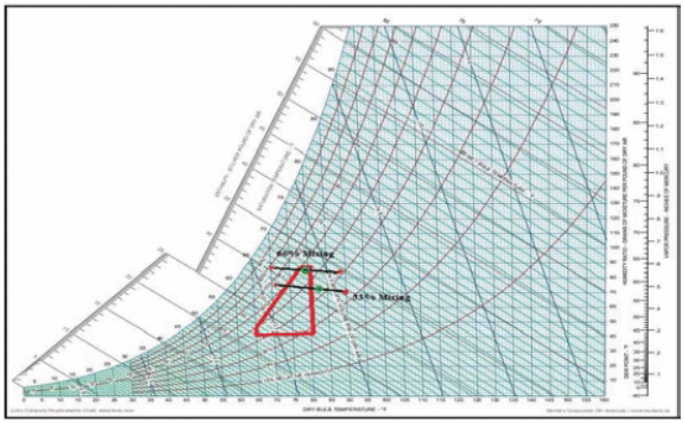

Figure 28: Psychrometric chart shows the mixing results of 33% and 66% wet

2.4.6 CONCLUSION

The vertically staging of DEC media has been successfully tested experimentally. The change in relative humidity and the temperature drop has been carefully reviewed and interesting results are found experimentally and theoretically by using the psychometric chart and adiabatic saturation equations. While operating the two unequal stage with similar assumed conditions these two stages can be turned on /off with mixing both the streams of air and bringing the mixed air inside the ASHRAE recommended and allowable envelops for both 66% and 33% wet running stages. The comparison of two configurations showed the un-equal configuration has better control on relative humidity than the single stage configuration. This clearly shows when the vertical split configuration is implemented for any number of staging, it would be beneficial, if the sections are un-equal.

This control on relative humidity and temperature greatly helps the data center environment to be run inside the ASHRAE's allowable range of relative humidity and temperature upon implementing the vertical split distribution system. This ultimately increases the reliability of the IT equipment and minimizes the cost associated with it. It also helps saving water utilization and power consumption.

2.4.7 Acknowledgement

This work is supported by NSF IUCRC Award No. IIP-1738811.

2.4.8 References

[1] V. Sreeram, Factors Affecting the Performance Characteristics of Wet Cooling Pads for Data Center Applications, 2014.

[2] C.-M. Liao and K.-H. Chiu, Wind tunnel modeling the system performance of alternative evaporative cooling pads in Taiwan region, 2002.

[3] B. Gebrehiwot, Maximizing Use of Air-Side Economization Direct and Indirect Evaporative Cooling for Energy Efficient Data Centers, 2016.

[4] Humidification Strategies for Data Centers and Network Rooms, [online] Available: http://www.apc.com/salestools/NRAN-5TV85S/NRAN-5TV85S_R3_EN.pdf.

[5] [online] Available: https://www.energylabs.com/web2/brochures/ELI_evaporative.PDF.

[6] HumiCool Division, Munters Corporation, 2003.

[7] Thermodynamics: An Engineering Approach, Yunus A. Cengel.

[8] Munters Corporation, [online] Available: https://webdh.munters.com/webdh/BrochureUploads/Munters%20General%20Psych%20Chart.pdf.

2.5 Indirect Evaporative Cooling with Wetted Air/Air Heat Exchangers for Data Center Cooling

2.5.1 INTRODUCTION

Servers in a Data Center (DC) are arranged in racks in a way to allow flow of cold air and hot air in separate channels. Thus, heat is drawn from the hot air side and replaced with cold air on the other side. Additionally, individual servers house fans that enable flow of cold air over itself to effectively dissipate the heat generated in its operation. This hot air is typically cooled using methods such as Direct Expansion (DX) type units (e.g., CRAC units) or Chiller based air conditioning systems. I.e., compressor-based equipment involving refrigerants. In this paper, these are further referred as Traditional Air-conditioning systems, "TAS", and Data Center as "DC".

Evaporative Cooling in Data Centers: DC engineers need to achieve strict Power Utilization Efficiency (PUE) targets. Apart from IT equipment, a major portion of the DC power is utilized for heat removal/ cooling. Traditional compressor-based air-conditioning systems (TAS) consume very high energy as compared to evaporative cooling. Therefore, in recent times, many companies are opting towards using evaporative cooling as the primary mode of operation. DC operating zone recommendation by the American Society of Heating Refrigerating and Air conditioning Engineers (ASHRAE) is considered as acceptable by the industry. Below is an illustration of DC operating zones, as recommended by ASHRAE in its TC9.9 "2011 Thermal Guidelines for Data Processing Environments" and a comparison with allowable operating conditions described by modern IT equipment suppliers, which clearly suggests a wider envelope for Evaporative Cooling.

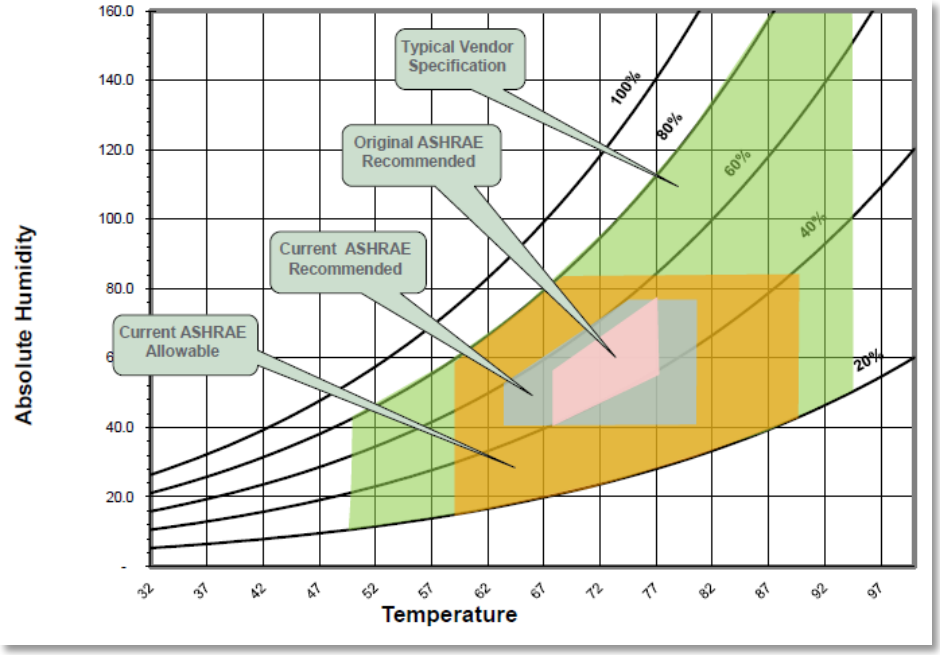

Figure 1: Recommended Data Center Operating Zone [1]

Introduction to Indirect Evaporative Cooling (IEC): Indirect evaporative cooling (IEC) is a system where a fluid is cooled by air on another side, without physically coming in contact, by the means of a heat exchanger. The fluid that brings in heat is considered primary, and the other side, secondary. Air on secondary side is obtained from the environment. It is further cooled by evaporation of water achieved by wetting the secondary side. This is achieved by spraying water in the secondary channel and forcing the movement of air in either con-current or countercurrent direction. Thus, the primary air is 100% sensibly cooled. Below is a typical crossflow plate heat exchanger that may be used in regular Air Conditioning applications.

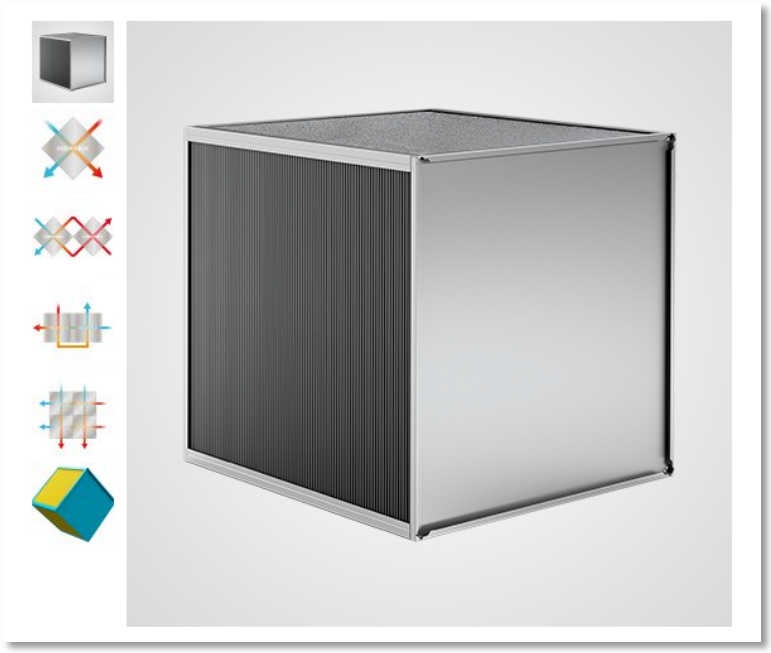

Figure 2: Crossflow Plate Heat Exchanger [2]

As explained above, on the primary side (can be also named as dry channel), air exchanges heat with the secondary side without mixing with each other. In the wet channel, secondary air is cooled by evaporation of the water film, which is formed by spraying water on the heat exchanger plates. In the wet channel, water film absorbs sensible heat of the air and converts it into the latent heat in the course of evaporation. As air carries more water vapor, it comes closer to its saturation point. In the process, the temperature of the water film and secondary air are decreased. Primary air flows in the alternative dry channels which is cooled by conduction of the separating plate between dry and wet channels.

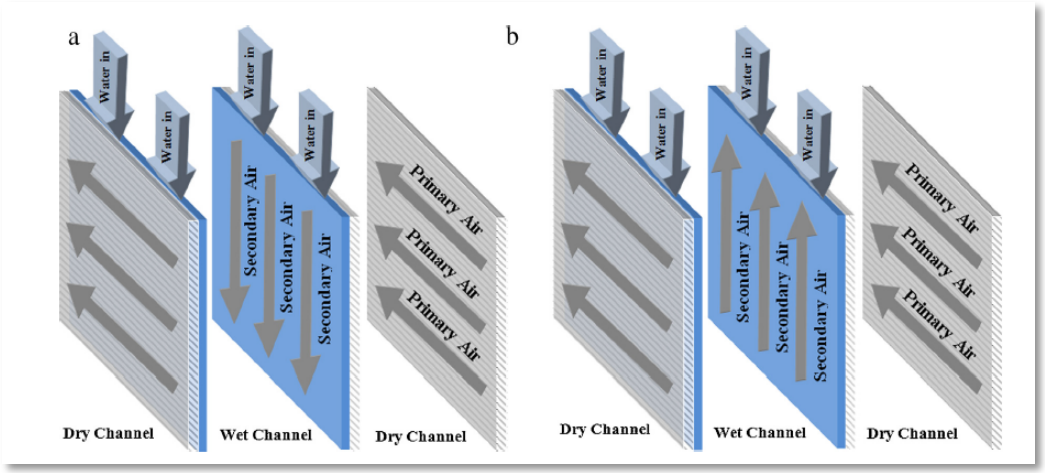

Figure 3: Dry and Wet Channels in the Indirect Evaporative Heat Exchanger

Indirect Evaporative Cooling (IEC) for Data Centers: A smart DC cooling system is designed with both TAS and IEC. While IEC acts as a basic mode of operation, TAS can be triggered when temperature or humidity approaches the outer bounds of set operating limits. Thus, based on the IT equipment heat load and ambient conditions, DC cooling can be operated in the below 3 modes: Air-to-Air IEC in dry mode, Air-to-Air IEC in wet mode, and Direct Expansion (DX) or Chilled water cooling (TAS).

The ASHRAE journal March 2011 describes DC operation with IEC. In this design, IEC module is designed to recirculate the DC air. Hot air from DC is forced through the primary side of the DC. Once cooled, it is pushed back to the DC servers through air channels, usually installed under raised floors. In this way, there is no contamination from outside environment or humidity fluctuation. The journal also describes a makeup air humidification/ dehumidification unit, designed at minimum 0.25 air changes per hour (ACH). Additionally, a filtration unit, is described with 6-10 ACH to filter the mixture of fresh air and hot DC air as it is supplied to the IEC unit.

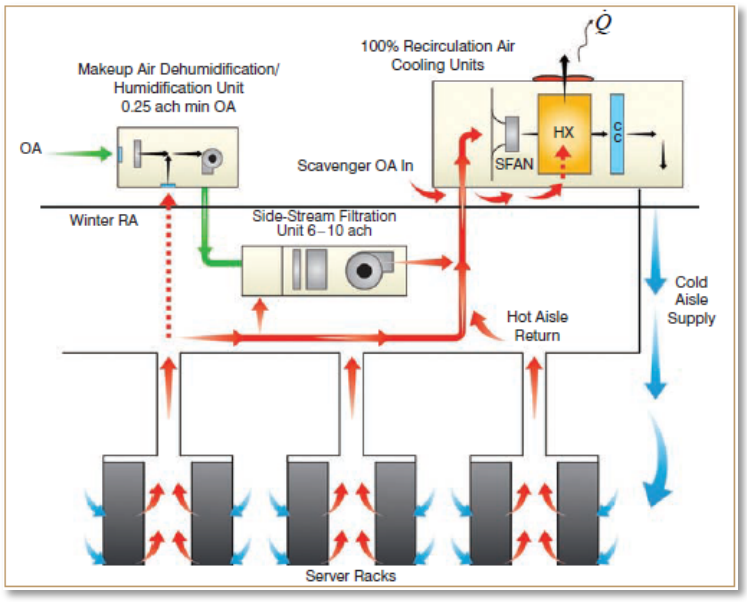

Figure 4: IEC System Design [4]

2.5.2 OBJECTIVES

The goal of this project is to provide best practices for using Indirect evaporative cooling technologies, develop deeper insight, and provide guidance in implementing, operating, controlling, and maintaining cooling systems integrated with air-side economization for data center cooling. This study lays the foundation for this project by defining a smart and extensive test method which will be invaluable in developing phenomenological models of IEC modules which can subsequently be used for developing IEC units at scale to help size and optimize equipment for Data Centers.

The principal objective of this study is to develop a method of testing, to help build IEC modules at larger scales and Improve characterization to help DC operators achieve stringent PUE targets. This study covers design parameters pertinent to sizing an IEC unit with technical selection of the components involved. We use information from existing research to develop optimum spray arrangement with spray header selection. The

components selected in this study can create +40Deg F temperature on both Primary and secondary sides. Thus, with this test method, we can create a wide range of hot dry and hot humid conditions from ambient climatic conditions of about 70 deg F, which is a standard condition in the enclosure of a factory or warehouse building.

The proposed method makes efficient use of saturated exhaust air on the secondary side for humidification of ambient air to adjust humidity and simulate a set climatic condition. A unique water collection grid is designed to accommodate at-least 10 minutes of experimental runtime, to record results in stable conditions. Finally, the proposed method allows estimation and characterization of cooling effectiveness, cooling capacity, water evaporation, water distribution, power usage, and total pressure drop.

2.5.3 TESTING SPECIFICATIONS OF INDIRECT EVAPORATIVE COOLERS

2.5.3.1 Standard rating conditions for data center cooling applications

A component indirect evaporative cooler (IEC Module), as defined in ASHRAE std. 143 -2015 [5], is an indirect evaporative cooling (IEC) device consisting of an IEC heat exchanger (HX), a means of delivering and distributing water to the wet passages of the heat exchanger, a basin for collecting water, a recirculating pump, and the piping that connects the basin and the water distribution system.

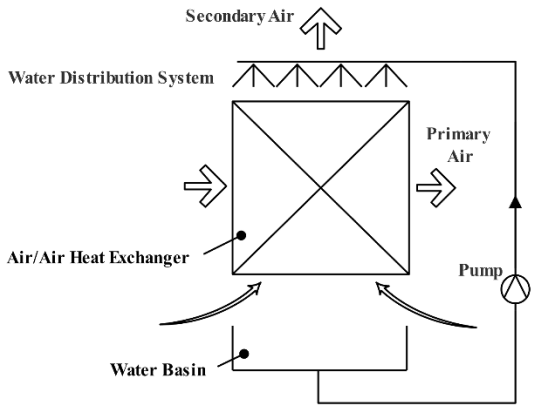

Figure 5: Schematic of an Indirect Evaporative Cooler Module

For a modular data center design focusing on scalability in deployment of IT and cooling, IEC presents an efficient option to condition air and water, if necessary, as a coolant. The effectiveness of an IEC module depends on its flow configuration, construction, heat transfer mechanism and the design specifications and requirements of a particular application. For data center cooling applications, territorial climatic conditions and the IT module cooling requirements prescribes the IEC module selection criteria and thereby its design characteristics. With the target supply air temperatures determined by the type of IT equipment and the desired controllability in a data center, a single IEC module can be sized and the total number of IECs required can be based on the total IT-load to be cooled and the territorial ASHRAE Climatic Design conditions.

2.5.4 EXPERIMENTAL SETUP FOR CHARACTERIZING AN IEC-BASED AIR HANDLING UNIT

The Test Setup is designed by carefully assessing and technically selecting components suitable for airflow of 8000 – 9000 cfm with a total static pressure not exceeding 3 in-wg (inches of water gage) on each side and the auxiliary unit. Special attention has been given to the face velocities to be maintained below 600fpm as per ASHRAE recommendations and pressure loss of equipment at 1000 fpm for an extreme case.

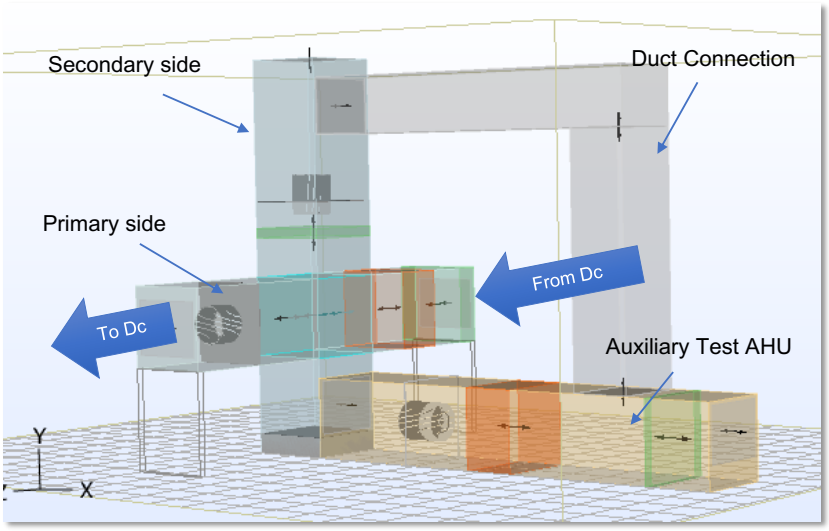

Figure 6: IEC-based Air Handling Unit Characterization Test Setup

2.5.4.1 Air-to-Air Plate Heat Exchanger

Our main interest is to build a module than can be used in multiple scales. Since DC Air Handling Unit (AHU) capacity can range from 20,000 to 100,000 cfm, we design a module for capacity 8,000 – 9,000 cfm. We begin by selecting a commercially available Plate Heat Exchanger (PHX) of an optimum size, capable of handling 8,000 - 9,000cfm of airflow. We select a reputed American manufacturer Heatex Inc.'s cross flow plate heat exchangers 48" x 48" x 48" with 5 and 10mm gaps between plates. Attached is a sample product selection report from manufacturer's selection software.

Air flow	CFM		8000	8000
Pressure drop (*)	inH_2O		0.809 (0.765)	0.911 (0.878)
Efficiency	- Wet		67	N/A
	- Dry		67	N/A
Effectiveness	- Wet		67	-
	- Dry		67	67
State before	Temperature		110°F	80°F
	Temp.wet bulb		86.6°F	68.1°F
°F	Relative humidity		40%	55%
	Absolute humidity		156.5 gr/lb*	84.16 gr/lb*
State after	Temperature		90°F	98.9°F
	Temp.wet bulb		82.4°F	73.4°F
°F	Relative humidity		73%	30.3%
	Absolute humidity		156.5 gr/lb*	84.15 gr/lb*
Air velocity (face/channel)	ft/min		514.27 / 1260.79	514.27 / 1260.79
Transferred power	BTU/h			161144.6

Figure 7: Manufacturer's Heat Exchanger Selection at 8,000 cfm [11]

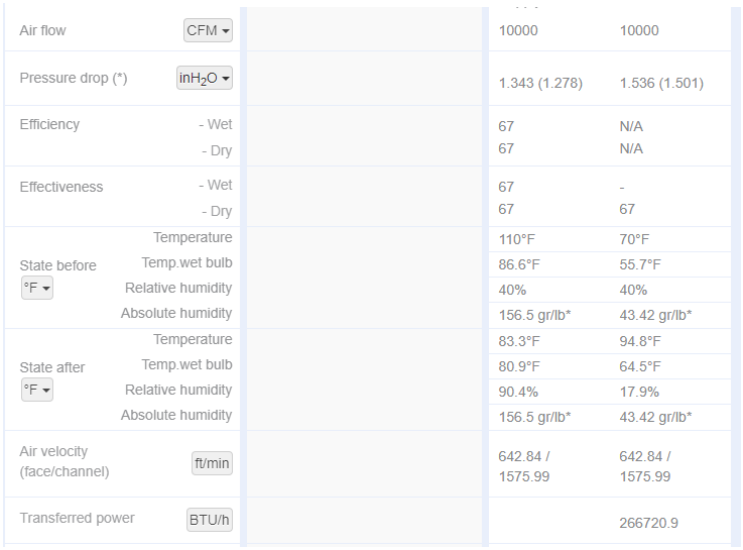

Air flow	CFM		10000	10000
Pressure drop (*)	inH_2O		1.343 (1.278)	1.536 (1.501)
Efficiency	- Wet		67	N/A
	- Dry		67	N/A
Effectiveness	- Wet		67	-
	- Dry		67	67
State before °F	Temperature		110°F	70°F
	Temp.wet bulb		86.6°F	55.7°F
	Relative humidity		40%	40%
	Absolute humidity		156.5 gr/lb*	43.42 gr/lb*
State after °F	Temperature		83.3°F	94.8°F
	Temp.wet bulb		80.9°F	64.5°F
	Relative humidity		90.4%	17.9%
	Absolute humidity		156.5 gr/lb*	43.42 gr/lb*
Air velocity (face/channel)	ft/min		642.84 / 1575.99	642.84 / 1575.99
Transferred power	BTU/h			266720.9

Figure 8: Manufacturer's Heat Exchanger Selection at 10,000 cfm [11]

This report provides an initial basis for more advanced calculations. It is to be noted that manufacturer's data cannot be entirely used as it does not truly consider the effect of different spray header arrangements. However, for developing a test method on a scalable IEC module, this selection software offers essential information of pressure drop in standard conditions. Pressure drop is likely to increase by the influence of water spray. It is to be noted that as the airflow increases from 8,000 cfm to 10,000 cfm, the pressure drops on both primary and secondary sides increases significantly, also raising the face velocities beyond ASHRAE's recommendation of 500 fpm. Hence, we design a test setup at 8000cfm with the described plate heat exchanger.

2.5.4.2 Primary, Secondary and Auxiliary Fan Selection

Fans are primarily classified based on their impeller type as Axial or Centrifugal. Axial fans are high-volume low-pressure fans. For a given amount of airflow and static pressure, centrifugal fans perform at higher efficiencies. However, Axial fans comparatively occupy lesser space and are a good choice in low static pressure requirements. A commercially available Centrifugal Plug fan with backward curved centrifugal impeller is selected. Reputed manufacturer Ziehl-Abegg's fan is considered. This fan is selected to deliver 8000 cfm of airflow @ 2.6 in-

wg at 1670 rpm. It comprises of a 6Kw, 3phase, IP 55 multi-speed electronically commutated (EC) motor. At maximum speed of 1860 rpm, the fan can deliver 8000cfm @ 4 in-wg or 9000cfm @ 3 in-wg static pressure. Fan/ cabinet spacing guidelines are considered from a reputed manufacturer's (KRUGER Ventilation [23]) data, which follows Air movement and control association's (AMCA) standard 211. Manufacturers can choose to design with axial fans to reduce the overall cabinet size and cost. This however depends on IT equipment heat load and extreme ambient conditions of the location.

Figure 9: Centrifugal Plug Fan [12]

fan data

SFP-class | SFP-value (P_{SFP})	- | Ws/m³	**3** | 1149
airflow volume (qv)	ft³/min	9534.7
air velocity	ft/s	49.20
pressure, **stat. (p_{sF})** | tot. (p_F)	in.wg.	**2.500** | 3.037
electrical power input (P_{sys})	W	5169
system eff., **stat. ($\eta_{sF,sys}$)** | tot. ($\eta_{F,sys}$)	%	**54.2** | 65.9
fan speed **(n)** | max. (n_{max})	rpm	**1864** | 1860
fan speed, set value (%n_{max})	%	100
frequency **(f_{BP})** | (f_{max})	Hz	**60** | 60
voltage (U_{DP})	V	460
current (I_{DP})	A	6.79
acoustics, suction side **($L_{w(A),5}$)** | ($L_{w,5}$)	dB	**87** | 93
acoustics, pressure side **($L_{w(A),6}$)** | ($L_{w,6}$)	dB	**94** | 99
dimensions (w x h x d)	in	26.38 x 26.38 x 21.14
product weight (m_{pr})	lb	154.3
k-factor nozzle pres. (k)	-	308
differential pres. nozzle ($p_{sF,nozzle}$)	Pa	2766

PF:PF_50; Anc:116180; STol:+-10 %

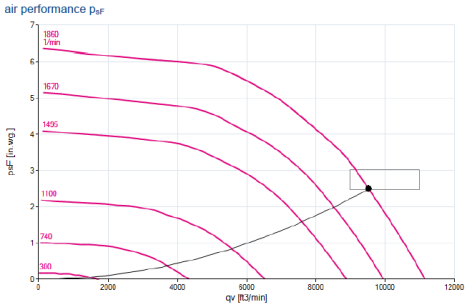

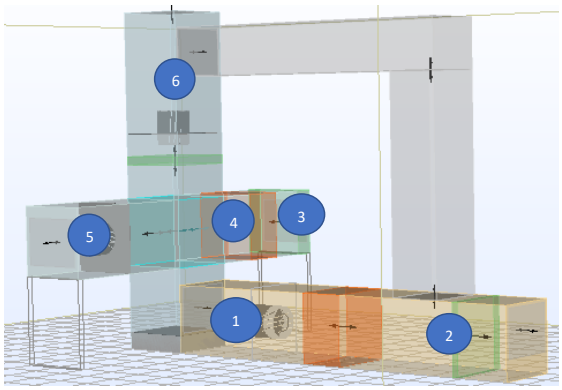

Figure 10: Ziehl Abegg fan selection and placement [12]

2.5.4.3 Airflow and Temperature Measurement

Airflow and temperature measurement stations are planned at various points for proper inspection of set conditions and accuracy of various calculations pertaining to performance rating. On the position 2 and 3, Airflow

and Temperature measurement is through in-duct measuring stations. We select a commercially available product from a reputed manufacturer. On positions 1, 4, 5, and 6 Airflow measurement is through fan's inbuilt module (except 4) and Temperature measurement through thermocouple sensors. A commercially available airflow station is considered from manufacturer Paragon controls.

Paragon Airflow and Temperature Measuring station

Figure 11: Airflow and temperature measuring station [13]

Accuracy of this station is reported within ±0.5% of actual flow through the velocity range of 200 to 1,200 fpm when installed in accordance with published recommendations and within ±5% at a velocity of 100 fpm. Our test method is designed for face velocities of 200 to 500 fpm. The measuring station selected is tested in accordance with ANSI/ AMCA 610-06/ 611-06 standards. Its operating temperature range is - 32 to 122°F (0 to 50ºC). Temperature sensor and transmitter's operating range -30 to 130 F. Pressure drop reported by the manufacturer is 0.13 in-wg @ 1148fpm. Additionally, thermocouple sensors that are used to measure temperature and humidity on position 1, 4, 5, and 6 can be selected with accuracy of +-1%.

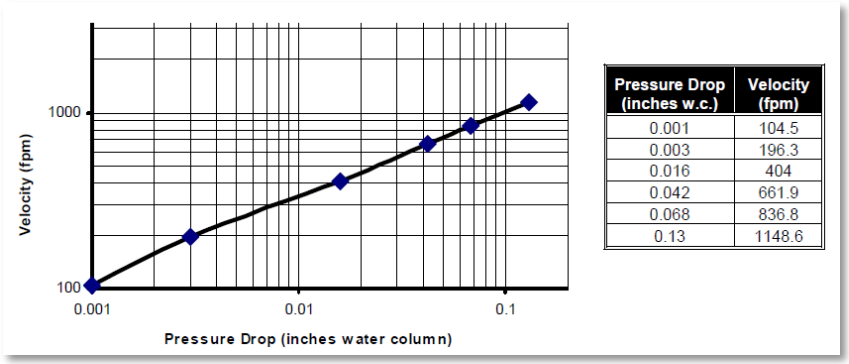

Pressure Drop (inches w.c.)	Velocity (fpm)
0.001	104.5
0.003	196.3
0.016	404
0.042	661.9
0.068	836.8
0.13	1148.6

Figure 12: System pressure drop across the measuring station [13]

2.5.4.4 Water Distribution Setup

Water spray arrangement can be done from top to bottom or bottom to top flow. In case of top to bottom, the secondary air acting is countercurrent. Therefore, it creates diffusion in the water spray and forces water droplets to join the water thin film on heat exchanger plates. Our main interest is to maximize the wetting of heat exchanger plates with minimum use of water by maximizing the residence time of water. In the top to bottom approach, based on spray header manufacturer's data, the spray manifolds shall be aligned vertically above the heat exchanger at a height of 8 to 16 inches. Based on previous literature review and manufacturer's data, we analyze several types of spray headers that are commercially available.

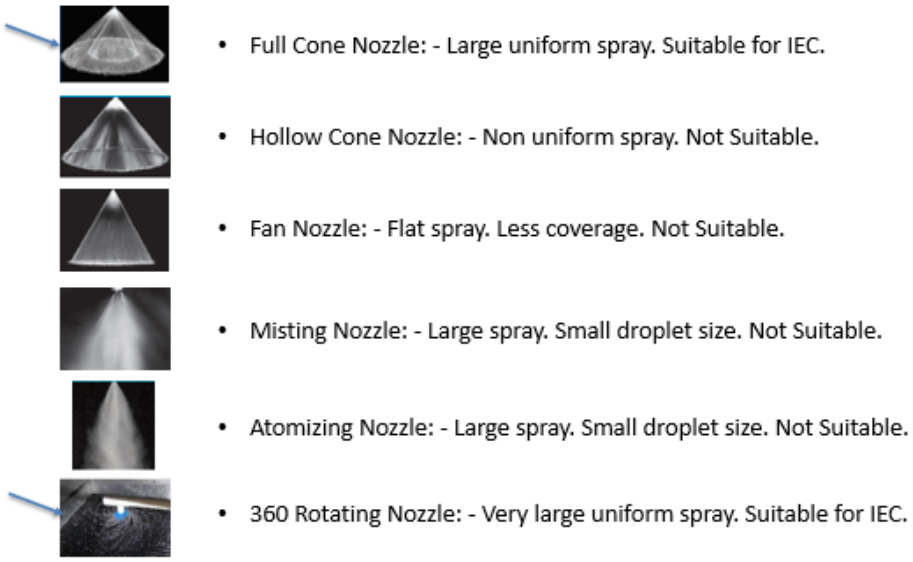

Figure 13: Spray patterns [7] [8]

For evaporative cooling, usually an atomizing type nozzle is the most preferred option. However, this shall not be a good choice for Indirect evaporative cooling as it creates very small droplets that can be easily drawn through by the pressure of the secondary fan. Smaller/ non-uniform coverage will cause inconsistent plate wetting. Therefore, we need to select a spray header that can cover a large area uniformly with considerably larger droplets. Several other factors such as spray angle, height of installation, coverage, flowrate, and pressure affect the overall performance of the secondary side of IEC module. Therefore, for our 48 x 48 x 48 in Heat exchanger, we finalize 1) Full cone type nozzle, and 2) 360° rotating header

Table 1: Spray Header Selection

Type	Model	Flow (GPM)	Press. (PSI)	Installation Ht. (in)	Coverage Dia. (Ft)	No. of headers
Full Cone	WL 120	1.08	20	8-10	2	6 (2 manifolds)
360 Rotating	3/32" inverted	1.1	20	12	15	1 (1 manifold)

Full Cone Nozzle:

- 2 Manifolds with 3 nozzles each.
- Flow and pressure measurement through gauges attached on top of each nozzle

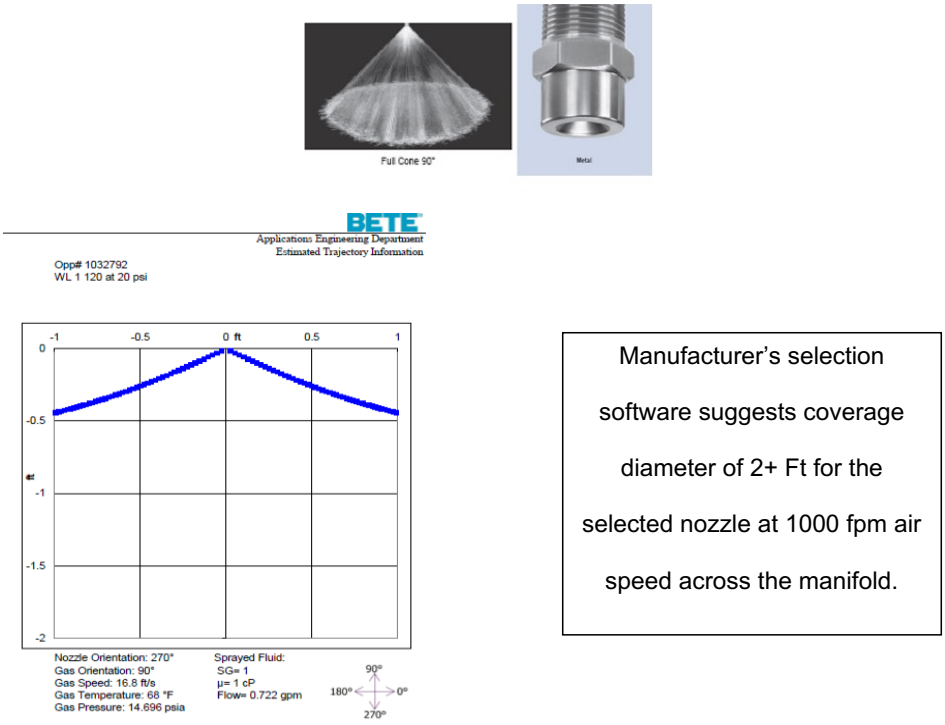

Manufacturer's selection software suggests coverage diameter of 2+ Ft for the selected nozzle at 1000 fpm air speed across the manifold.

Figure 14: Bete Nozzle Selection Software [7]

We use an online tool to calculate the manifold length and diameter at the selected flow rate and pressure. Each manifold shall hold 3 nozzles, equally spaced from each other.

Spray manifold sizing:

Minimum Pipe Diameter Size

This calculates the minimum pipe size for a pipe with equally spaced outlets such as a sprinkler lateral or manifold given a maximum allowable pressure loss.

Flow Rate In The Pipe:

3.3 gpm

Maximum Allowable Pressure Loss:

20 psi

Number of Outlets:

3

Pipe Length:

44 in

Pipe Material:

Plastic

Calculate

Minimum Pipe Diameter:

0.24 in

Figure 15: Manifold Sizing [14]

360° Rotating Spray Header:

	PSI	
	20	25
#5 Nozzle - Beige (5/64")		
Flow (GPM)	0.75	0.84
Diameter at 3.0 ft. ht.	30.0	31.0
Diameter at 6.0 ft. ht.	32.0	32.5
#6 Nozzle - Gold (3/32")		
Flow (GPM)	1.10	1.25
Diameter at 3.0 ft. ht.	31.0	31.4
Diameter at 6.0 ft. ht.	34.0	34.5

Figure 16: Selection of a spray header [14]

2.5.4.5 Electric Coil Heaters

Electric Heaters are selected on 1) Primary side of the IEC module to simulate hot DC return air; 2) Auxiliary AHU to simulate hot (and humid) ambient condition for the secondary side. Both heaters are designed to

sensibly heat air from 70F to 110F in 3 coil-steps with total installed power of 102 Kw. This power is controlled to achieve the desired heating.

Duct Heaters			Dimensions (in)						CFM	FPM	Electrical Data					Stages		
Item	Qty	Model (See Legend)	Heater			Control Box					P (kW)	VAC-Ph	I (A)	Ctrl V	Signal	Qty	kW	A
			W	H	D	A	B	C										
1	Tag(s): BDH-1, BDH-2																	
	2	DF CI00HB	50.00	48.00	6.00	9.00	49.50	10.00	8000	500	102.0	460-3	128.0	24	Mod 0-10V	3X	34.00	42.67
	Elec. Opts.: FC-CA-SF-AC-MC-TR-TF-CF-PDN-HECB-STC8-TXM-SCR-CGC Mech. Opts.: N1-BCC-CC																	

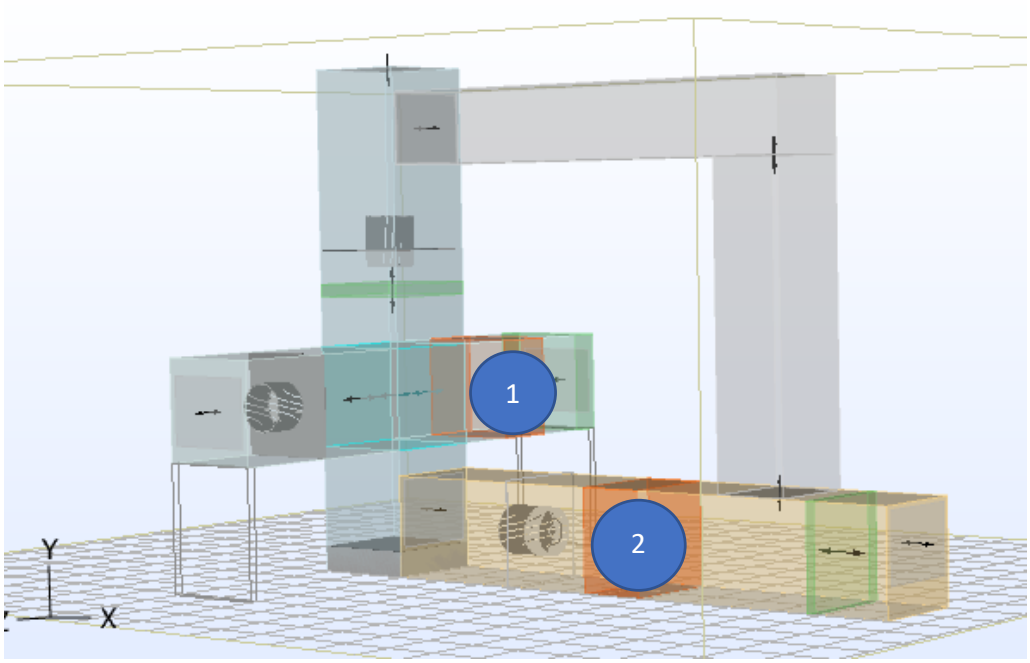

Figure 17: Neptronic Heater Selection and Placement [15]

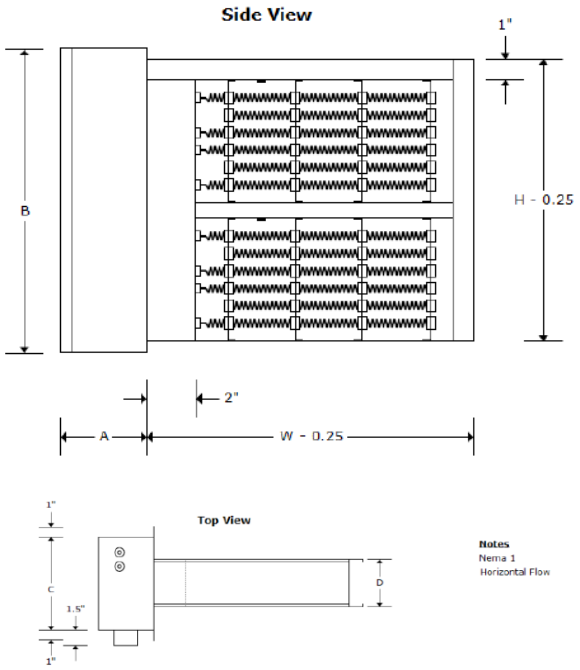

Figure 18: In-duct Heater – General Drawing [15]

Heat required (KW) = (Airflow (cfm) x dT (F))/3160 [Source: Marley Engineered products]

2.5.4.6 Pre-filters

Standard MERV (Minimum Efficiency Reporting Value) 8 air filter selected, assembled from 12 x 12 x 2 in panels. Filters are installed at the suction of primary side and auxiliary AHU to protect against dust particles entering with the airstream.

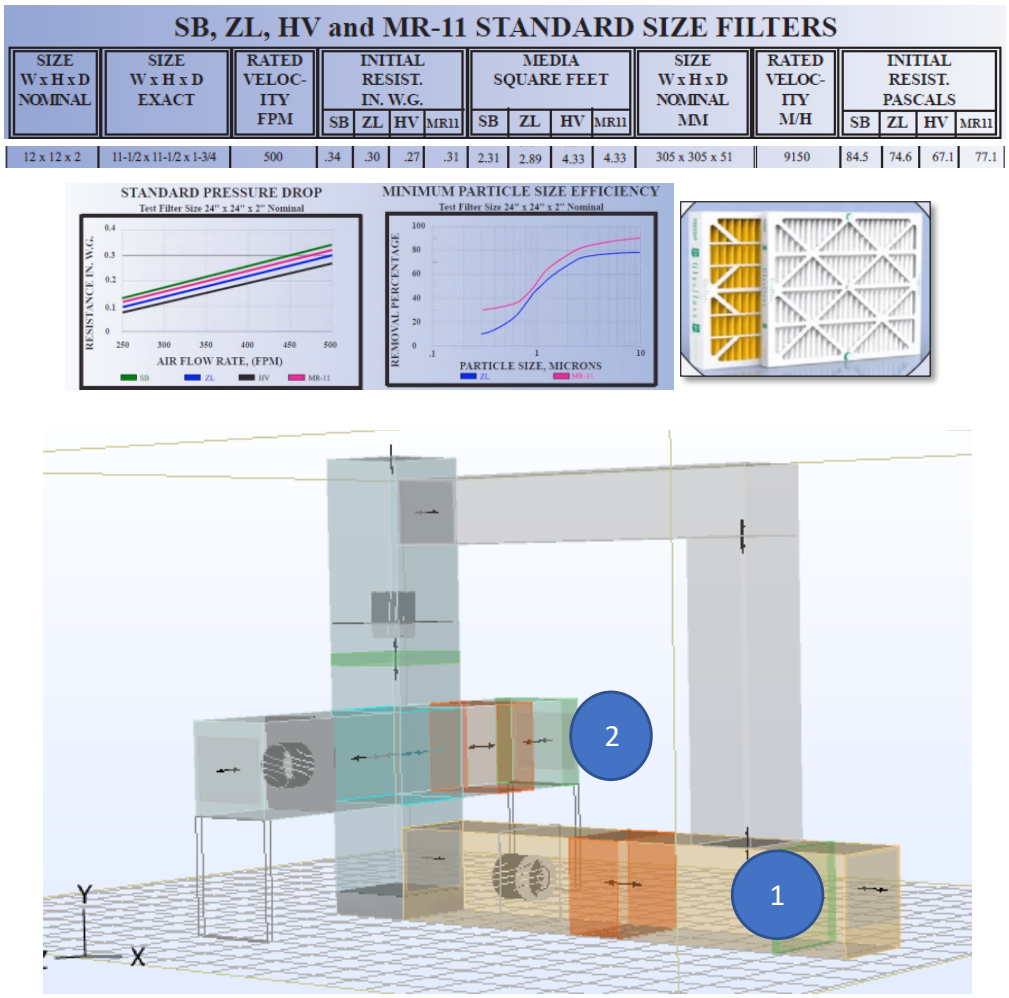

Figure 19: Air Pre-filters selection and Placement [16]

2.5.4.7 Mist/Drift Eliminators

Drift eliminator protects the water droplets from carryover due to countercurrent airflow. This not only saves precious water, but also allows us to estimate the water resident in the system. We select a commercially available Mist eliminator of size 48 x 48 x 2 (or 4) inches.

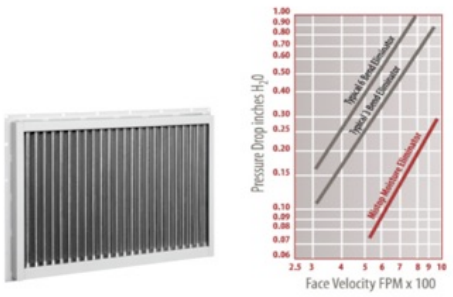

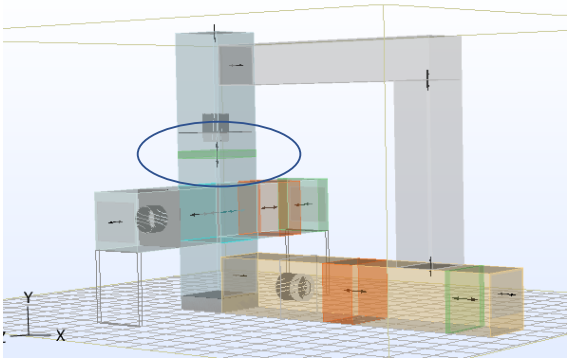

Figure 20: Mist/Drift Eliminator Selection and Placement [17]

2.5.4.8 Motorized Airflow Volume Control Dampers (VCD)

We select commercially available VCDs. These dampers should have a modulating operating mode that enables them to constantly change the opening based on control signals. 4 VCDs are selected to vary the mixture of return and fresh air as per set condition.

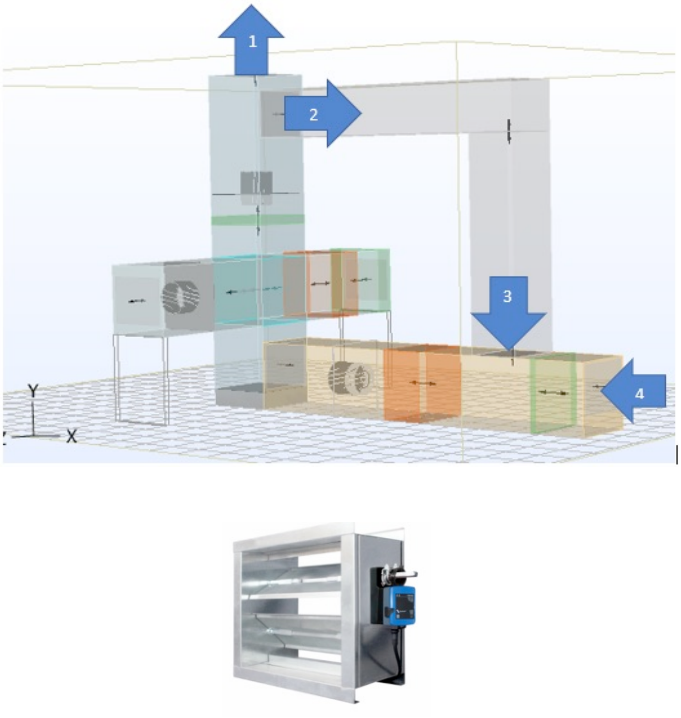

Figure 21: Motorized VCD selection and placement [18]

2.5.4.9 Sump Water Collection Grid

We design a plastic water collection sump – 48 x 48 x 12 inches, divided in 36 equal grids, aligned vertically below the Heat Exchanger. The 36 grids allow us to study water distribution across the heat exchanger.

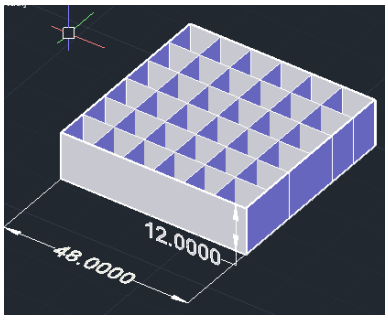

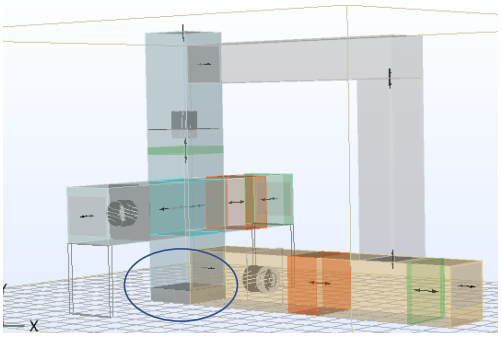

Figure 22: Sump water collection grid and placement [19]

2.5.5 DESIGN OF EXPERIMENTS

This setup should create temperature and humidity conditions, emulating a typical DC, to measure and report performance under several parameters.

Table 2: Sample DC condition setpoints on Primary side

Primary Side				
Ambient		Process	Test Condition	
Temp (F)	R.H (%)		Temp (F)	R.H (%)
70	30	Sensible heating	90	16
70	30	Sensible heating	100	12
70	30	Sensible heating	110	9.05

Table 3: Sample DC Condition Setpoints on Secondary Side

Secondary Side				
Ambient		Process	Test Condition	
Temp (F)	R.H (%)		Temp (F)	R.H (%)
70	30	Not Applicable	70	30
70	30	Return Saturated Air mixing + Sensible heating	90	50
70	30	Return Saturated Air mixing + Sensible heating	110	60

2.5.5.1 Process path of Secondary Air

Secondary air process is a mixture of adiabatic and sensible cooling. As air enters the secondary side, before reaching the heat exchanger, it is cooled adiabatically by the water spray. In this process, air gains humidity and approaches its saturation point. As air is forced through the heat exchanger channels, it exchanges heat with the thin water film on the heat exchanger plate of secondary side, that gains heat through conduction from the primary airstream. As we know the primary air is hot DC return air, the secondary side airstream can be seen as a forced laminar flow over an isothermal plate. The convection heat transfer to secondary air stream due to primary side can be calculated using Newton's law of cooling [22].

Heat convected from a hot isothermal plate in forced laminar flow [22] is given by,

$$Q = h_{plate} A (T_w - T_\infty)$$

$$\dot{Q}_{\text{plate}} = 0.664 \cdot (Pr)^{1/3} \cdot \sqrt{\text{Re}_L} \cdot \frac{kA}{L} \Delta T$$

While secondary air gains heat, its water carrying capacity increases. This air, being in continuous influence of the water spray, is constantly cooled adiabatically. Below is general schematic to understand the process path of secondary air in an IEC module.

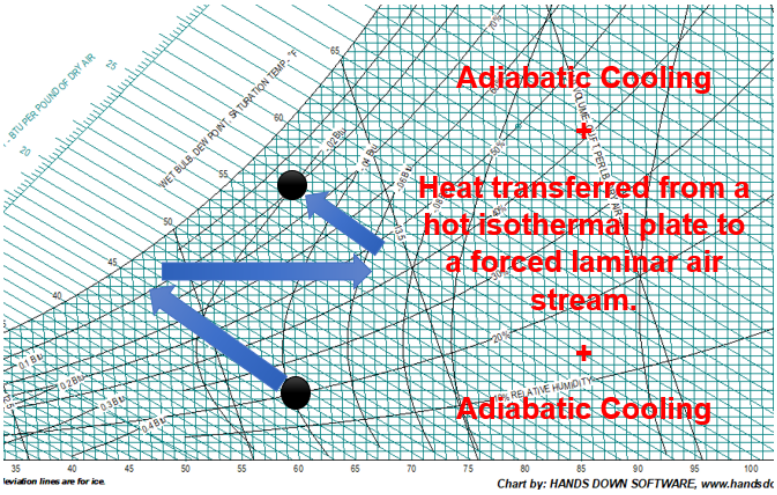

Figure 23: Process plot on Psychrometric Chart [20]

2.5.5.2 Control of condition on Secondary side

Let us consider a case study where we want to create 110 F @ 35 % R.H with +-1% for 8000 cfm of air. Please note that these numbers and processes are samples to explain the process path of secondary air. In this designed test method, secondary side air shall be measured at the designated measuring stations. Further control settings shall be dependent on measurements from these stations.

Table 4: Secondary Side – Auxiliary AHU Return Air Mixing

	Temp (F)	R.H (%)
Primary side air set temperature	110	9
Ambient air	70	30

Process state	1	
	Air at the inlet of Secondary side at the start of the cycle	
	Temp (F)	R.H (%)
Cycle 1	70	30

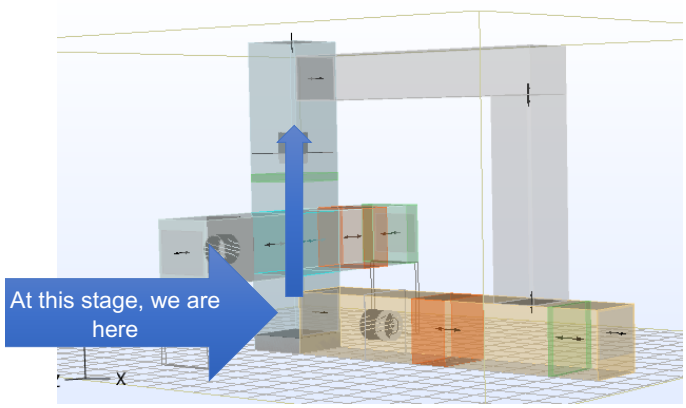

Figure 24: Secondary Side – Downstream of Auxiliary Return Mixing Chamber

Air entering the secondary side is adiabatically cooled due to the influence of water spray.

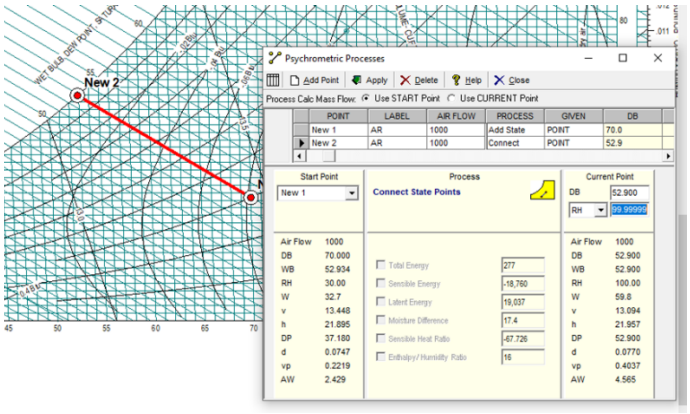

Figure 25: Process plot on Psychrometric Chart for Table 4 [20]

Table 5: Secondary Side - Auxiliary AHU Return Air Mixing

Process state	1		2		3	
	Air at the inlet of Secondary side at the start of the cycle		Adiabatic cooling		heat transfer due to convection	
	Temp (F)	R.H (%)	Temp (F)	R.H (%)	Temp (F)	R.H (%)
cycle 1	70	30	52.9	100	81.5	37

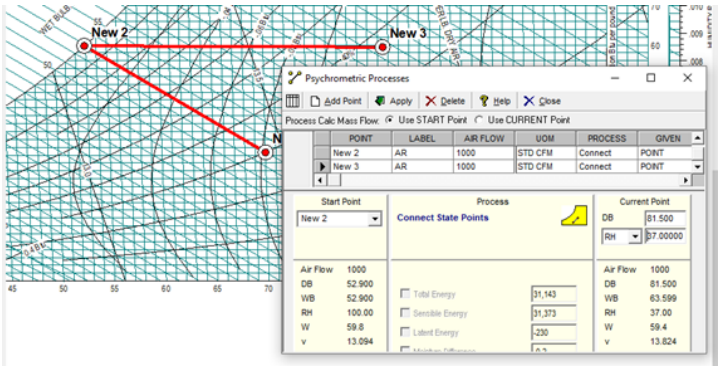

Figure 26: Process plot on Psychrometric Chart for Table 5 [20]

As air reaches the heat exchanger plates, it gains heat convected by hot primary side plate. Therefore, in large number of miniscule steps, air gains heat sensibly and again cools adiabatically.

Table 6: Secondary Side – Auxiliary AHU Return Air Mixing

Process state	1		2		3		4	
	Air at the inlet of Secondary side at the start of the cycle		Adiabatic cooling		heat transfer due to convection		Adiabatic cooling	
	Temp (F)	R.H (%)	Temp (F)	R.H (%)	Temp (F)	R.H (%)	Temp (F)	R.H (%)
cycle 1	70	30	52.9	100	81.5	37	63.6	100

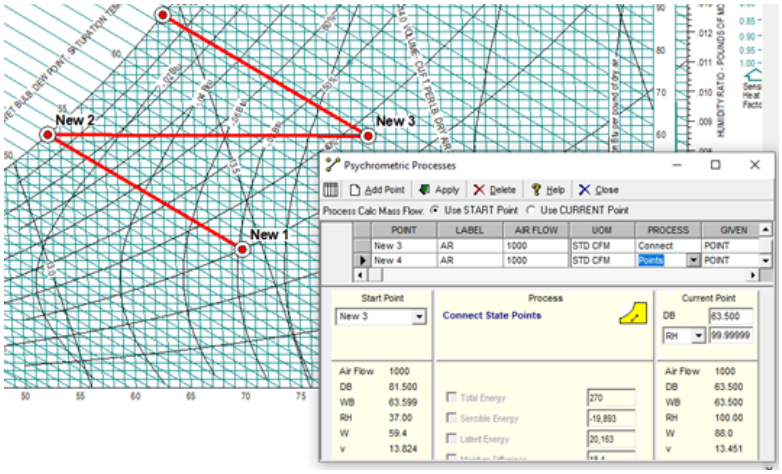

Figure 27: Process plot on Psychrometric Chart for Table 6 [20]

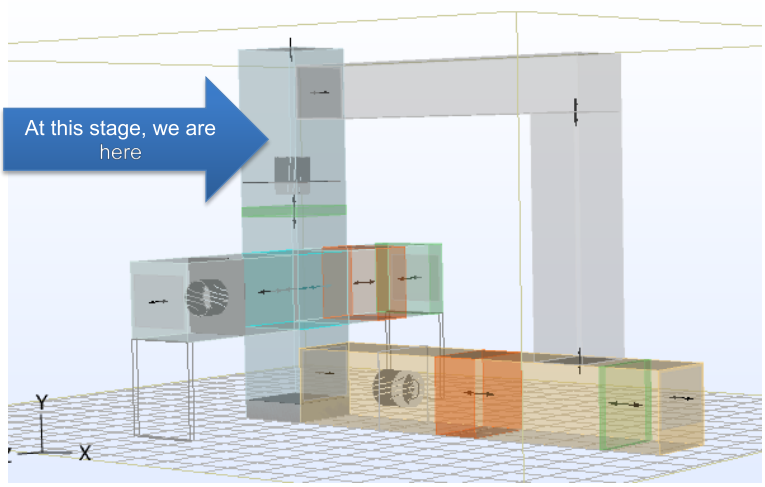

Figure 28: Secondary Side – Downstream of Auxiliary Return Mixing Chamber after Table 6

From this point, we exhaust certain amount of air and recirculate the rest back to the auxiliary unit to create a mixture with the ambient air. For this sample calculation, we assume 75% of return air and balance 25% of ambient fresh air. As discussed above, 4 motorized Volume Control Dampers (VCD) are selected to modulate the return air and fresh air percentage in the system. We use an online tool to calculate the result of this mixture.

Inputs:

English Units

	① Outdoor Air	② Return Air	③ Additional Air Stream (optional)
cfm	2,000.0	6,000.0	Add. Air Volum
Dry Bulb Temperature	70.0	63.6	T, aa, db
Wet Bulb Temperature	52.9	63.6	T, aa, wb

Reset Calculate

Results:

Total Air Volume:	8000.00 cfm
Mixed Air, Dry Bulb:	65.20 oF
Mixed Air, Wet Bulb:	60.93 oF

Figure 29: Return and Ambient Air Mixture [21]

Table 7: Secondary Side – Auxiliary AHU Return Air Mixture

	Air at the inlet of Secondary side at the start of the cycle		Adiabatic cooling		heat transfer due to convection		Adiabatic cooling		Return air VCD opening	Ambient air VCD opening	Air Mixture in Auxiliary AHU	
	Temp (F)	R.H (%)	Temp (F)	R.H (%)	Temp (F)	R.H (%)	Temp (F)	R.H (%)	75%	25%	Temp (F)	R.H (%)
cycle 1	70	30	52.9	100	81.5	37	63.6	100	6000 cfm	2000 cfm	65.2	78.6

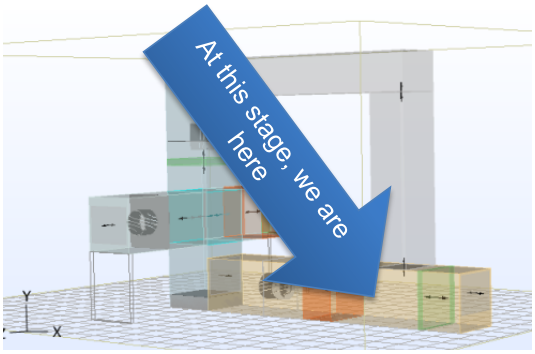

Figure 30: Secondary Side – Downstream of Auxiliary Return Mixing Chamber after Table 7

This air mixture is heated by the auxiliary electric heater that is set to sensibly heat the air to 110 Deg F as a starting assumption of this sample calculation. This heated air enters the secondary side suction as beginning of cycle 2.

Table 8: Secondary Side - Auxiliary AHU Return Air Mixture

	1		2		3		4		5		6		7	
	Air at the inlet of Secondary side at the start of the cycle		Adiabatic cooling		heat transfer due to convection		Adiabatic cooling		Return air VCD opening	Ambient air VCD opening	Air Mixture in Auxiliary AHU		Sensible heating set to 110F	
	Temp (F)	R.H (%)	Temp (F)	R.H (%)	Temp (F)	R.H (%)	Temp (F)	R.H (%)			Temp (F)	R.H (%)	Temp (F)	R.H (%)
cycle 1	70	30	52.9	100	81.5	37	63.6	100	6000 cfm	2000 cfm	65.2	78.6	110	19.2
cycle 2	110	19.2	74.9	100	92.5	57	79.48	100	6000 cfm	2000 cfm	77.13	81.8	110	29.5

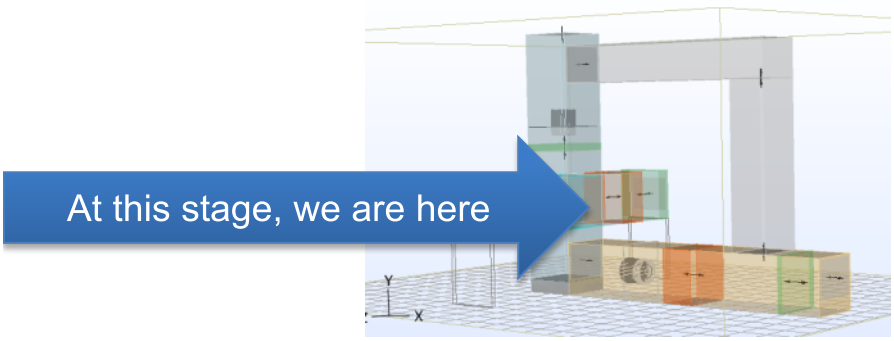

Figure 31: Secondary Side – Downstream of Auxiliary Return Mixing Chamber after Table 8

In this way a desired condition can be achieved by running various cycles. For a uniform and stable condition, it is advisable to achieve small increments in temperature and humidity by mixing the return and fresh air with close proportions. Due to response time for VCD opening adjustment, a stable condition can be achieved with slow increments over a period of 5-6 minutes.

Table 9: Secondary Side - - Auxiliary AHU Return Air Mixture

	1		2		3		4		5		6		7	
	Air at the inlet of Secondary side at the start of the cycle		Adiabatic cooling		heat transfer due to convection		Adiabatic cooling		Return air VCD % open	Ambient air VCD % open	Air Mixture in Auxiliary AHU		Sensible heating set to 110F	
	Temp (F)	R.H (%)	Temp (F)	R.H (%)	Temp (F)	R.H (%)	Temp (F)	R.H (%)			Temp (F)	R.H (%)	Temp (F)	R.H (%)
cycle 1	70	30	52.9	100	81.5	37	63.6	100	6000 cfm	2000 cfm	65.2	78.6	110	19.2
cycle 2	110	19.2	74.9	100	92.5	57	79.48	100	6000 cfm	2000 cfm	77.13	81.8	110	29.5
cycle 3	110	29.5	81.183	100	95.6	63.5	84.45	100	6000 cfm	2000 cfm	80.88	82.58	110	34
cycle 4	110	34	83.67	100	96.8	66.5	86.56	100	6000 cfm	2000 cfm	82.45	82.87	110	35.5
cycle 5	110	35.5	84.58	100	97.3	67.5	87.35	100	6000 cfm	2000 cfm	83.05	82.98	110	36.5
cycle 6	110	36.5	85	100	97.5	68	87.71	100	5700 cfm	2300 cfm	82.61	80.48	110	35

As we can see above, the desired temperature and humidity was achieved in cycle 4. As the humidity starts to deviate, air mixture was adjusted in cycle 6 to maintain the humidity at the set condition of 35%. This adjustment is achieved by varying the VCD opening with the help of a programmable controller.

2.5.6 MEASUREMENTS

Measurements of airflow, differential pressure, temperature, and humidity are taken across the 6 designated stations for further calculations. Parameters are numbered according to the station. E.g.: 2T_db = Dry bulb temperature recorded at station 2, which is at suction of auxiliary AHU.

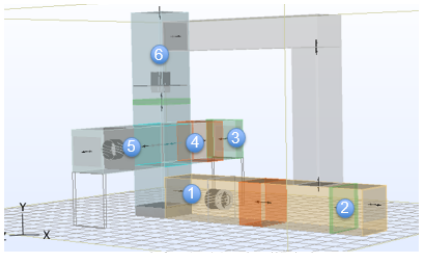

Figure 32: Measurement station locations

Below table describes sample (assumed) readings to demonstrate implementation of the test method.

Table 10: Measurements table – Refer to Figure 32 for Measuring station locations

Primary Suction				Primary Heater			Primary Fan (near discharge)					Aux. Suction				Aux. discharge/ Secondary Suction						Secondary Fan (near discharge)				
3	3	3	3	4	4	4	5	5	5	5	5	2	2	2	2	1	1	1	1	Hx Face Velocity (fpm) = 1_cfm/ 16 sq.ft (Face area of Hx)	1	6	6	6	6	6
T_Db	T_Wb	R.H (%)	cfm	T_Db	T_Wb	R.H (%)	T Db	T Wb	R.H (%)	cfm	dP	T Db	T Wb	R.H (%)	cfm	T Db	T Wb	R.H (%)	1_cfm	1_Fv	DP	T Db	T Wb	R.H (%)	cfm	DP
70	52.9	30	8000	90	60.8	16	76	61.9	40	8000	2.8	70	52.9	30	2000	110	86.79	40	8000	500	1.8	87.7	87.7	100	8000	3.1
70	52.9	30	8000	90	60.8	16	79	63.4	40	8000	2.75	70	52.9	30	2000	110	86.79	40	7000	437.5	1.78	87.9	87.9	100	7000	3
70	52.9	30	8000	90	60.8	16	80	63.4	40	8000	2.7	70	52.9	30	2000	110	86.79	40	6000	375	1.7	89.14	89.14	100	6000	2.75

2.5.7 CALCULATIONS AND REPORTS

Below are IEC module performance calculations on sample (assumed) measurement data to demonstrate implementation of the test method.

2.5.7.1 Cooling Effectiveness and Capacity

Table 11: IEC Cooling Effectiveness and Capacity Calculation

Cooling effectiveness	Cooling capacity
$C\_E = (T_{db4}-T_{db5}) / (T_{db5}-T_{wb4})$	$C\_q\ (BTU) = 1.08 \times q_5 \times (T_{db4}-T_{db5})$
C_E	C_q
0.95	207360
0.60	95040
0.52	86400

Where ,

T_{db4} – Entering air temperature, dry bulb

T_{db5} – Exiting air temperature, dry bulb

T_{wb4} – Entering air temperature, wet bulb

q_5 – airflow (cfm) recorded at exit

2.5.7.2 Water Evaporated

Table 12: Total Water Evaporated Calculation

Water Evaporated				
humidity density of T_Db1 Lb/cub.ft	humidity density of T_Db6 Lb/cub.ft	water content (kg/min) = (hd x cfm)/2.2		Total Water Evaporated (kg/ min) = W_hd6 - W_hd1
hd1	hd6	W_hd1	W_hd6	W_Ev
0.0687	0.0713	249.82	259.27	9.45
0.0687	0.0712	218.59	226.55	7.95
0.0687	0.071	187.36	193.64	6.27

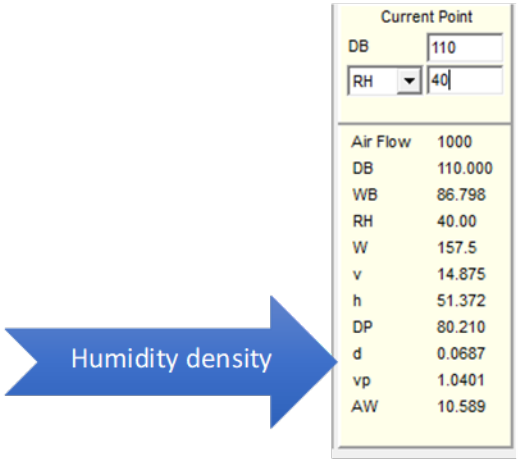

Figure 33: Humidity calculation on Psychrometric Analysis tool [20]

T_db1 – Secondary side entering air temperature, dry bulb

T_db6 – Secondary side exiting air temperature, dry bulb

2.5.7.3 Water Consumption

Table 13: Total water consumption calculation

Water Consumption									
Mass of Water spray: Nozzle 1 (kg/min)	Mass of Water spray: Nozzle 2 (kg/min)	Mass of Water spray: Nozzle 3 (kg/min)	Mass of Water spray: Nozzle 4 (kg/min)	Mass of Water spray: Nozzle 5 (kg/min)	Mass of Water spray: Nozzle 6 (kg/min)	Total Mass of Water Spray (kg/ min) W_s = sum (Nz1 to 6)	Mass of water Collected in grid(kg/min)	Total Water consumption (kg/min)= W_Ev + W_g	Mass of Water resident on Heat Exhanger plates (kg/min) W_r = W_s - (W_g+W_Ev)
W_Nz1	W_Nz2	W_Nz3	W_Nz4	W_Nz5	W_Nz6	W_s	W_g	W_c	W_r
4.158	4.158	4.158	4.158	4.158	4.158	24.948	14.6	24.05	0.893
4.158	4.158	4.158	4.158	4.158	4.158	24.948	12.6	20.55	4.393
4.158	4.158	4.158	4.158	4.158	4.158	24.948	12	18.27	6.675

2.5.7.4 Fan characteristics

Table 14: Calculation of fan performance and operating characteristics

Fan Characteristics										
Primary Fan airflow (cfm)	Total Pressure drop (in-wg)	Velocity Pressure (in-wg)	Primary Fan static pressure (in-wg) = Total Pressure - Velocity pressure	Primary Fan absorbed Power (watts)	Secondary Fan airflow (cfm)	Total Pressure drop (in-wg)	Velocity Pressure (in-wg)	Secondary Fan static pressure (in-wg) = Total Pressure - Velocity pressure	Secondary Fan absorbed Power (watts)	Total Fan Power absorbed (watts)
P_cfm	P_Tp	P_vp	P_sp	P_pw	S_cfm	S_Tp	S_vp	S_sp	S_pw	F_pw
8000	2.8	0.3	2.5	3400	8000	3.1	0.35	2.75	3600	7000
8000	2.75	0.25	2.5	3350	7000	2.85	0.25	2.6	3500	6850
8000	2.7	0.2	2.5	3325	6000	2.75	0.35	2.4	3300	6625

2.5.7.5 Reports

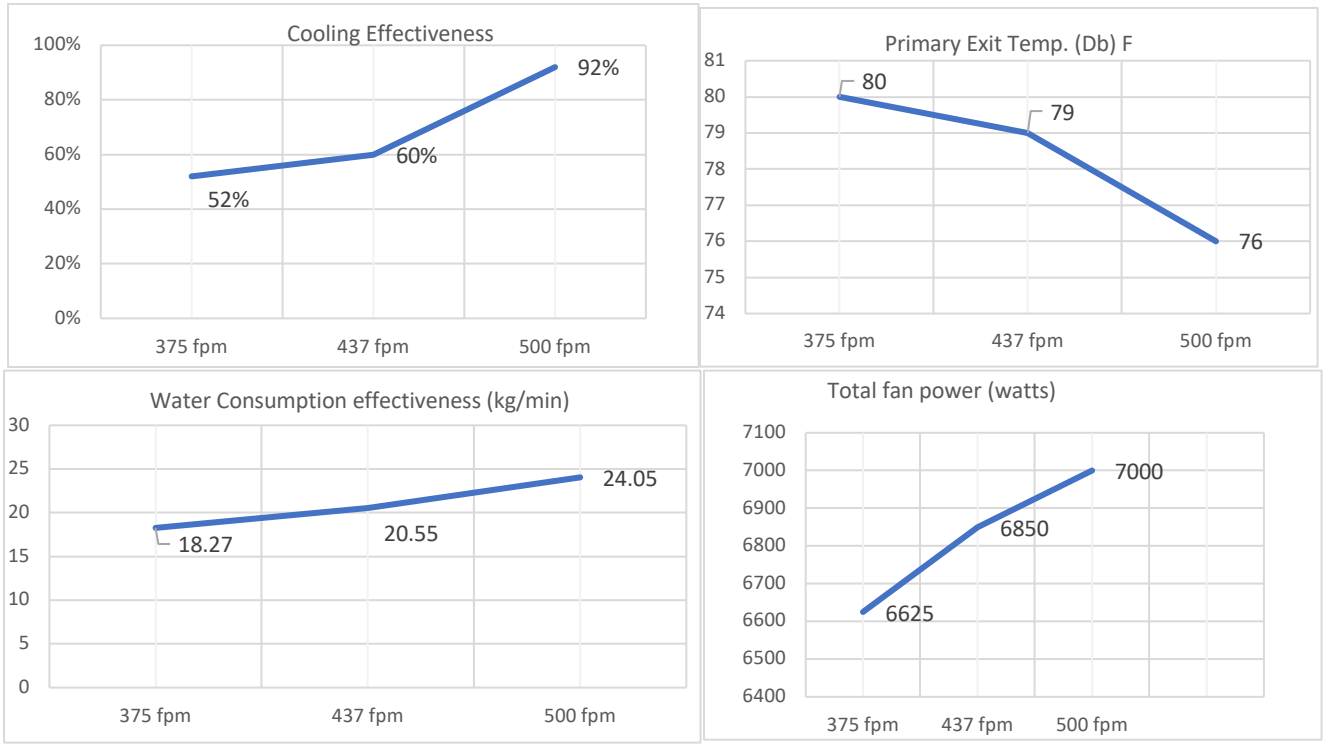

Figure 34: Sample plots based on assumed measurements and calculations: Cooling effectiveness, Primary exit temperature, total fan power & water consumption effectiveness (Clockwise)

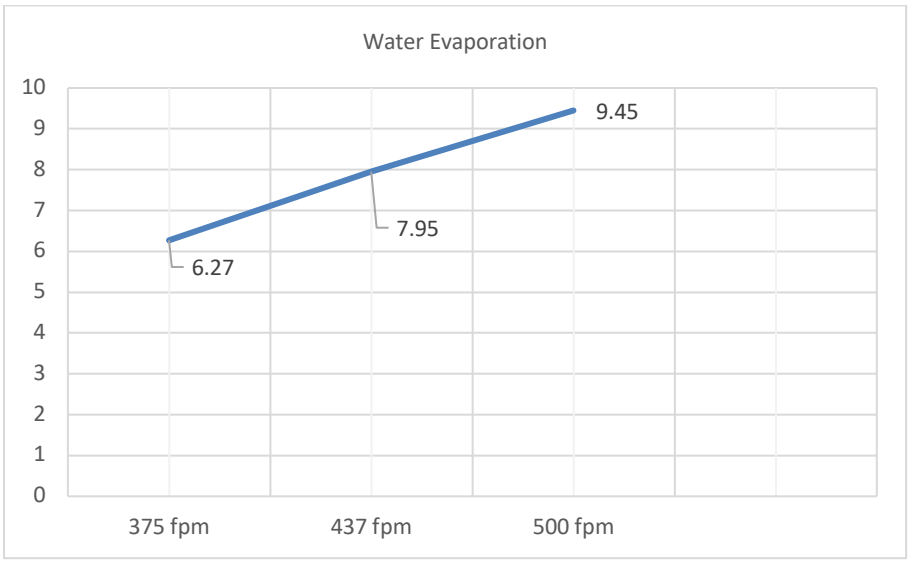

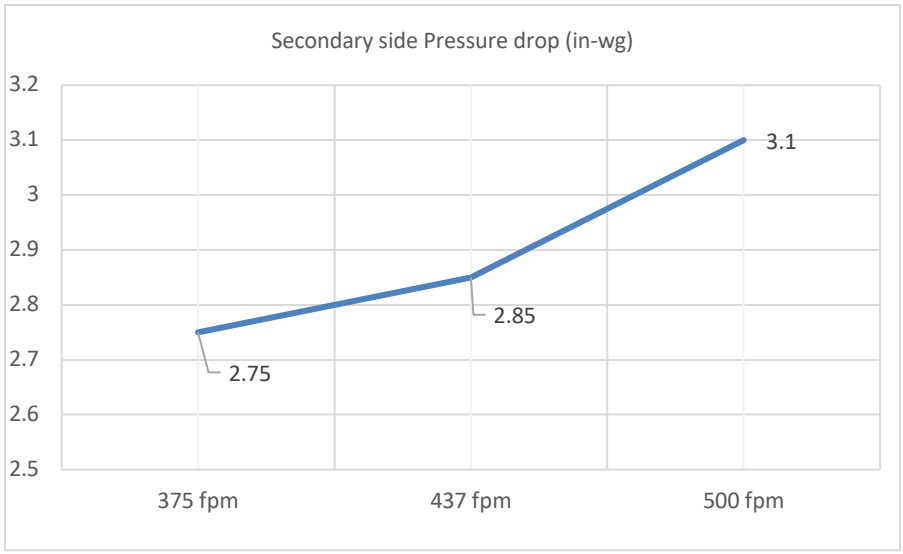

Figure 35: : Sample plots based on assumed measurements and calculations: water evaporation (top) and secondary side pressure drop (bottom)

2.5.8 SUMMARY

Characterization of primary side exit temperature, cooling effectiveness, secondary side power consumption, and water usage allows DC operators to maximize PUE. For e.g., in the given sample calculations,

while operating at 6000cfm of secondary air, we can achieve 80F on the primary side. This stays within the ASHRAE's recommended zone. In this choice, the operator saves 9% on fan power and 35% on water consumption. The Test method lets us create stable conditions of hot-humid environment. Evaporative cooling efficiency drops as the conditions become and hot and humid. Thus, this method allows testing the outer operating limits of IEC modules for DC. Various spray methods can be employed and tested to maximize cooling effectiveness. This Test method can be used to scale IEC modules in the multiples of 8000cfm in non-stacked arrangement of crossflow plate heat exchangers.

2.5.9 REFERENCES

[1] High Efficiency Indirect Air Economizer-Based Cooling for Data Centers, White Paper 136 (Schneider), By Wendy Torell. The Expanding Operating Environment.

[2] Heatex Official Website, Product Data, And Engineering Information Available On: www.heatex.com/products/cross-flow

[3] Novel Modeling Of An Indirect Evaporative Cooling System With Cross-Flow Configuration By Ghassem Heidarinejad And Shahab Moshari.

[4] 2011 Dunnavant Ashrae Journal Data Center Heat Rejection Indirect Air Side Economizer Cycle.

[5] Ansi/Ashrae Standard 143-2015, Method Of Test For Rating Indirect Evaporative Coolers.

[6] Evaporative Cooling Design Guidelines Manual For New Mexico Schools And Commercial Buildings. Author: J. D. Palmer, P.E., C.E.M. Nrg Engineering, Funded By: United States Department Of Energy And New Mexico Energy Minerals And Natural Resources Department Energy Conservation And Management Division

[7] Bete Product Catalogues and Engineering Information.

[8] Experimental Investigation Of Water Spraying In An Indirect Evaporative Cooler From Nozzle Type And Spray Strategy Perspectives. Tiezhu Sun A, Xiang Huang A, Yi Chen B, Hong Zhang A.

[9] Numerical And Experimental Study On Spray Cooling System Design For Cooling Performance Enhancement Of Natural Draft Dry Cooling Towers, Yubiao Sun.

[10] 6sigma Data Center Cooling Design And Simulation Software By Future Facilities, Usa.

[11] Product Selection By Heatex Selection Software https://heatexselect.heatex.com.

[12] Ziehl Abegg Product Information And Software Selection Output.

[13] Paragon Controls Airflow and Temperature Measurement Product Information.

[14] Manifold Sizing Calculator Available on Washington State University Website Source:
Http://Irrigation.Wsu.Edu/Content/ Calculators/ General/ Pressure-Loss-With-Outlets.Php

[15] Heater Product Selection and General Arrangement Drawing By Neptronic, Canada.

[16] Merv 8 Pre-Filter Product Selection and Engineering Information From Glasfloss Product Catalogue.

[17] Mist Eliminator Product Selection and Engineering Information From Manufacturer “Mistop”.

[18] Volume Control Damper (VCD) Product Image from Prudentaire Website: https://www.prudentaire.com/.

[19] Water Collection Grid Designed Using Autocad 2018 Student Version.

[20] Heating and Cooling Process Plot Using Carrier Version Handsdown Software Free Package.

[21] Air Mixture Calculation On: https://www.adicotengineering.com/air-mixing-calculator.

[22] Heat Convection From Hot Isothermal Plate To Forced Laminar Flow Theory And Calculation On Efunda.Com, Including Online Calculator:
https://www.efunda.com/formulae/heattransfer/convectionforced/calclamflowisothermalplate.cfm.

[23] Cabinet Sizing Of Centrifugal Plug Fan Guidelines From Kruger Ventilation Bnb Series Product Catalogue.
https://www.krugerfan.com/.

[24] Systems with Manifolds by Mario Doninelli (Caleffi).

[25] Mathematical Modelling of Flows In Dividing And Combining Flow Manifold By A.K. Majumdar.

[26] Adding More Fan Power Can Be A Good Thing by Ronnie Moffitt, P.E., Member Ashrae.

[27] HVAC Cooling Systems for Data Centers By A. Bhatia, Ced Engineering.

Chapter 3

Operations and Maintenance

3.1 Introduction

3.1.1 DIRECT EVAPORATIVE HEAT EXCHANGER

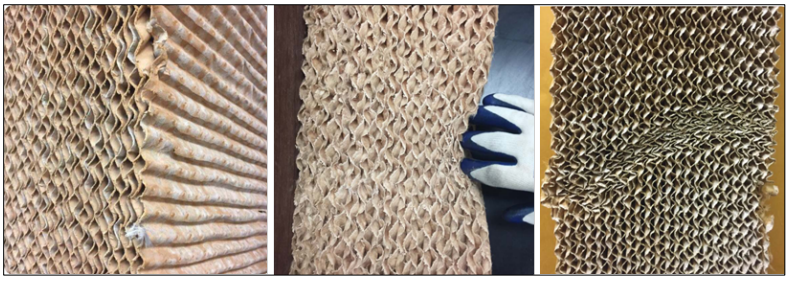

Figure 1: Scale formation, softening and collapsing of media pad (Left to Right)

3.2 Accelerated Degradation Testing of Rigid Wet Cooling Media to Analyze the Impact of Calcium Scaling

Hemanth N. Dakshinamurthy
University of Texas at Arlington
Arlington, TX, USA

Ashwin Siddarth
University of Texas at Arlington
Arlington, TX, USA

Abhishek Guhe
Mestex
Dallas, TX, USA

Rajesh Kasukurthy
University of Texas at Arlington
Arlington, TX, USA

James Hoverson
Mestex
Dallas, TX, USA

Dereje Agonafer
University of Texas at Arlington
Arlington, TX, USA

3.2.1 ABSTRACT

Rigid wet cooling media is a key component of direct and indirect evaporative cooling systems. Evaporation is the process of a substance in a liquid state changing to a gaseous state. When water evaporates only water molecules gets evaporated and the other chemicals in the water is left behind on the surface as residue. Many studies have been conducted on how the change in air flow velocity, media depth, porosity, water distribution affect performance of the cooling system. The operational efficiency of the cooling media varies over its life cycle and depends primarily on temperature and speed of inlet air, water distribution system, type of pad and dimension of the pad.

Although evaporative cooling when implemented with air-side economization enables efficiency gains, a trade-off between the system maintenance and its operational efficiency exists.

In this study, the primary objective is to determine how calcium scale affects the overall performance i.e., saturation efficiency and pressure drop across the media pad. Areas of the pad that are not wetted effectively allow air to pass through without being cooled and the edges between wetted and dry surface establish sites for scale formation. An Accelerated Degradation Testing (ADT) by rapid wetting and drying on the media pads at elevated levels of calcium was planned on the media pad. This research focuses on monitoring the degradation that occurs over its usage and establish a key maintenance parameter for water used in media pad.

As a novel study, preliminary tests where mandatory because there were no established standards for media pad degradation testing. It was clearly found that scale deposition on media pads does not affect the media pad performance. Water conductivity is the key maintenance parameter for monitoring sump replenishing cycles

which will result in reduced water usage. The average water conductivity in the sump during wetting cycles reduced continuously when ADT was performed on an already used media pad. Whereas the average conductivity of water during wetting cycles had different results when ADT was performed on a completely new pad.

3.2.2 NOMENCLATURE

DEC	Direct evaporative cooling
RH	Relative humidity
FPM	Foot per minute
GPM	Gallon per minute
ADT	Accelerated degradation testing
SEM	Scanning electron microscope
EDS	Energy dispersive spectroscopy

3.2.3 INTRODUCTION

Prudent use of water as a resource is a key factor when operating evaporative cooling units in regions of strained water availability. Calcification occurs due to how media pads are currently operated. The effect of wetting/drying cycles on the media performance is seldom given consideration during operation and the primary monitoring parameter at the water sump is the water itself. From the different media pad manufacturers maintenance guide, it was quite clear that calcium carbonate is the scale forming component on the media pad. The common suggestion from all the cooling media pad manufacturers is to avoid rapid wetting and drying cycles for a long period of time but the effect of this operation was not studied [1]. Study on calcium carbonate scale deposition by Hasson [2] helped in understanding the mechanism of Calcium Carbonate ($CaCO_3$) formation on heat transfer surfaces. Furthermore, the effect of parameters like temperature and flow rate on calcium carbonate scale deposition was reported in that study. A knowledge base was established on what affects calcium scaling on

media pads. An important step in an accelerated test is to define the type of failure and before choosing the critical factor to be accelerated and establishing a monitoring parameter [3]. Media pad degradation is a soft failure, it suggests that the pad will not come to a point where it fails completely but the performance drops drastically, and it is not on par with the recommended standards. This recommendation helped in choosing the critical factor as rapid wetting and drying of media pad. [4] Evidence based guidelines for defibrillation pads by Drury used accelerated testing for establishing a maintenance guide.

3.2.4 DEGRADATION MODEL

Accelerated degradation test involves choosing a proper degradation model, establishing a connection between the critical factor and the performance factor that equates to the failure condition. Since the testing involves two parameters i.e., the elevated calcium hardness of water to increase the rate of scaling and the rate of wetting and drying comes under degradation due to usability. These models will be correlated for recommending maintenance criteria for cooling media pads. A model based on the usability rate is established. This usability rate can be used as a factor based on the timing of wetting and drying cycles i.e., actually in use. The degradation based on used rate is well explained in [5]. Analogous model based on the literature review was created for this degradation model.

$$\boldsymbol{Usability\ Rate} = \frac{\boldsymbol{Actual\ Wetting\ Time}}{\boldsymbol{Wetting + Drying\ Time}} \qquad (1)$$

This along with elevated hardness test results and usability rate can be used to establish an empirical relation between conductivity and number of cycles. This empirical relation can be used to control replenishing rates for media pad washing. This can control water usage and create better understanding of sump drain water cycles. Existing maintenance procedures for media pad is 1) allowing the media to dry completely once in a 24-hour cycle. 2) washing the media down with continuous water flow (this would just be ON cycle of the evaporative

cooler) twice a season. There is no reason behind this maintenance, and it is a simple method for extending the life of media pad.

3.2.5 EXPERIMENTAL TEST SETUP

An Airflow test bench with suitable ductwork, equipped with a sump and a water distribution header, is designed to operate the wet cooling media pad. Further details of the test up involving the airflow bench is detailed in [6].

The model of the test setup is depicted in Figure 1. Before every ADT the sump was cleaned thoroughly. The air flow bench conditions were set according to the requirement. Pump was controlled using Arduino. All the monitoring parameters will start recording once the first wetting cycle starts. Table 1 lists the parameters of significance in the degradation testing.

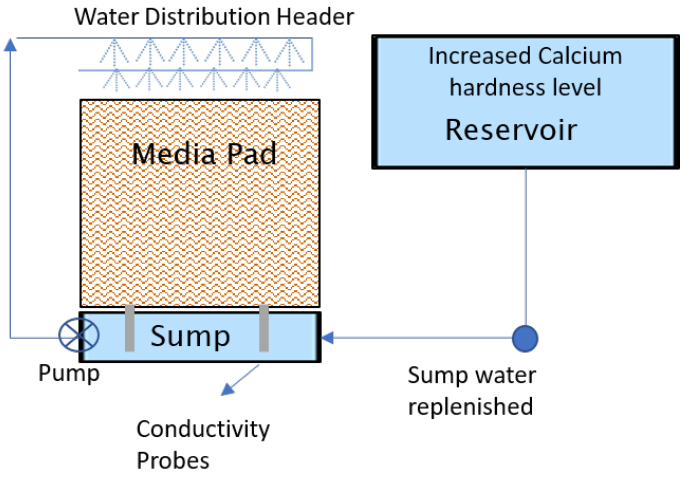

Figure 1: Test setup used for accelerated degradation testing

Table 1: Characteristics of the parameters

Parameter	Equipment used	Properties	Role in ADT
Airflow measured in Cubic Feet per minute (CFM)	Air flow bench with blast gate	Desired flow rates can be achieved by using desired nozzles and blower fan speeds	Maintained constant throughout the test
Elevated Calcium level in water in parts per million (ppm)	Calcium hardness increaser	5lbs of $CaCO_3$ in 10000 gallons of water increases hardness by 10 ppm.	Adjusted according to testing requirement
Sump Water Conductivity in micro Siemens/cm	Conductivity meter operated with Arduino	Output Signal: 0-5V; Range: 0-5000 micro Siemens/cm	Monitored continuously
Temperature (^{o}F) and Relative Humidity (%)	RF code sensors	18 wireless sensors were used. 9 at inlet and 9 at outlet.	Monitored continuously
pH	Digital pH meter	Range: 0 to 14	Monitored at regular intervals
Pressure drop (inches of Water)	Dwyer A-302F-A	Pitot tubes, 4 upstream and 4 downstream of pad	Monitored continuously
Water Temperature (^{o}C)	T-type thermocouple	Directly recorded in Agilent	Monitored continuously
Water flow rate in gallons per minute (GPM)	Submersible pump	Flow rate can be adjusted	Maintained constant throughout the test

Preliminary testing regional water is conducted to establish the elevated level of calcium hardness to be considered for the degradation test. Table 2 lists the Calcium levels of the regional tap water. A reservoir of 55 gallons capacity was setup to continuously replenish water supply to the sump at the required calcium hardness level. Desired calcium concentration in sump water was achieved and verified. Finally, after the completion of test all the data was analyzed. Dip test was performed using calcium hardness testing strip. It will give us the range of amount of calcium present in the sample when compared with the provided chart. The titration gives us the exact amount of calcium present in the water. Both the titration and dip test were performed by using Lammote calcium testing kit. The second result from Table **3** shows that the conductivity of water increased after washing the media pad.

Table 2: Preliminary testing of regional water

Type of water	Type of test	Ca level in ppm
Tap water	Dip test	60-120
Tap water	Titration	110
Drinking water	Dip Test	60-120
Drinking water	Titration	80
Few pellets of $CaCO_3$ added to tap water	Dip test	>180

Table 3: Conductivity of water for initial understanding

Type of Water	Conductivity
Tap water	325 micro Siemens/cm
Conductivity of water washing old pad	1143 micro Siemens/cm

3.2.6 METHODOLOGY

Preliminary tests are run to estimate the rate of wetting and drying for a fixed water flow rate over the media pad. Tests are carried out with tap water and with sump water at elevated Calcium hardness levels. Wetting and drying duration in the experiment is 3 minutes and 7minutes respectively and together they compromise a cycle. The reason behind the above timings is that complete media pad wetting can be achieved during the wetting cycle and longer drying time is provided for water in the pad to get evaporated.

As shown in Figure 2 , the sump water conductivity varies in accordance with sump water levels. The water level starts from 10gallons. The observed trend from this testing was when the water level starts dropping in the sump the conductivity started increasing and once the sump was filled back to its full capacity water conductivity dropped. To perform an accelerated test for long duration a decision was made to provide a continuous supply of water to the sump to maintain a constant volume in the sump for the entire duration. The conductivity results are plotted below in Figure 2 and Figure 3.

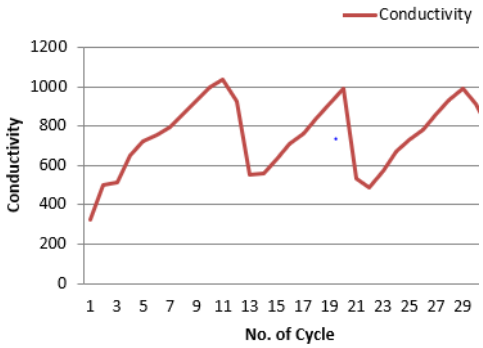

Figure 2: Conductivity of water without continuous supply of water to the sump.

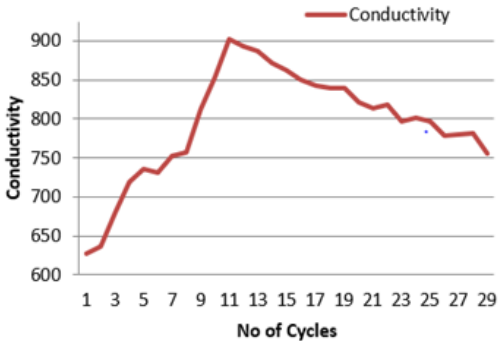

Figure 3**:** Conductivity in sump water with continuous tap water supply to the sump

An EDS (Energy dispersive spectroscopy) test was conducted to quantify the chemical composition of the scaled media pad. A sample from the media pad, pre-used and utilized again for preliminary testing, was analyzed under a Hitachi 3000N SEM machine. SEM Test set up: Vacuum Pressure Range is between 10Pa to 270Pa. 30Pa was used for testing with a working distance of 15mm. Beam current: 25kV.

It is clear from the **Error! Reference source not found.** and **Error! Reference source not found.** that there is a stark difference in calcium level. This result proves that rapid wetting and drying cycles on media pad at elevated levels results in significant deposition of calcium on the pads.

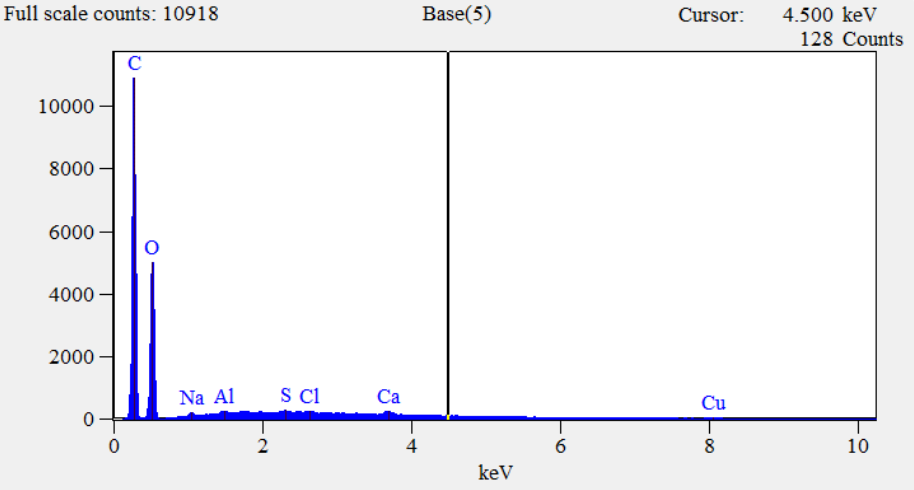

Figure 4: Calcium content in an unused/new media pad

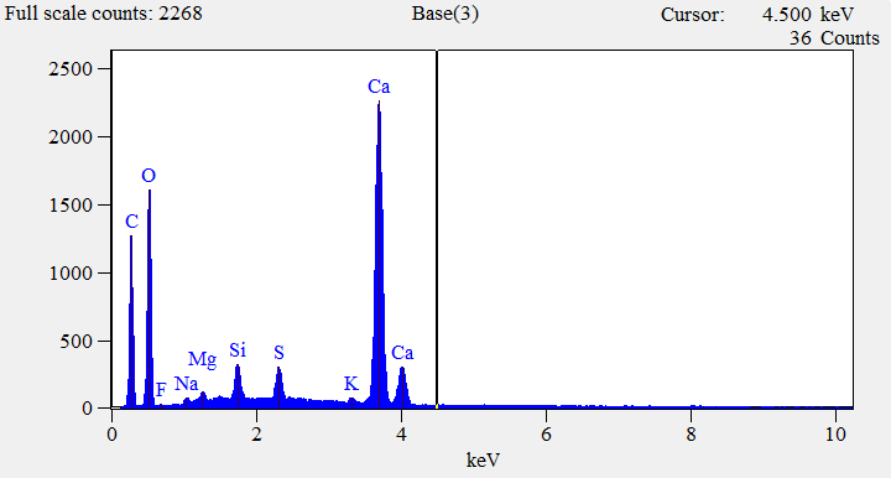

Figure 5: Increased Calcium deposits evident in a used media pad

Table 4: Degradation testing with elevated Calcium hardness levels for extended period of time

S.No	Type of water used	Type of pad used	Number of cycles
1.	300 ppm of calcium maintained in water reservoir	KUUL 12in cellulose media pad previously used in lab conditions [6]	288cycles (2 days)
2.	300 ppm of calcium maintained in water reservoir	Munters CELdek 12in media pad in new condition	720 cycles (5 days)

3.2.7 RESULTS AND DISCUSSION

3.2.7.1 Observations from Test 1

Based on the initial 48 hours test, several observations can be made regarding the media pad degradation. The average conductivity of the water in the sump during the wetting cycle decreased over the testing period as shown in Figure 4.

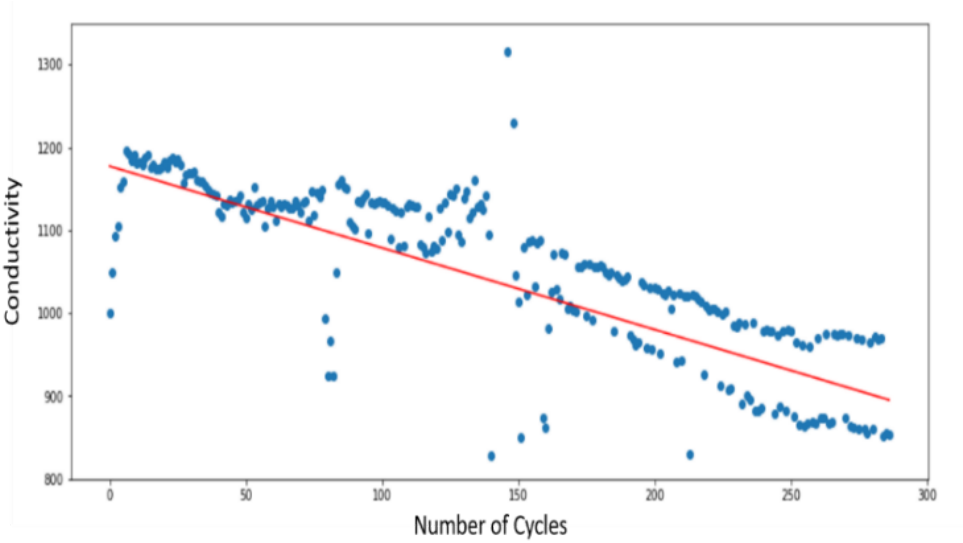

Figure 4: Plot between average conductivity during wetting cycles vs number of cycles.

Based on the observed trend in Figure 4, a line equation is predicted for average conductivity during wetting cycles, given by $\mho$, with respect to the total number of wetting cycles, n.

$$\mho = -0.985(\mathrm{n}) + 177.252 \qquad (2)$$

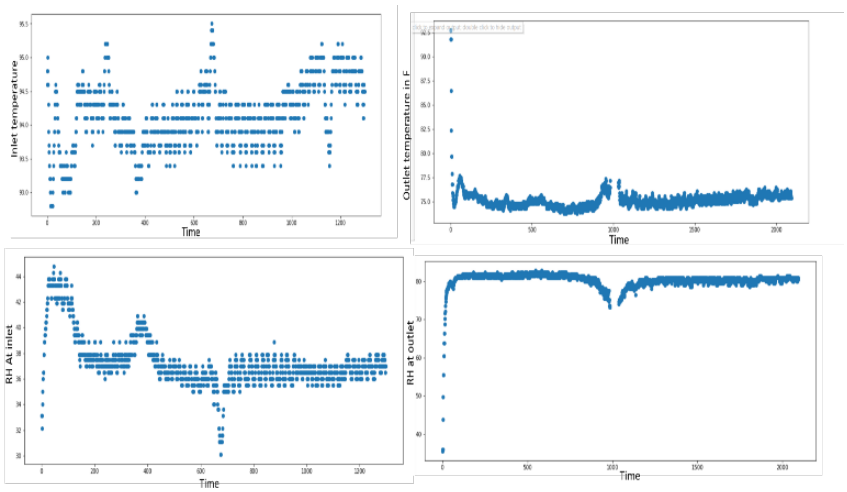

Figure 5: Top two pictures depict the variation in temperature in inlet and outlet. Bottom two pictures depicts the variation in RH in inlet and outlet.

The temperature and relative humidity was not affected by the scale deposition. Figure 5 clearly vindicates the observation and it also matches with manufacturers guide. Scale formation on the pads were clearly visible to naked eyes as shown below in Figure 6. Scale formation was very high on the inlet face of the media, where upstream hot air meets the water and almost negligible at outlet face of the pad.

Figure 6: Scale deposition more pronounced at the inlet of the media pad

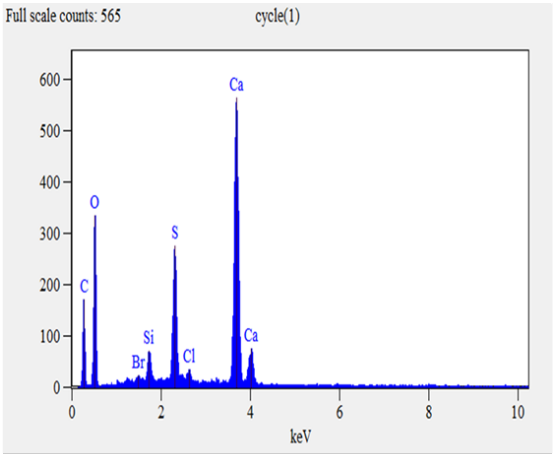

Element Line	Net Counts	ZAF	Weight %	Norm. Wt.%	Atom %
C K	934	3.616	29.45	29.45	40.97
O K	1942	8.071	45.96	45.96	48.00
Si K	564	1.557	1.22	1.22	0.73
S K	2889	1.233	5.64	5.64	2.94
Cl K	311	1.292	0.68	0.68	0.32
Ca K	6855	1.134	16.75	16.75	6.98
Br K	9	1.398	0.29	0.29	0.06
Total			100.00	100.00	100.00

Figure 7: EDS results of media pad sample after accelerated degradation test

A sample was taken from the media pad for EDS test. The testing conditions was same as previous SEM test setup. The results are represented in Figure 7. The spike in calcium content shows the clear deposition of calcium on media pad. A trend which was very confusing was sudden drop of the conductivity during wetting and drying cycles as shown in Figure 8. Once wetting cycle was done there was a sudden drop of conductivity from 1000's to 600's next second. The reason behind this sudden drop must be clarified or analyzed. This drop in conductivity was not on a regular basis or there was no trend attached to it, it happened on a random basis. If there was no drop in conductivity it stayed almost the same with small difference in conductivity during wetting and drying cycles. Weight of the pad also seemed to increase after the testing. The weight of the new pad was not recorded so we were not able to compare the increase in weight. The weight recorded after the testing was 3487 grams.

3.2.7.2 Observations from Test 2

The cooling performance of the media pad did not degrade even though there was good deposition on the pad. Temperature across the media pad just changed slightly according to day and night variation. The plot between temperature at the outlet and number of cycles clearly depicts the change was very low as shown in Figure 8.

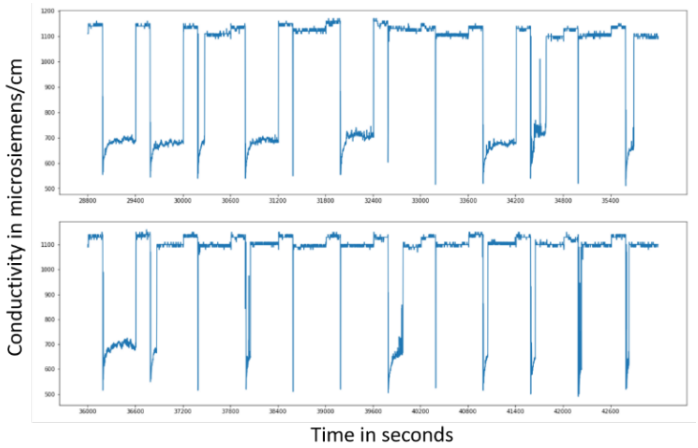

Figure 8: Sample of the conductivity plot with respect to time.

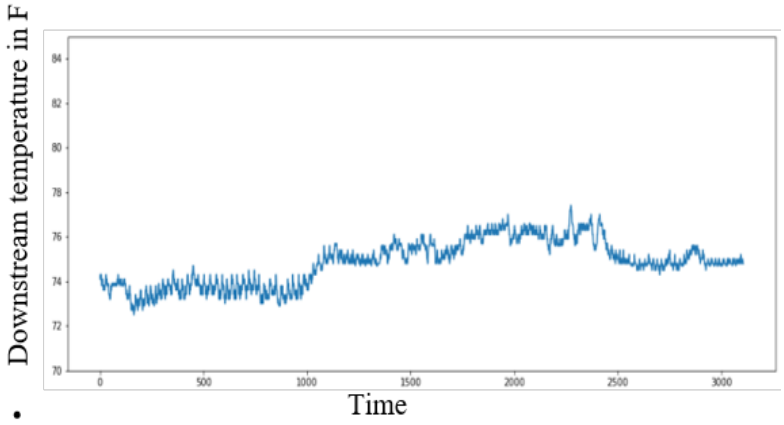

Figure 10 Variation of outlet temperature during the ADT test.

The pressure drop varied between the 0.10-0.18 inches of water. Water temperature varied in the range between 22-25(degree Celsius) as shown in Figure 9. Significant changes were observed only in conductivity and

pH of the sump water and this justifies using water conductivity as the monitoring parameter. Table 5: pH data after each day of **testing**.

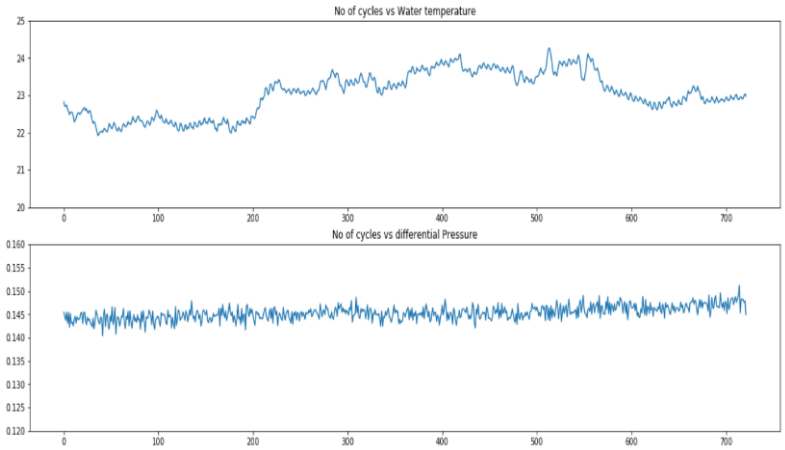

Figure 9: Plot between number of cycles and water temperature, pressure drop.

Table 5: pH data after each day of testing

Day	pH of the sump water
Before testing	7.5
After day 1	7.75
After day 2	7.96
After day 3	8.23
After day 4	8.46
After completion of test	8.65

As there was no bleed off cycle maintained the pH of the sump water kept increasing with increase in scale formation on the pad. During the initial stages of testing the conductivity remained in the 500-600 (micro siemens/cm) range with slight variation. After the 300th cycle there was an increase in conductivity of the water from 600 and started moving to 700. This rate of increase was plotted using a degree 2 curve. Equation of the curve plotted above in Figure 10 is Equation 3.

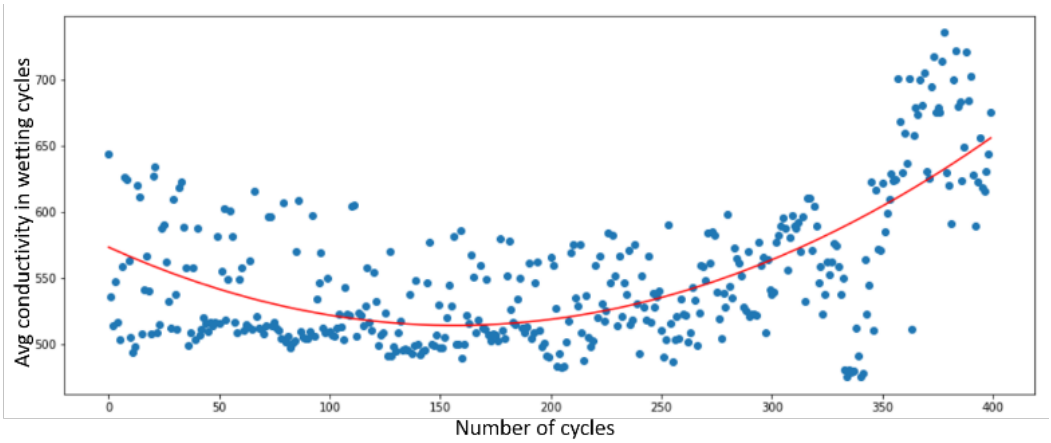

Figure 10 Conductivity plot for the initial 400 cycles.

$$\mho av = 0.0024\ (n^2) - 0.754\ (n) + 537.25 \qquad (3)$$

where $\mho$av is the average conductivity of sump water during wetting of media pad.

When the above equation was extrapolated to the ASHRAE limits the number cycles required to reach the extreme value can be found out. As per the [7] ASHRAE, allowable range is 350-3500microsiemens/cm. Based on above equation, it will take 1272 cycles to reach 3500. This kind of empirical relationship between a monitoring parameter and time will be very helpful for the manufacturers to guide their customers for maintenance of the pad.

3.2.8 CONCLUSION

The accelerated degradation testing performed by rapid wetting and drying clearly proved that it leads to scale deposition on the pads. However, the performance of the media pad i.e. the efficiency of the media pad does not drop drastically with scale deposition. This ADT leads to better understanding of maintaining a media pad based on water quality. Based on the conductivity of water in the sump, water can be replenished accordingly. By this way water is treated as a commodity and use of water can be controlled.

3.2.9 ACKNOWLEDGMENTS

This work is supported by NSF IUCRC Award No. IIP1738811.

3.2.9 REFERENCES

[1] J. D. Palmer, “Evaporative Cooling Design Guidlines Manual for New Mexico Schools and Commercial Buildings,” *NRG Eng.*, 2002.

[2] Hasson, D., M. Avriel, W. Resnick, T. Rozenman, and S. Windreich. "Calcium carbonate scale deposition on heat transfer surfaces." Desalination 5, no.1(1968): 107-119 .

[3] M. Hamada, “Maintenance oriented optimal design of accelerated degradation testing,” no. December, 2006.

[4] N. E. Drury, G. W. Petley, F. Clewlow, and C. D. Deakin, “Evidence-based guidelines for the use of defibrillation pads,” *Resuscitation*, vol. 51, no. 3, pp. 283–286, 2001.

[5] J. W. McPherson, *Reliability Physics and Engineering*. 2010.

[6] A. Al Khazraji, A. Siddarth, M. Varadharasan, A. Guhe, D. Agonafer, J. Hoverson and M. Kaler, “Experimental Characterization of Vertically Split Distribution Wet- Cooling Media Used in the Direct Evaporative Cooling of Data Centers,” IEEE 17th Intersociety Conference on Thermal and Thermomechanical Phenomena in Electronic Systems (ITherm), San Diego, CA, USA, 2018.

[7] R. A. Steinbrecher and R. Schmidt, “Data center environments ASHRAE’s evolving thermal guidelines,” *ASHRAE J.*, vol. 53, no. 12, pp. 42–49, 2011.

3.3 Evaluation of Cooling Control Strategies in Airflow Provisioning Modular Data Centers

3.3.1 ABSTRACT

To achieve energy efficiency and reduce operational costs in data centers with modularized Information Technology and cooling infrastructure there is an ongoing trend to minimize the use of mechanical cooling and instead use outdoor air in favorable environmental conditions for cooling purposes. The cooling module can comprise of evaporative cooling systems which use direct, indirect or a combination of direct/indirect evaporative cooling units to provide adequate cooling. The degree of cooling achieved in the IT module depends on the effective airflow provisioned and the air distribution methods employed. In this study, a modular data center which is equipped with a direct/indirect evaporative cooling unit is considered. The IT module consists of a row of four 42U racks populated with 1U web servers. The conditioned air is supplied through a ducted vent flooding into the cold aisle and the return hot air is exhausted out when not necessary and utilized for mixing purposes otherwise when operating in economizer mode. Commercial CFD tool- 6SigmaRoom is used to develop a CFD model of modular data center and validated with existing research facility in Dallas, TX. To ensure adequate airflow provisioning, a comparison of temperature-based and pressure differential-based measurements in IT module is carried out to control the supply fans in the cooling module. Also, different cooling architectures are studied to determine the impact on thermal performance and efficiency of the cooling solution. The results shall be used to optimize the air distribution on existing research data center facility.

3.3.2 INTRODUCTION

Data centers are equipped with power conversion and backup equipment to maintain reliable power supply and cooling facilities to maintain proper temperature and humidity conditions within the data center. Within the last two decades the amount of digital data generated, stored and transmitted has greatly increased due to the rapid evolution of IT and telecommunication products and technologies. In 2011, IDC [1] reported that the zettabyte barrier was surpassed in 2010 and estimated that the amount of information created and replicated

will surpass 1.8 zettabytes (1.8 trillion gigabytes) in 2011 a nine-fold increase in just five years. The size of the digital world is predicted to increase by a factor of 44 by 2020 [2].

Figure 1: A Data Center Facility [27]

3.3.2.1 Modular Data Centers

A modular data center system is an alternate way to construct the traditional data center in a portable way. Modular data center systems can offer scalable data center capacity with multiple power and cooling options. The modular data center can be shipped anywhere in the world to be added, integrated, or retrofitted into the customer's existing data center footprint. Modular data centers can be the best solution for energy efficiency, reduction in both cost and development time.

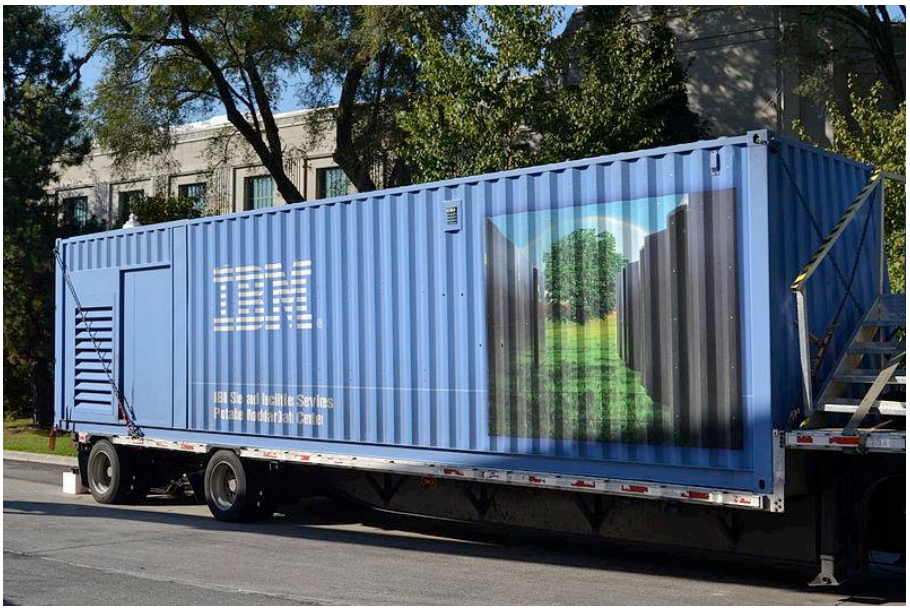

Figure 2: An IBM Modular Data Center [3]

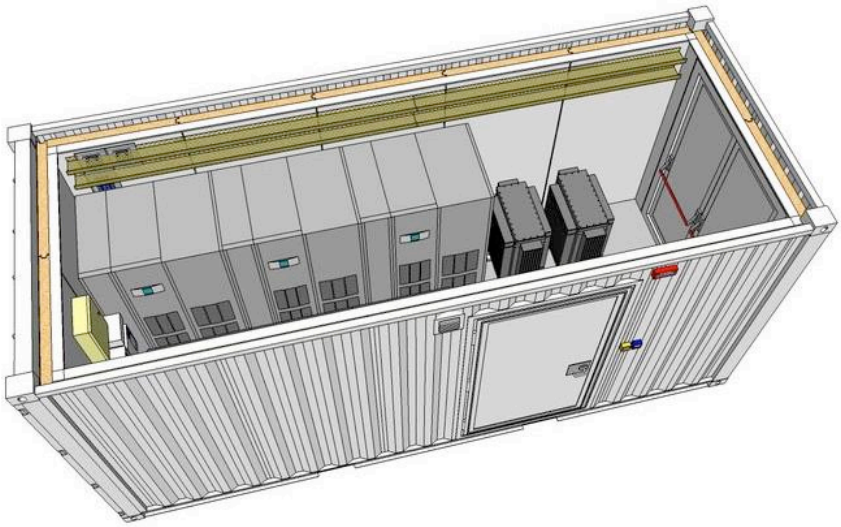

Figure 3: An example of a Modular Data Center

3.3.2.2 Importance of Data Center Cooling and Airflow Management

The degree of cooling achieved depends on the effective airflow provisioning and the distribution methods employed. Recent air cooling advancement includes three basic cooling options (a) room-based cooling, (b) row-based cooling and (c) rack-based cooling.

Room-Based Cooling: The CRAC units are associated with the room and operate to handle the total heat load of the room. Room-based cooling may consist of one or more CRAC units without any predefine air provisioning paths ducts, dampers, vents, etc. Sometimes in raised floor or overhead supply/return airflow provisioning the supply and/or return airflow can be partially constrained. The room level cooling significant fraction of the air from CRAC units bypass the IT loads and return directly to the CRAC. This bypass air represents CRAC airflow that is not assisting with cooling of the loads; which results in a decrease in overall cooling capacity.

Rack-Based Cooling: For row-based configuration, the CRAC units are associated with a row and operate to handle the heat load of a particular row. The CRAC units are located in between the IT racks or they may be mounted overhead. Compared with the traditional uncontained room-based cooling, all of the rated capacity of the CRAC can be utilized due to shorter and well-defined airflow path.

Rack-Based Cooling: With rack-based cooling, the CRAC units are associated with a rack which is dedicated to meet heat load of a rack. The CRAC units are directly mounted to or within the IT racks. Compared with room-based or row-based cooling, the rack-based airflow paths are even shorter and exactly defined. Different airflow provisioning approaches are shown in Figure 4.

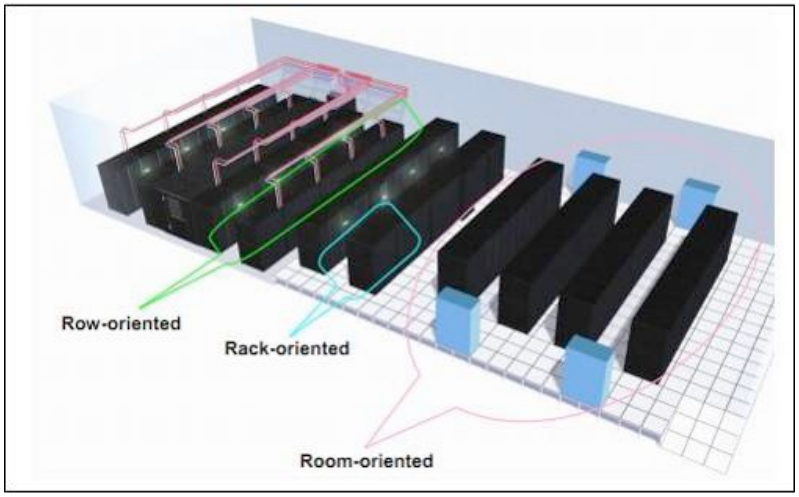

Figure 4: Various Data Center Airflow Provisioning Approaches

This research presents optimization control strategies of airflow provisioning and comparison of various airflow provisioning methods for the modular data center. The computational fluid dynamics model was generated with rack units installed in the facility with emphasize on pressure distribution, airflow pattern, and rack inlet temperature. Study of the effect of different control strategies on server fan performance was carried out.

The candidate airflow provisioning configuration studied includes:

(1) Ducted supply and ducted outlet with containment (2) Raised floor with containment.

Different airflow control strategies considered for study:

(1) Fixed airflow and (2) Pressure differential (CA/HA Pressure differential) based control

3.3.3 MODELING OF MODULAR DATA CENTERS

3.3.3.1 Computational Fluid Dynamics and Fan Affinity Laws

Flow nature inside the data center is always found to be complex due to the high flow rate of cooling air from the cooling unit which results in turbulent flow with large variability in flow velocity magnitude. This kind of complex flow inside the data center required computational fluid dynamics (CFD) and heat transfer to investigate thermal performance of data center. There are several commercially available CFD which can efficiently solve the problem of data center thermal performance. These CFD codes solve incompressible Navier-Stokes equation with

k-∈ turbulence model and energy equation to compute flow and temperature distribution within the data center. The governing equations for the incompressible Newtonian fluid with constant thermal conductivity, k, are provided below [12].

Conservation of mass:

$$\boldsymbol{\nabla} \cdot \vec{V} = 0 \tag{1}$$

Conservation of linear momentum (NS Equation):

Where ν is the constant kinematic viscosity.

$$\frac{\partial \vec{V}}{\partial t} + (\vec{V} \cdot \nabla)\vec{V} = -\frac{1}{\rho}\nabla p + \nu \nabla^2 \vec{V} + \vec{f} \tag{2}$$

Conservation of energy:

$$\rho c_p \left[\frac{\partial e}{\partial t} + (\vec{V} \cdot \nabla)T\right] = k\nabla^2 T + \phi \tag{3}$$

Where Cp is specific heat, φ is the dissipation function representing the work done against viscous forces, which is irreversibly converted into internal energy. It is defined as

The k-ε model

The k-ε model is the most common turbulence model in numerical modeling of data center due to its low computational expenses and better numerical stability. Turbulent viscosity is given by $\phi = (\bar{\bar{\tau}}.\nabla)\vec{V} = \tau_{ij}\frac{\partial v_i}{\partial x_j}$

(4)

where $C\mu$ is a constant, k is the turbulence kinetic energy, and ε is its rate of dissipation. The parameters k and ε are obtained by solving two additional differential equations; for complete details, see Launder and Spalding (1974) [13].

Fan Affinity Laws

Change in fan speed (RPM) alters the air flowrate, static pressure rise, power necessary to operate at new speed.

1st law

$$Q_{N2} = Q_{N1}\left(\frac{N_2}{N_1}\right) \tag{4}$$

Where, $N1$ and $N2$ are fan speed (RPM), $QN1$ and $QN2$ are airflow rates corresponding to speed $N1$ and $N2$ respectively.

2nd law

$$\Delta P_{N2} = \Delta P_{N1}\left(\frac{N_2}{N_1}\right)^2 \tag{5}$$

Where, $N1$ and $N2$ are fan speed (RPM), $\Delta PN1$ and $\Delta PN2$ are static pressure rise across the fan corresponding to speed $N1$ and $N2$ respectively

3rd law

$$W_{N2} = W_{N1}\left(\frac{N_2}{N_1}\right)^3 \tag{6}$$

Where, $N1$ and $N2$ are fan speed (RPM), $WN1$ and $WN2$ are fan power corresponding to speed $N1$ and $N2$ respectively.

Multiple fans system

Fans in series: "n" fans in series will increase pressure "n" times at a given flow rate, with no additional free delivery flow.

Fans in parallel: "n" fans in parallel will increase flow "n" times at a given pressure level, with no additional shutoff pressure generated.

$$\dot{V}_n = \dot{V}_1 \times n \tag{7}$$

Where, V_1 is airflow rate of a single fan unit, n is number of fans within the system

3.3.3.2 Research Modular Data Center

To study efficient cooling approaches like Air-side economization, Direct and Indirect Evaporative cooling and effect of gaseous and particulate contamination, a modular data center has been built at Mestek Inc. Dallas, Texas. This data center is shown in Figure 5 and Figure 6. The schematic of IT pod is shown in Figure 8. IT pod is configured in a cold aisle (CA) / hot aisle (HA) configuration (see Figure 7) and contain four 42U Panduit P/N S6212BP cabinets. The cabinets contains total 120 HP SE1102 servers. Cold air from a cooling unit, Aztec Sensible Cooling Model ASC-15-2A11-00, is delivered to the cold aisle through a supply duct. Supply duct has inlet vent at one end which is configured with 45º angled louvers to guide the airflow inside CA. Hot air from the hot aisle is being supplied to the cooling unit while return cycle is in operation (DEC and IEC) or exhausted to the ambient (ASE). The return duct has pressure relief dampers for pressure control. Description of the cooling unit's construction can be found in its technical guide [14].

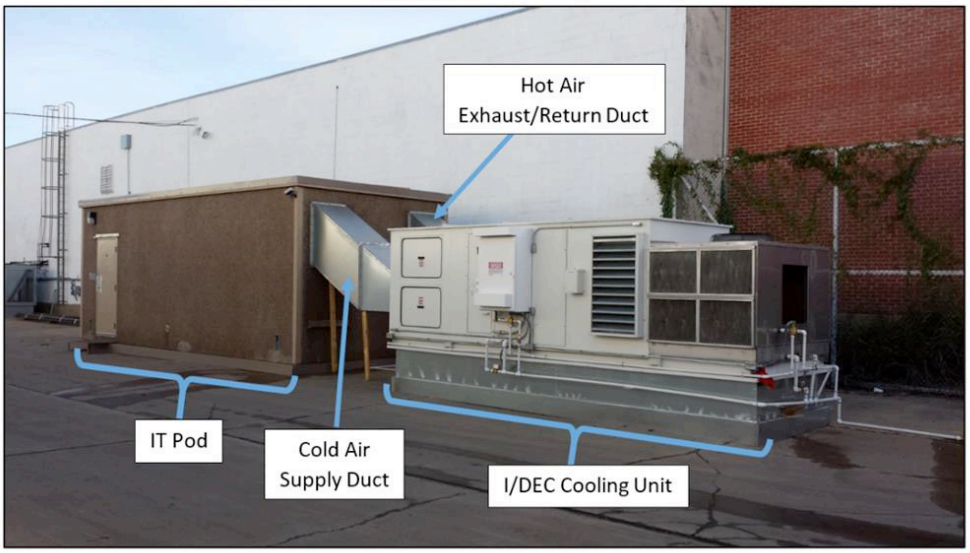

Figure 5: Research Modular Data Center [15]

Figure 6: Return Duct Arrangement of MDC [15]

Figure 7: Cold Aisle/Hot Aisle Containment in the MDC

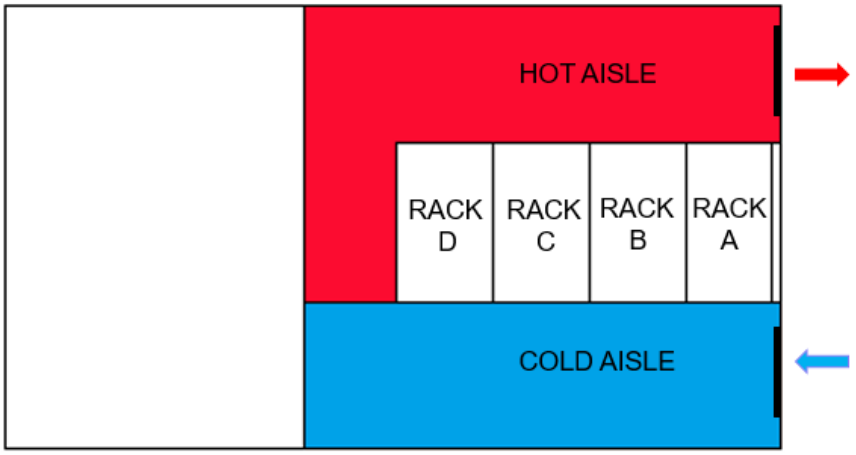

Figure 8: Schematic of rack layout in the MDC

3.3.3.3 ITE specification

Internal details of the server are shown in Figure 9. Server contains a total of four Sunon PMD1204PJB-1 fans in parallel connection and one power supply fan. Details of the fan geometry and flow configuration can be found in manufacturer's manual [17]. Estimation of the power consumption and airflow requirement of the server is included in following sections.

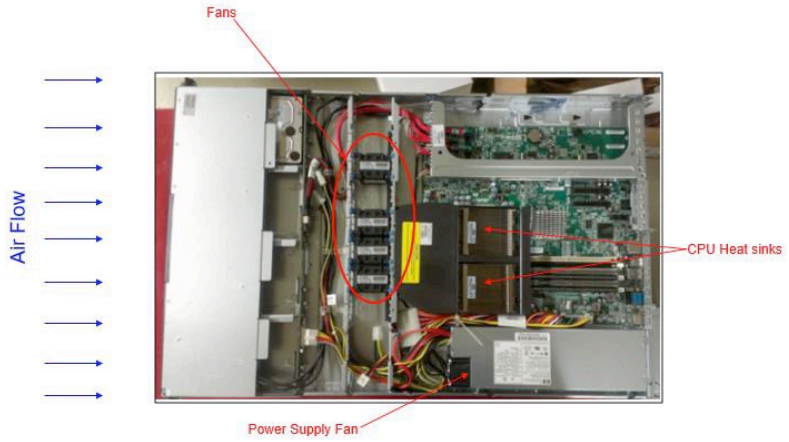

Figure 9: A typical 1 rack unit server – HP SE1102

B.Gebrehiwot [16] investigated estimated power consumption of HP SE1102 server using Lookbusy test and Prime 95 test. I have included results of the prime 95 test which provides a good estimation of power consumption. When the server is stressed using the Small FFTs setting, it draws about 180 W as shown in Figure 10 whereas when it's stressed using In-place large FFTs setting, it draws about 195 W as shown in Figure 11.

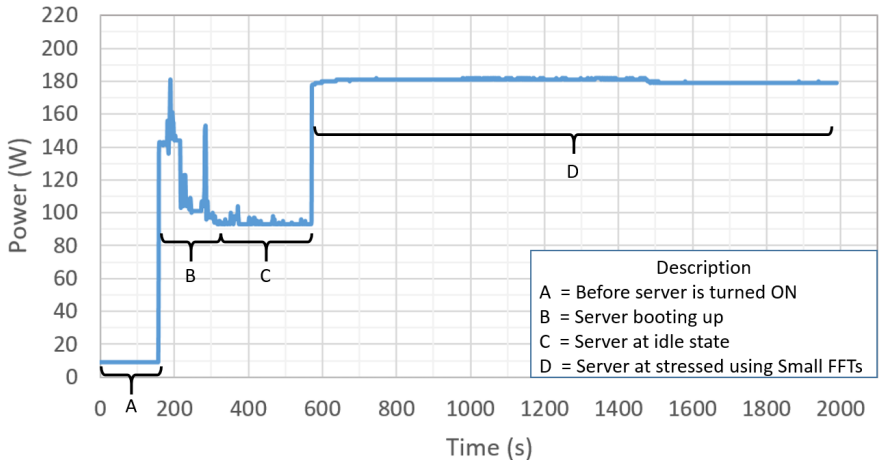

Figure 10: Server Power Estimation Result from Prime95 Test (Small FFTs) [16]

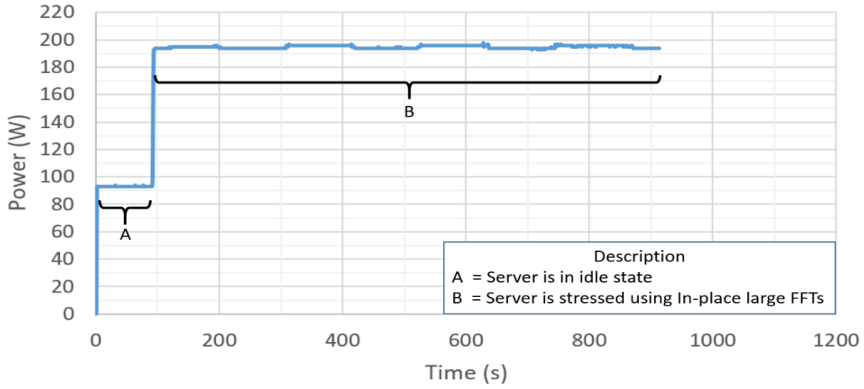

Figure 11: Server Power Estimation Results Prime95 (Large FFTs) [16]

3.3.3.4 MDC Airflow Requirement

Airflow required by the IT pod was calculated using the relation between CFM and KW

$$CFM = \frac{\text{Watts}}{0.316 \times \Delta T} \tag{8}$$

Where, CFM (Cubic Feet per Minute) airflow rate, Watts= Total power of IT pod, ΔT= Temperature Difference across Rack in°F. For this study total power of IT pod was 24 KW, ΔT= 25°F which results in 3037 CFM. This CFM value is considered for fixed airflow provisioning.

To estimate the airflow required by the server first fan manufacturer's data [17] is considered. Using fan affinity laws discussed below, total airflow require for a single server is estimated to be 60 CFM for free air delivery (design) point. Single fan curve, server impedance curve, and total fan curve are shown in Figure 12.

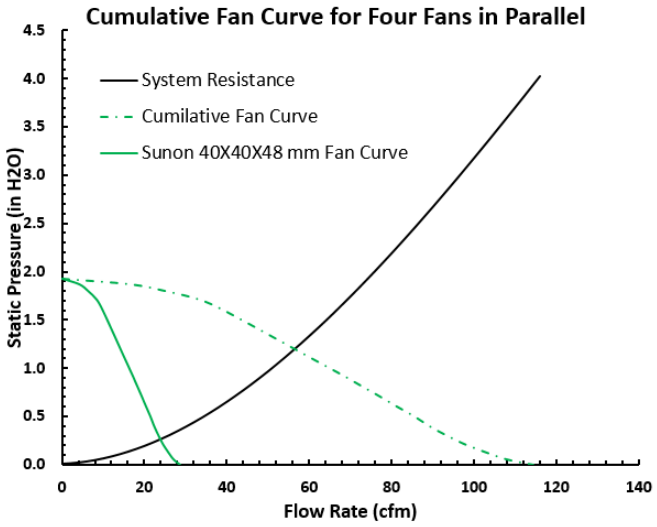

Figure 12: Cumulative Fan Performance Curve for 4 Fans in Parallel Arrangement

Active flow curve approach for airflow estimation: To estimate total airflow required for the IT pod, an HP SE1102 server is first tested on a 30-inch diameter airflow bench (see Figure 13) to find out how much airflow is required for its operation. Active flow curve methodology is used to obtain the flow curve as discussed in the literature. The server is mounted on the airflow bench as shown in Figure 14. General guidelines for setting up the airflow bench test and methodology to obtain active flow cure are followed as provided in [18].

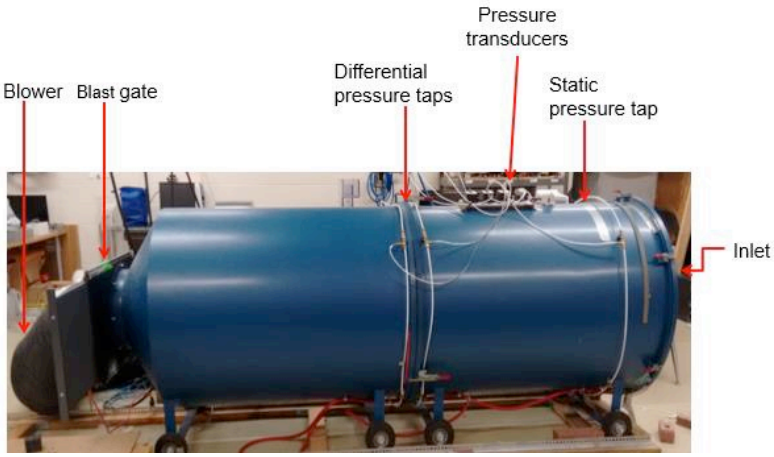

Figure 13: Airflow Bench

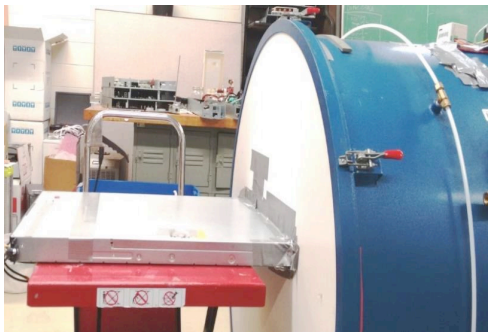

Figure 14: HP SE1102 1-RU server mounted on the airflow bench

Experimental results and comparison with theoretical data are shown in Figure 15. Results from the test indicate that server required 36.5 CFM approx. for free air delivery condition which was in very good agreement with the research carried out by A. Husam [19].

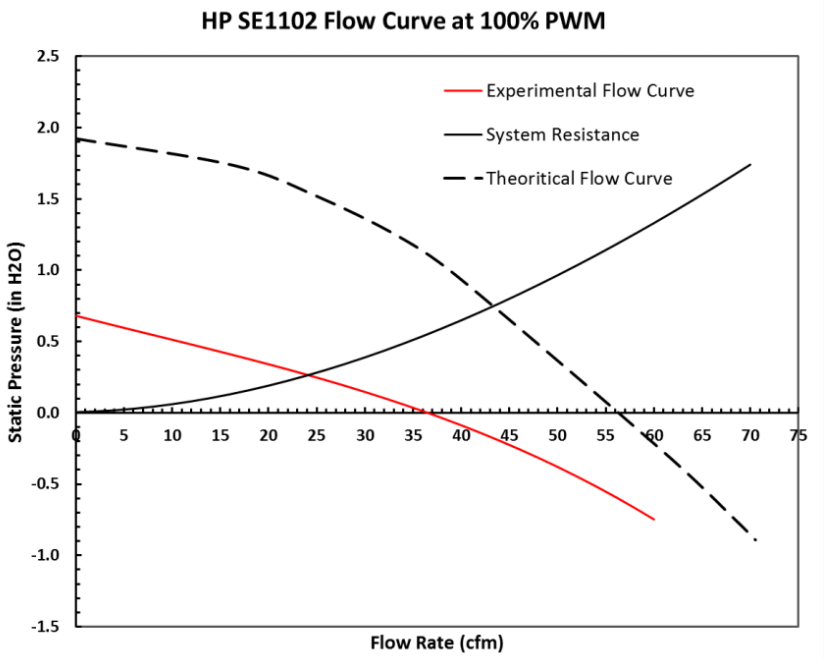

Figure 15: Active flow curve obtained experimentally

For the 120 servers inside the IT pod, a minimum of 36.5 CFM x 120 server = 4380 CFM is needed. This calculation did not take into account the air flow requirement of additional IT equipment, such as switches, expected increase in airflow rate if inlet air temperature is at a higher temperature, or possible increase in the number of servers in the future.

3.3.3.5 CFD Model of Research Modular Data Center

Security and reliability concerns allow limited access to operating data center for thermal characterization and airflow behavior study. Large data center facilities exhibits constrain for temperature and pressure data measurement across the facility. Use of computational fluid dynamics and heat transfer is the most common approach to predict the airflow and temperature distribution inside the data center.6Sigma DC commercially available CFD code was used to develop a numerical model of research data center. The component of data center includes total 4 racks. Racks are populated with total 120 HP SE1102 servers, servers are mounted in similar

pattern to existing stacking pattern in research data center. The effective active flow curve was obtained by mounting the server to airflow bench and varying the flow rate and pressure while the server fans were operating. CFD model of a modular data center is shown in Figure 16.

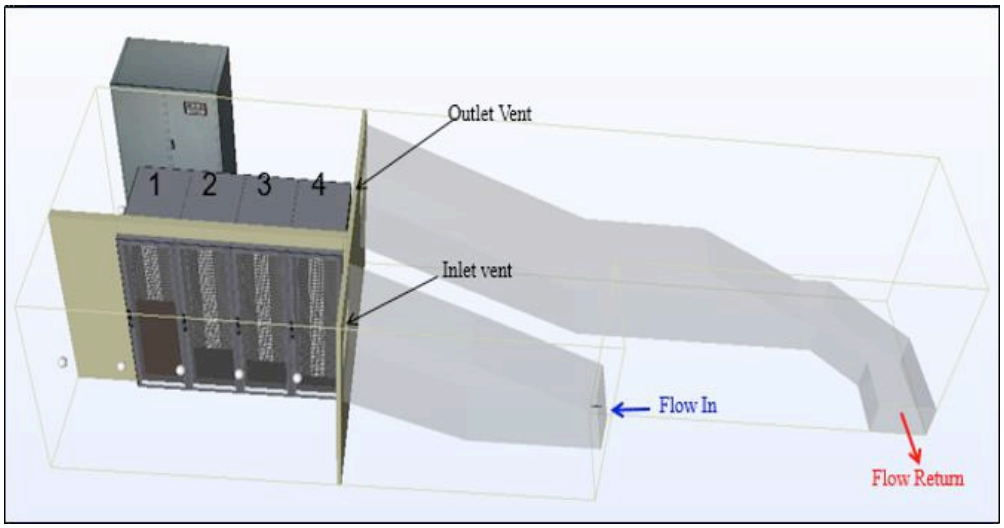

Figure 16: CFD Model of the research modular data center

In actual data center facility airflow entering the CA at very high-velocity results in large amount of recirculation of airflow inside CA. Recirculation creates low-pressure area at the center of the circulation and makes it harder for server fans, which are close to the center of circulation, to draw in air. Another reason for maldistribution of air flow through the servers is that air enters the cold aisle at high speed and perpendicular to the direction of air intake to the servers. This kind of maldistribution further increases the difficulty in drawing air in. With an increase in IT load, the amount of volume flow rate that needs to leave from HA increases but due to insufficient outlet vent area airflow gets trapped inside HA which results in high pressure in HA.

CFD analysis is used to provide the prediction of the airflow distribution, pressure, and temperature distribution. Blanking panels were installed in racks in the absence of the server. Blanking panels were provided with 5% equally distributed leakage over the panel area to monitor the effect of negative pressure differential across the server rack. In pressure differential control configuration, a pressure controller is used to control the

airflow rate of the CRAC upon satisfying the specific pressure differential. Five pressure sensors are placed in CA and HA each, the average of the sensor at each side is taken then the pressure differential is measured and checked to meet the set point criteria.

The pressure differential $\Delta P = P_{cold} - P_{Hot}$. Pressure differential set point considered for the study was +0.04 in/H_2O (over provisioning).

3.3.4 RESULTS AND DISCUSSION

3.3.4.1 Fixed Airflow Provisioning

Pressure distribution plot for the fixed airflow provisioning is shown in Figure 17. As results indicate due to high pressure in HA and low pressure in CA, the pressure differential across the server racks is $-0.202\ in.\ H_2O$. Negative pressure differential causes entrainment of hot air from the HA to CA (backflow).

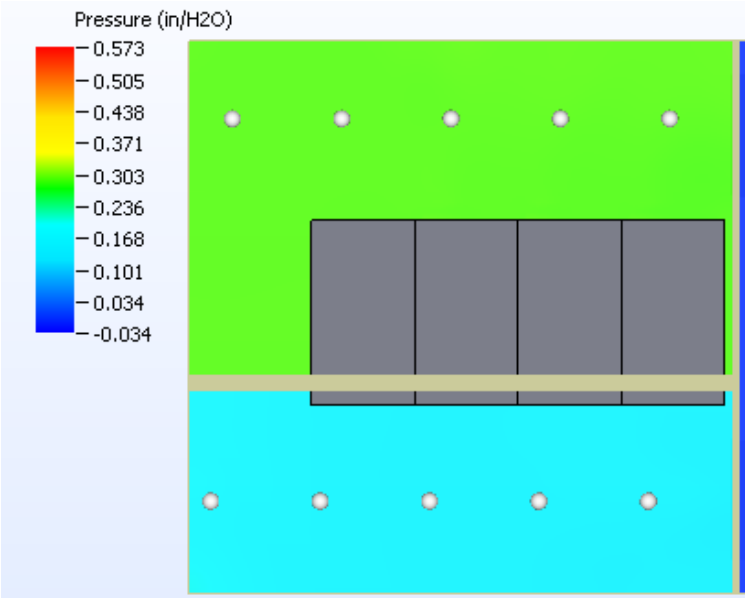

Figure 17: Pressure distribution in the MDC

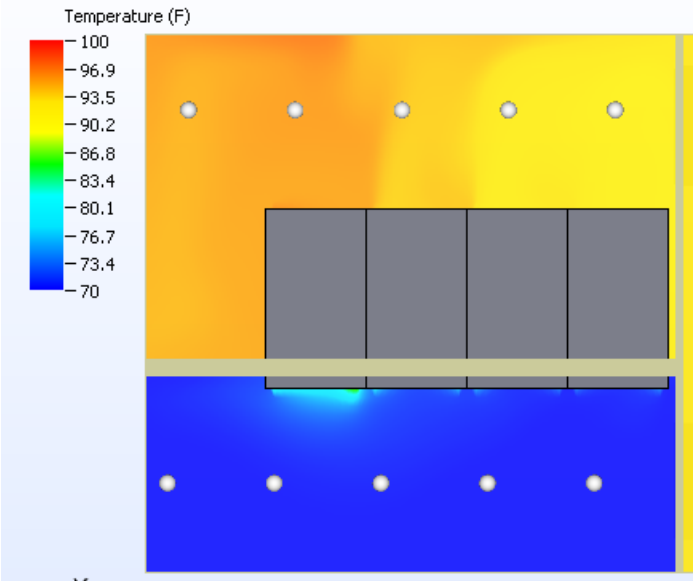

Figure 18: Temperature contour in the MDC

Temperature distribution in CA-HA indicates that hot air from the HA gets mixed with cold air at the inlet of a server rack. Due to backflow, the temperature at the rack inlet increases which results in decrease in cooling capacity of the cold air. Temperature plot at the server inlet is shown in Figure 19 indicates some temperature hot spots at server inlet that may cause effects as drastic as a failure of the server component.

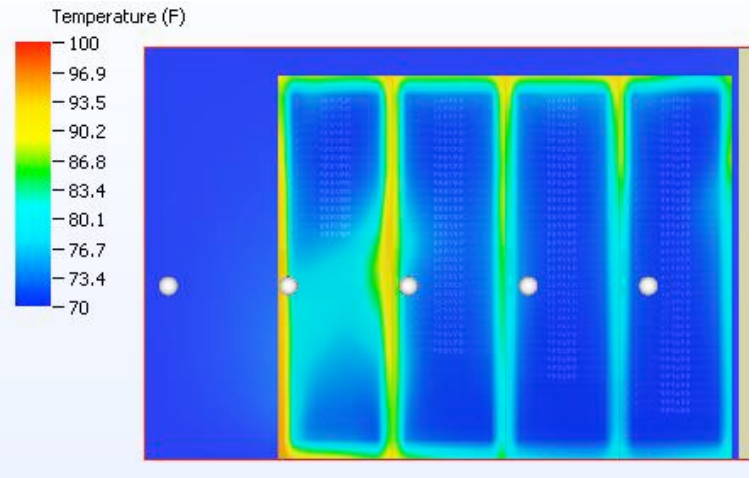

Figure 19: Temperature distribution at the rack inlet

To avoid the adverse effect of recirculation of hot air into cold aisle perfect containment of the CA and HA can be the solution. The temperature distribution plot at the inlet of the racks in for the perfectly contained CA and HA in Figure 20 indicates that there is no hot air mixing with cold air due to recirculation. In practical applications, perfect containment of the CA and HA is impossible to achieve because always there between racks, under racks, door seams and between blanking panel.

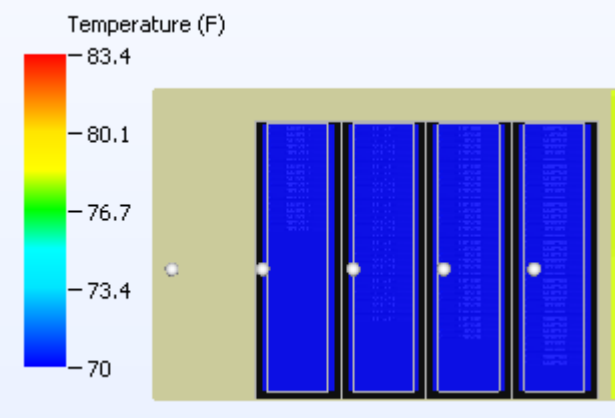

Figure 20: Rack inlet temperature distribution for ideal containment scenario in the MDC

3.3.4.2 Pressure Differential Controlled Airflow Provisioning

Pressure distribution in CA and HA is shown in Figure 21 indicates that pressure differential across the server rack is at set point 0.04 in/H_2O. CFM required to obtain set point pressure differential was 4912 CFM. Temperature distribution in CA and HA as well as at inlet of server rack is shown in Figure 22 & 23.

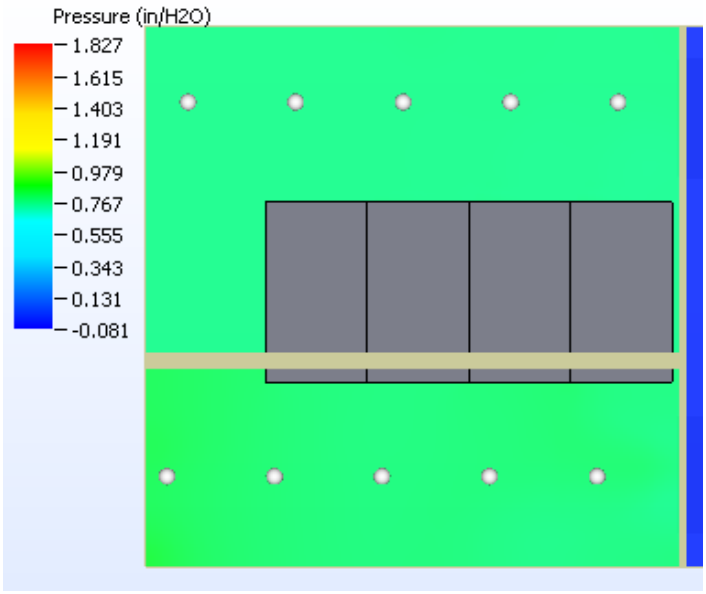

Figure 21: Pressure distribution in the MDC

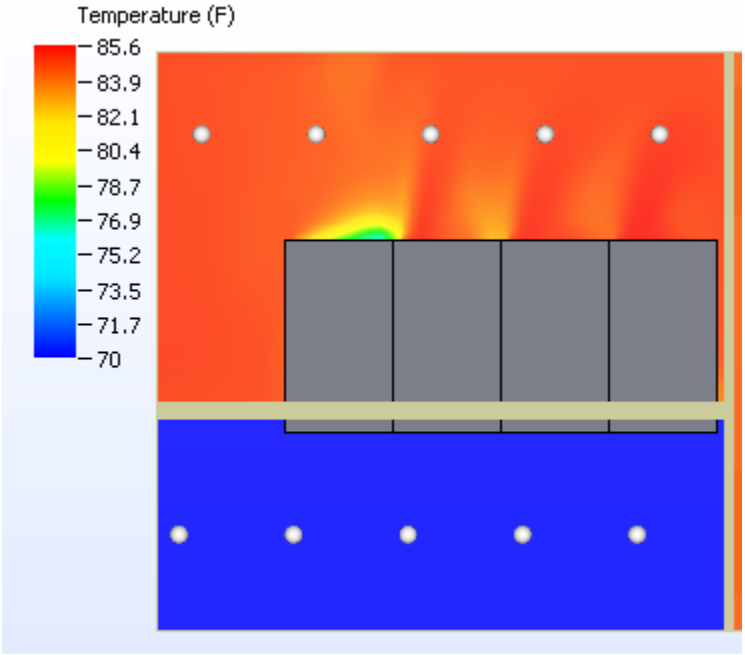

Figure 22: Temperature distribution in the MDC

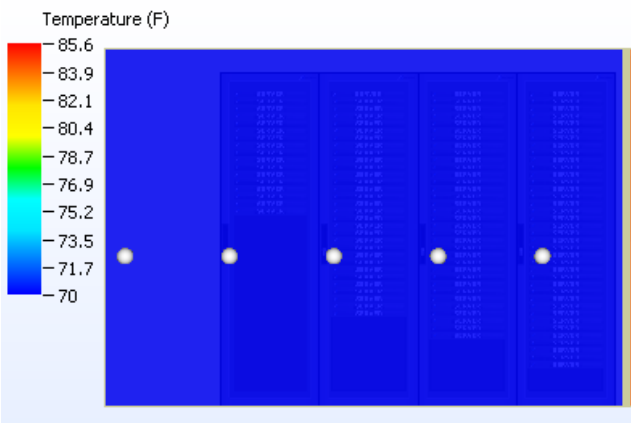

Figure 23: Rack inlet temperature distribution in the CA of the MDC when a positive pressure differential is maintained across the row of racks

Temperature distribution indicates that due to high pressure in cold aisle there is no back flow from the hot aisle. Even though backflow problem is solved, Figure 21 indicates that due to a positive pressure differential cold air from the CA is directly passed through the leakage and get mixed with hot air in HA which results in low-temperature CRAC return air. Low-temperature CRAC return airflow reduces CRAC unit efficiency. Iterative study to investigate the pressure differential set point to just remove the backflow effect can stop cold airflow mixing with hot air directly through leakage.

3.3.4.3 Effect of Airflow Provisioning on Server Performance

To understand the effects of different control strategies airflow provisioning on server performance and impact on total energy consumption three servers from the each rack was monitored for this comparative study. From each rack top, middle and lower most server was taken under consideration. In CFD study equipment inlet temperature and airflow rate of server fans were consider as monitor criteria and measured for both fixed airflow provisioning method as well as provisioning method to maintain positive pressure gradient across the racks.

Effect on equipment inlet temperature: Equipment inlet temperature results are shown as a chart form in Figure 24 and Figure 25. Equipment inlet temperature is most likely to rise due to backflow effect. Hot air

penetration into the cold aisle plays a significant impact on inlet temperature. At top of the rack due to the presence of the gap and at bottom of the rack due to blanking panel leakage backflow is most likely to take place. A temperature rise of the equipment is a result of backflow which leads to high-temperature value of top and bottom server as compared to middle one. On the other hand, equipment temperature for overprovisioned pressure differential control airflow provisioning falls under the acceptable range of ASHRE 2011 compliance [22] and uniform over the rack.

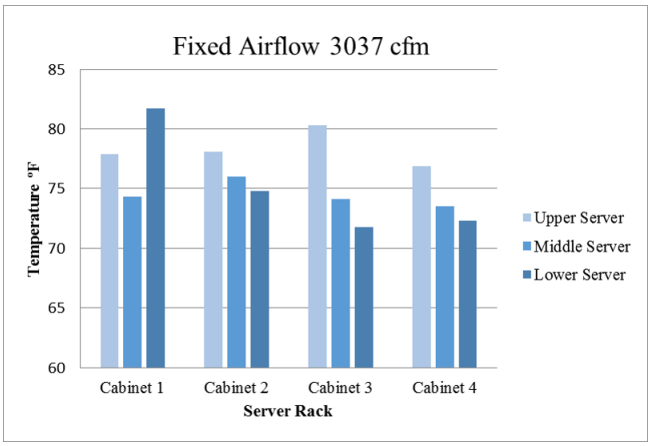

Figure 24: Server flow rates for fixed flow provisioning

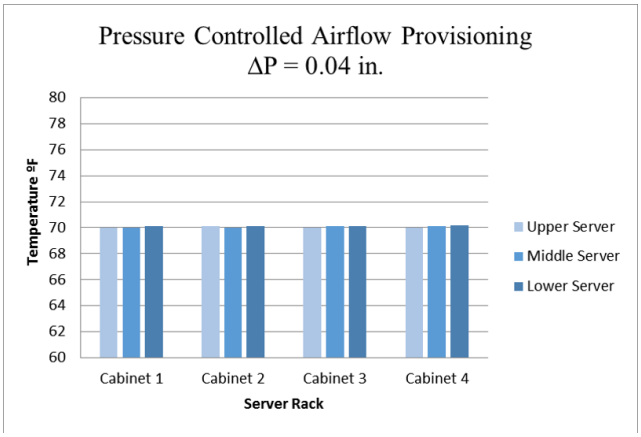

Figure 25: Server flow rate upon overprovisioning of airflow

Effect of server flow rate: Figure 26 and Figure 27 demonstrate server flow rate for lower, middle and top server for fixed and over provisioned airflow provisioning. Operating flow rate of the server is governed by the experimentally measured flow curve discussed in earlier section. Free air delivery point on active flow curve is 36.5 CFM.

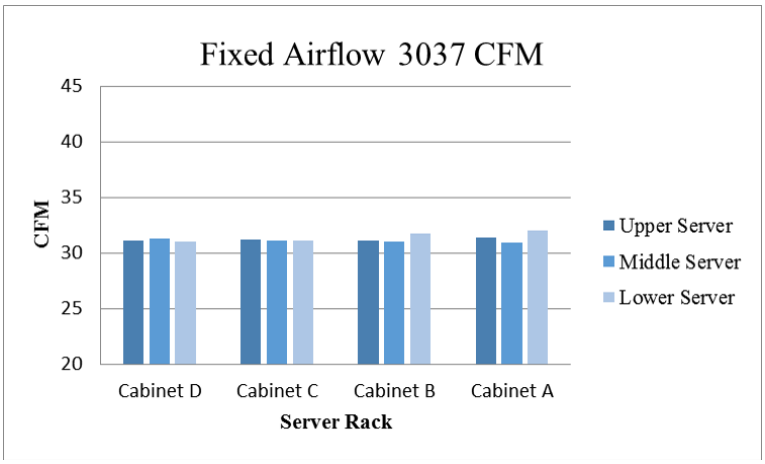

Figure 26: Server flow rates for fixed flow provisioning

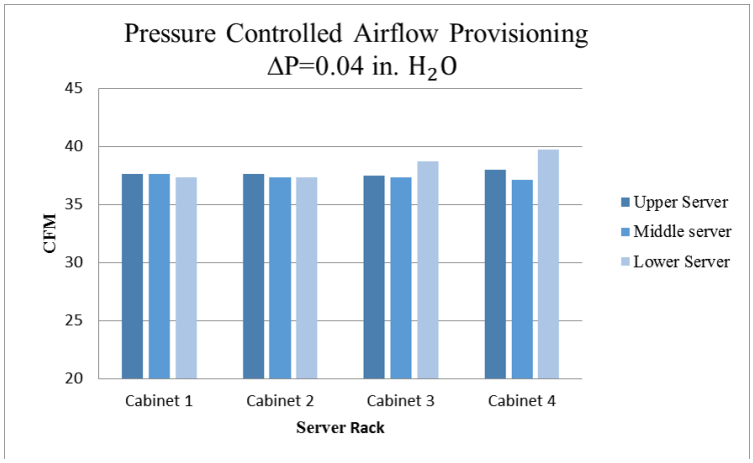

Figure 27: Server flow rates upon overprovisioning of airflow

High pressure in HA generates resistance for flow to pass through the server for fixed airflow provisioning. As shown in Figure 26 for fixed airflow provision servers are operating at lower flow rate than free air flow rate and

operating point falls in the hindering region on flow curve. Reduction in server flow rate can create the adverse effect on server performance like an increase in temperature and more power consumption to meet the design criteria. For over-provisioned airflow supply due to higher pressure in cold aisle server flow rate exceeds the free air delivery point 36.5 CFM. Airflow operating point lies in aiding region of the active flow curve. The increase in flow rate helps in improvement of server performance by keeping the temperature value in the acceptable range.

Over-provisioning of airflow by maintaining positive pressure gradient across the server rack can be useful to avoid hot air penetration from HA to CA up to certain threshold value of leakage (perforation in containment). The threshold value for the leakage is 15% of total containment area [21]. For the leakage ratio less than the threshold value, overprovisioning can be used to get high enough pressure distribution in CA to prevent hot air leakage in CA. For leakage greater than threshold value any overprovisioning of airflow will result in loss of cold air. A higher value of leakage may allow cold air to pass directly through the perforation instead of servers will results in loss of cold air.

If the server fan can ramp down when possible depending on component temperature using intelligent fan speed control algorithm [22]. During overprovisioning, server fan can be ramped down to reduce airflow rate to certain level and server can still operate allowable temperature range of the component. Less server airflow results in the reduction of total airflow demand from the CRAC unit to save a significant amount of energy.

3.3.4.4 Comparison of Airflow Provisioning Architectures

Thermal management of data center incorporates various cooling techniques at the chip level, server level, rack level, and room level. At room-level cooling, several alternate air supply and return configurations are employed. Different provisioning architectures with containment are considered as a key cooling solution for data center industries. Containment configuration includes cold aisle containment (CAC) and hot aisle containment (HAC), which segregate cold and hot air inside the data center. Containment enhances energy saving by operating cooling unit to at high return temperature and avoid mixing of hot air with cold air.

Raised floor plenum cooling architecture is commonly used in data center industries because of liberty of server rack arrangement provided by it. For the raised floor room-level cooling configuration, perforated tiles are placed in the cold aisle which supplies cold air to rack. To complete the airflow loop hot air from the rear of the rack is extracted from the ceiling vent and returned to CRAC unit. Comparison between raised floor and ducted supply/return configuration is included in following part of a study.

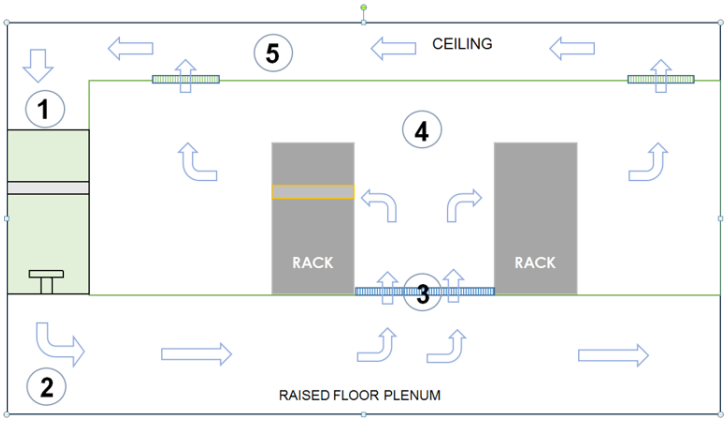

Figure 28: Schematic of a raised floor data center [25]

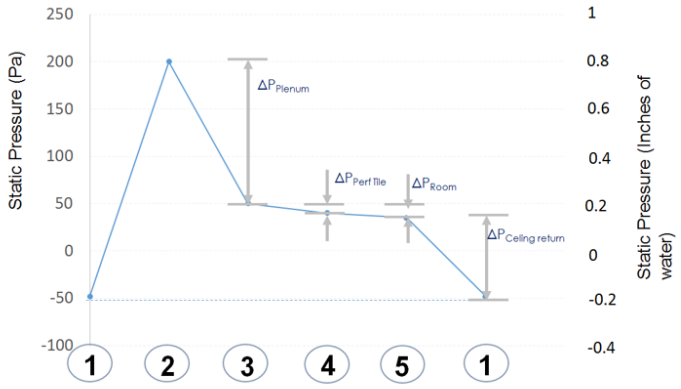

Figure 29: Variation of the static pressure profile in a raised floor data center [25]

CFD Modeling of Raised Floor Data Center Configuration:

Security and reliability concerns allow limited access to operating data center for thermal characterization and airflow behavior study. Large data center facilities exhibits constrain for temperature and pressure data measurement across the facility. Use of computational fluid dynamics and heat transfer is the most common approach to predict the airflow and temperature distribution inside the data center. 6Sigma DC commercially available CFD code was used to develop the numerical model of research a data center. The component of data center includes total 4 racks. Racks are fully populated with total 120 HP SE1102 servers. The effective active flow curve was obtained by mounting the server to airflow bench and varying the flow rate and pressure while the server fans were operating. CFD model of the modular data center is shown in Figure 30.

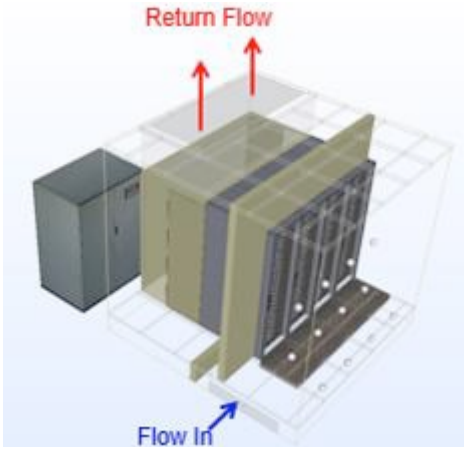

Figure 30: CFD model of the raised floor data center configuration considered in the comparative study

Total IT load is 30.4 KW which required 4810 CFM to meet the power capacity. Perforated tile with 50% perforation area tiles is placed for each rack to supply cold air from the plenum. Parametric study and literature study is carried out for a suitable height of raised floor. For the floor are less than 1000 square feet area 12 inch raised floor height is suitable.[26]

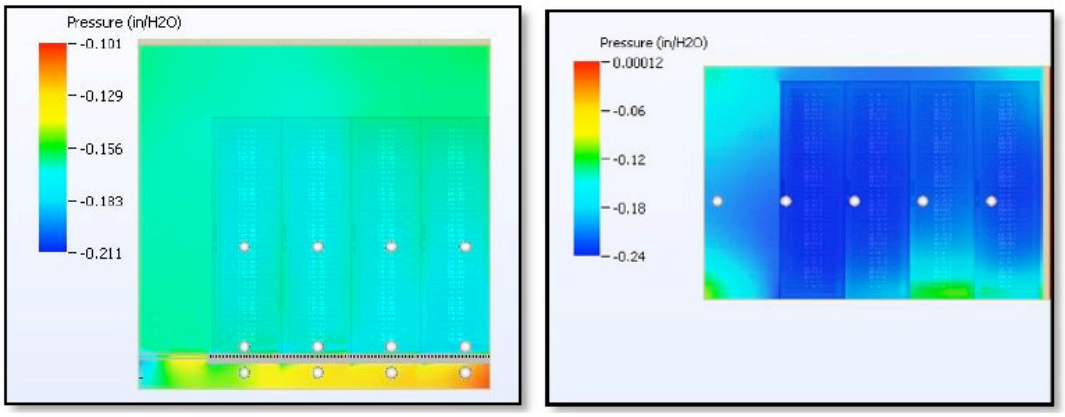

Figure 31: Pressure distribution of the raised floor (Left) and ducted system (Right)

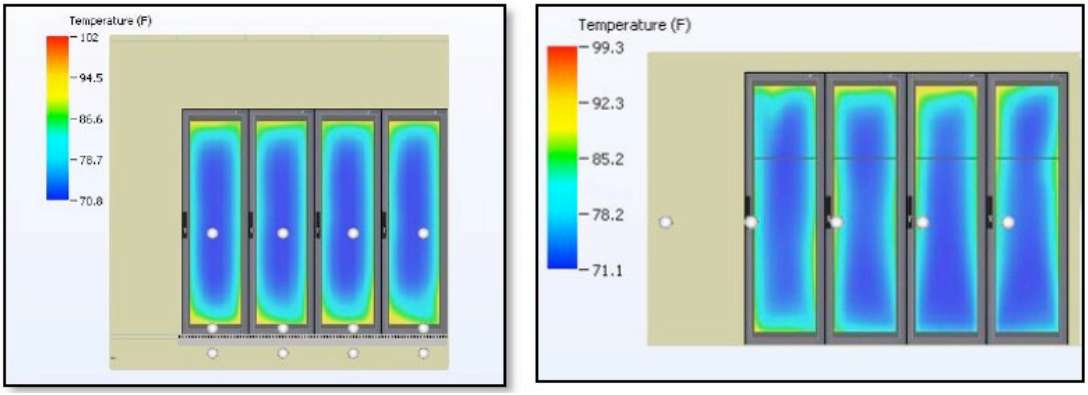

Figure 32: Temperature distribution for raised floor (left) and ducted system (right)

Temperature distribution at the rack inlet is shown in Figure 32 for raised floor data center and ducted supply/return configuration. Temperature at the bottom of racks is very high due to lack of airflow and temperature on the top of the racks increases due to recirculation of hot air into cold aisle through leakage. ASHRAE thermal compliance plot in Figure 33 and Figure 34 represents equipment temperature which provides better comparative sight for thermal performance of different architectures. Results indicates that there are more number of server which falls in acceptable temperature range. In case of raised floor data center configuration very few servers are in acceptable temperature range.

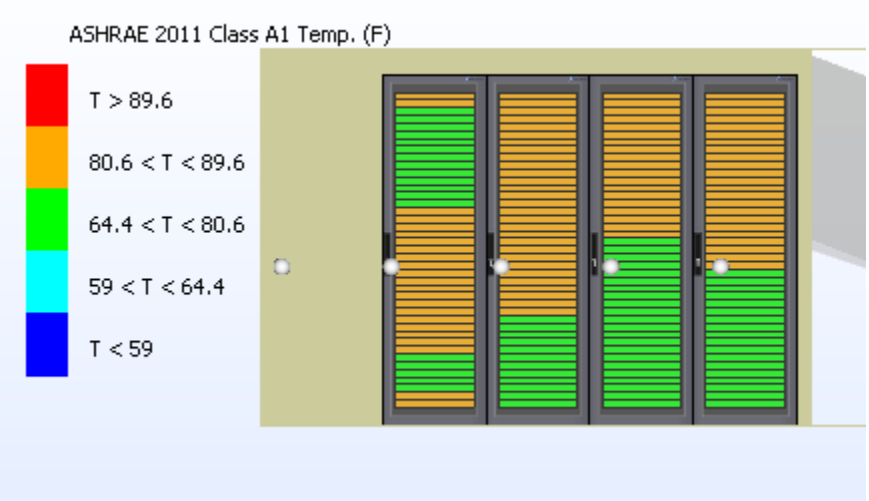

Figure 33: ASHRAE 2011 Class A1 Thermal Compliance for Ducted System Airflow Provisioning Architecture

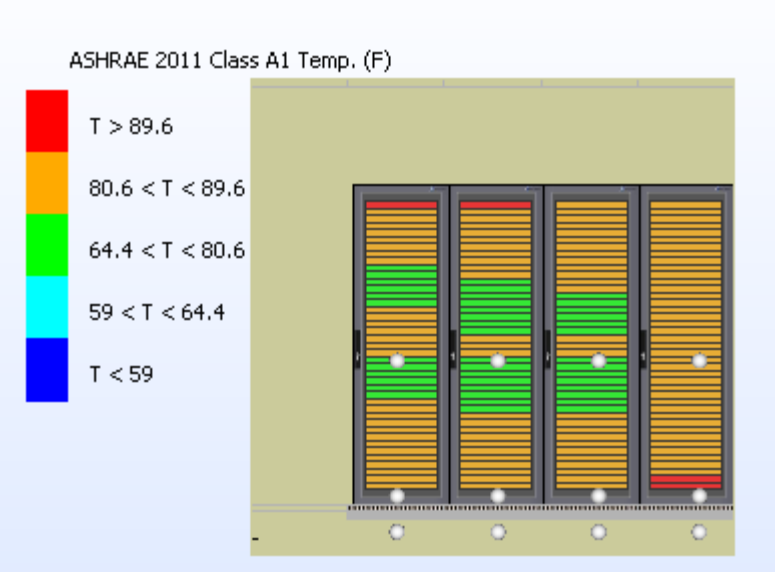

Figure 34: ASHRAE 2011 Class A1 Thermal Compliance for Raised Floor Airflow Provisioning Architecture

3.3.5 CONCLUSION

Data center houses IT equipment which is used for digital data storage, processing, and transmission. Use of high-performance microprocessor, high-density electronic packages and high heat load capacity racks in data

centers resulted in high heat dissipation rate. For reliable data center operation, removal of dissipated heat and proper cooling has become the main concern of data center industries. Reduction in energy consumed by the cooling unit cooling unit can significantly improve the energy efficiency of data centers. Use of proper airflow provisioning and control system can significantly reduce airflow demand and proper extraction of heat can be done.

In this study, different approaches for efficient airflow management is discussed. Depending on the data center capacity and architecture different airflow provisioning can be deployed to meet the efficiency criteria. To study the effect of different airflow provisioning strategies research modular data center that uses direct and indirect evaporative cooling unit has been used. In actual data center facility, pressure inside CA is very low due to maldistribution of airflow. Also, with the increase in IT load, the amount of volume flow rate that needs to leave from HA increases but due to insufficient outlet vent area airflow gets trapped inside HA which results in high pressure in HA. This kind of imbalance of pressure in CA and HA results in negative pressure gradient across the rack and increases the risk of backflow.

Estimation of power consumption in IT pod earlier research study results was considered. Airflow bench test to obtain active flow curve to determine the airflow requirement. Using practical data detail CFD model was created to get pressure and temperature distribution inside the IT pod for different airflow provisioning. Results suggest that to reduce the risk of backflow and to maintain positive pressure gradient across the rack instead of fixed airflow provisioning, pressure differential-controlled airflow provisioning should be deployed. To estimate the correct amount of airflow requirement for IT pod additional efforts should be applied to determine pressure loss due to various factors like recirculation, Venturi effect, and losses due to friction presented by airflow path. Different cooling architecture has its own benefits and drawbacks. The second part of the study is focused to determine the effectiveness and comparison of different data center cooling architecture. Rack inlet temperature highly depends on the airflow management. Configurations presented with various assumptions like inlet louvers

angle, server fan operating speed, leakage ratio, and distribution, perforated tile design et cetera, depending on the performance requirements, configurations need to be changed. As per the results for efficient thermal performance of modular data center with small capacity ducted supply/return configuration, overhead supply/return system is suitable configuration. For data centers with large capacity and floor area raised floor data center is ideal due to liberty in rack arrangement.

3.3.6 REFERENCES

[1] J. Gantz and D. Reinsel, "Extracting Value from Chaos," June 2011.

[2] Forsythe_Technology/the-data-center-now-and-in-the-future 2013

[3] https://commons.wikimedia.org/wiki/File:IBMPortableModularDataCenter2.jpg

[4] http://www.seedit.asia/index.php/background

[5] United States Environmental Protection Agency Energy Star program (2007) Report to congress on server and data center energy efficiency public law 109-431, 2 Aug 2007

[6] J. Koomey. Growth in data center electricity use 2005 to 2010. Analytics Press. Oakland, CA. 2011[Online]. Available: http://www.analyticspress.com/datacenters.html.

[7] P. Delforge. (2015, February 6). *America's Data Centers Consuming and Wasting Growing Amounts of Energy* [Online]. Available: http://www.nrdc.org/energy/data-center-efficiency-assessment.asp.

[8] http://www.lgcnsblog.com/wp-content/uploads/2015/06/robot_02.png

[9] Madara, S., “Best Practices in Data Center Cooling”, www.afcom.com data center management magazine article, Nov./Dec. 2004 issue

[10]Stal L, Belady C (2001) “Designing an alternative to conventional room cooling,” in 23rd international telecommunication energy conference, Edinburgh, 14-18 Oct 2001, p 109-115

[11] White paper 130, “Choosing between Room, Row, and Rack-based Cooling for Data Centers” Schneider Electric’s Data Center Science Center, DCSC@Schneider-Electric.com,p 3-7

[12] http://users.metu.edu.tr/csert/me582/ME582%20Ch%2001.pdf Finite Element Analysis in Thermofluids Dr. Cüneyt Sert

[13] Launder, B.E. and D.B. Spalding, 1974, The Numerical Computation of Turbulent Flows, Computer Methods in Applied Mechanics and Engineering, Vol. 3, pp. 269 – 289.

[14] Aztec Sensible Cooling. Indirect and indirect/direct evaporative units. *(TGASC-1),* 2010. Available: http://www.appliedair.com/modules/news/upload/%7BBC036927-4E95-47BD-A79B-F6B55467BD7A%7D_TGASC-1.pdf

[15] S. Sathyanarayan, B. Gebrehiwot, V. Sreeram, D. Sawant, D. Agonafer, N. Kannan, J. Hoverson and M. Kaler. Steady state CFD modeling of an IT pod and its cooling system. Presented at Thermal Measurement, Modeling & Management Symposium (SEMI-THERM), 2015 31st. 2015. DOI: 10.1109/SEMI-THERM.2015.7100159.

[16] B. Gebrehiwot, "Maximizing Use of Air-Side Economization, Direct and Indirect Evaporative Cooling for Energy Efficient Data Centers ", February 2016

[17] Sunonwealth Electric Machine Industry Co., Ltd. *SUNON Specification for Approval: DC Brushless Fan, Model PMD1204PJB1-A, P/N (2)*. Available: http://datasheet.octopart.com/PMD1204PJB1-A-Sunon-Fans-datasheet-126742.pdf.

[18] *Instruction Manual for AMCA 210-99 Airflow Test Chamber*. Available: http://www.fantester.com/.

[19] Alissa, H., A., Nemati, K., Sammakia, B., Seymour, M., Schmidt, R., Schneebeli, K." Chip to Facility Ramifications of Containment Solution on IT Airflow and Uptime," IEEE 2015.

[20] Alissa, H. A., Nemati, N., Sammakia, B., Seymour, M., Schneebeli, K., Schmidt, R., " Experimental And Numerical Characterization Of A Raised Floor Data Center Using Rapid Operational Flow Curves Model," InterPack 2015, San Francisco, CA, USA, 2015

[21] S. Alkharabsheh, 'Effect of Cold Aisle Containment Leakage on Flow Rates and Temperatures in a Data Center', 2013

[22] ASHRAE TC 9.9 Mission Critical Facilities, Technology Spaces, and Electronic Equipment. *2011 Gaseous and Particulate Contamination Guidelines For Data Centers*. Available: http://tc0909.ashraetcs.org/documents/ASHRAE%202011%20Gaseous%20and%20Particulate%20Contamination%20Guidelines%20For%20Data%20Centers.pdf.

[23] A. Siddarth, "Experimental Study on Effects of Segregated Cooling Provisioning on Thermal Performance of Air Cooled Servers in Data Centers", 2015

[24] http://data-centers.in/reduce-power-consuption-in-data-center

[25] P. Kumar and Y. Joshi, "Fundamentals of Data Center Airflow Management", *Springer*, pp. 199–236, 2012

[26] Michael A. Bell, "Use best Practices to Design Data Center Facilities" Gartner Research Publication Date: 22 April 2005/ID Number: G00127434

[27] http://www.datacenterjournal.com/

3.4 Artificial Neural Network Based Prediction of Control Strategies for Multiple Air-Cooling Units

Vibin Shalom Simon, Ashwin Siddarth, Dereje Agonafer

Mechanical and Aerospace Engineering

The University of Texas at Arlington,

P.O. Box 19023

Arlington, Texas, United States, 76019

3.4.1 ABSTRACT

A data center cooling system consists of a hierarchy of systems with dedicated control algorithms dictating their operational states. There exists a wide range in spatial and temporal parameter space in an ensemble of non-linear dynamic systems, each executing a control task, while the global objective is to drive the overall system to an optimum operating condition i.e. minimum total operational power at desired rack inlet temperatures. Certainly, it is beneficial in optimizing workload migration at temporal scales but, solving the instability of the cooling systems operating at design points helps in understanding the whole system and make predictions to have better control strategies. Several techniques are available to realistically capture and make predictions. Data-driven modelling/Machine learning is one such method that is less expensive in terms of cost and time compared to other methods like validated CFD simulation/experimental setup. The objective of this study is to develop a control framework based on predictions made using machine learning techniques such as Artificial Neural Network (ANN) to operate multiple Computer Room Air Conditioning Units (CRAC) or simply Air-Cooling Units (ACU) in a hot-aisle contained raised floor datacenter. This paper focuses on the methodology of gathering training datasets from numerous CFD simulations (Scenarios) to train the ANN model and make predictions with minimal error. Each rack has a percentage of influence (zones) based on the placement of ACUs and their airflow behavior. These zones are mapped using steady state CFD simulation considering maximum CPU utilization and cooling provisioning. Using this map, ITE racks are targeted and given varying workload to force the corresponding

ACU that is responsible for provisioning, to operate at set points. Number of such scenarios are simulated using the same CFD model with fixed bounds and constraints. Using large samples of data collected from CFD results, the ANN is trained to predict values that correspond to the activation of the desired ACU. Such efficient control network would minimize excessive cooling. The validated prediction points are used to model a control framework for the cooling system to quickly reach the operating point. These models can be used in real-time data centers provided; the training data is based on in-house sensor values.

3.4.2 INTRODUCTION

Data centers are facility buildings, housing Information Technology Equipment (ITE) and provide power and cooling. Technological advancement and price erosion enabled high growth rate of electronic packaging [1]. In 2014, data centers in the U.S. consumed an estimated 70 billion kWh, representing about 2% of total U.S. electricity consumption, and is estimated to increase to 75 billion kWh by 2020 [2]. A large data center at an industrial-scale operation uses as much electricity as a small town in the United States.

Managing cooling infrastructure is important to guarantee ITE reliability, working time, and operating scenarios for best performance. The scale of power consumption depends on workload, design and the longevity of data centers. Effective air distribution and provisioning of ITE will have a significant impact on energy consumption and equipment reliability [3]. The energy used by a typical rack of state-of-the art servers, consuming 20 KW of power at a cost of 10 cents per kWh is more than $17,000 per year in electricity. Data centers holding hundreds of such racks constitute an energy-intensive building. Efforts to improve energy efficiency in data centers can pay big dividends [4].

However, the cooling is generated and distributed by various systems, but airflow management is a key to optimum cooling of ITE and corresponding energy consumption. Optimizing the delivery of cool air and the removal of heat generated by the ITE can involve many design and operational practices. The general goal is to minimize or eliminate inadvertent mixing between supplied air to the ITE and hot air removed from it. Hot-aisle

containment is one method to maintain the cold air supplied to the racks as generated by the cooling unit so that they are evenly distributed throughout the ITE without significant change in the temperature or humidity due to recirculation [4].

Generally, multiple Computer Room Air Control (CRAC) units respond altogether increasing cooling power to provision a localized hotspot which result s in excessive cooling for other ITEs especially in a co-located datacenter. The unnecessary cooling expenditure can be cut down by establishing a new strategy that could involve a particular CRAC unit or a combination of them to provision any localized hotspot. Knowing the fact that ITE workload fluctuation results in time-based temperature variation, the cooling unit also requires a certain time interval to respond to the scenario and make changes to address the situation.

Data center Facilities are of various types in terms of design, layout, ITE workload distribution and cooling strategies. Our data center design is chosen based on the literature survey from small-scale raised-floor data centers having indoor Computer Room Air Control (CRAC) Unit and hot aisle containment. The necessity of this design is to intentionally use the CRAC unit to provision localized hotspots due to workload distribution at any specific ITE so that the cooling power consumption can be optimized based on the need. The CFD model of the datacenter room does not involve Power distribution units, cables, pillars, exhaust vents and other supplementary equipment since they are considered insignificant in this study.

A robust CFD software, 6SigmaRoom provided by Future Facilities is used to model and simulate the temperature and flow characteristics based on a Blackbox model of ITE and several other units in a datacenter. The difficulties when using this software is that it needs explicit domain knowledge and time expensive to produce the results for steady state/transient simulations. Since data centers are dynamic, CFD is not a suitable tool to produce real-time results to improve the power usage. Research has been conducted previously on such applications and it is found that Data-Driven Modeling (DDM) is viable option to analyze the data from the CFD model and validate with real-time raw data from the datacenter facility. Also, the methodology adopted to move forward in this

research is based on the workflow demonstrated by Athavale et al. [5]. One such modeling technique is machine learning and the appropriate tool being used is Artificial Neural Network (ANN) to learn and mimic the behavior of airflow patterns and thermal characteristics in a datacenter. ANN has been used in various HVAC applications as well as in Datacenters for predicting parameters to control cooling unit based on the weather and psychrometric bins [6]. Predictions were made on different modes of cooling provided to datacenters depending upon the operational psychrometric bins and climatic conditions [7]. In our case the training dataset is generated by the CFD model having various configurations for cooling strategies for multiple Air-cooling units. The data driven model learns the non-linearity of physics-based systems and predicts parameters to modify the action space. The ANN is trained until it delivers the least error without overfitting the sample data, such that its prediction can be validated with in-house sensors deployed at specific locations in a datacenter facility.

Observing various configurations and types of data center we chose a model that is predominantly built in a small-scale raised-floor data center. The model is purposefully designed in such a way that the provisioning of ITE is visualized and quantified for various hotspot scenarios.

3.4.3 OBJECTIVES AND STRUCTURE

The objectives of this study were to:

1. Understand the provisioning of ITE before an event of hotspot based on the zone of influence of the Air Cooling Units over the servers.
2. Construct an ANN model using the CFD generated dataset for predicting temperature and airflow control parameters to operate the Air-cooling unit at desired operating points.

Table 1: Data center room specifications

Raised Floor Hot Aisle Contained Data Center	
Total Room Capacity	300 KW
No. of racks per row	12
No. of Rows	3
Power per rack (KW)	8.4 (max.)
Cooling system	3 Air cooling Units (ACU) of 1140 KW max. sensible cooling

3.4.4 CFD MODEL AND ITE SPECIFICATION

CFD analysis is carried out using the model showed in Fig. 1. The model has underfloor supply and false-ceiling return configuration. The model has 2ft raised-floor design containing 36 racks, 12 racks per row provisioned by 3 ACUs. Ceiling is built at 14ft from the floor for the hot air to escape from the hot aisle containment to the return duct of the ACU. Solid obstructions are built from the hot-aisle containment to the vents in the ceiling to direct the hot air upwards. Similarly, the obstructions are built to direct the air from the ceiling to the return duct of the ACU. Floor grills of size (2 x 2) ft^2 with 50% open dampers are arranged in-line in front of the rack inlet to direct the cold-air upwards.

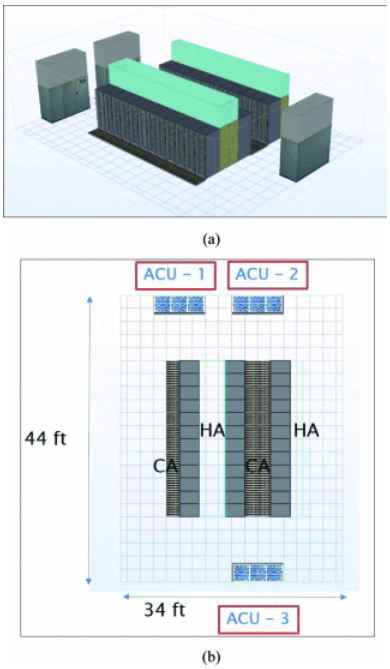

Figure 1: (a) Data Center room model showing hot-aisle containment (b) Naming scheme for ACUs

The underfloor plenum pressure is maintained using two sensors, one at the bottom of the tiles and the other above the rack. Usually these sensors are placed in the middle of the room.

Each rack is filled to its capacity with 1U servers of 200 W, a total of 42 servers per rack as shown in Fig. 2. Three Inlet and outlet temperature sensors are equally spaced along the air flow direction at the cold aisle and hot aisle respectively to capture the temperature stratification. Typical air leakages of 5% is set to all the racks. Initially, workload is distributed equally through all the servers, typical load of 40 W per ITE is given at idle conditions and 180 W per ITE is given at peak usage conditions. The above parameter is one such boundary conditions given during the simulation. The server used for modeling and analysis is HP SE1120 having an outflow pressure curve measured using experimental analysis using air flow bench [8].

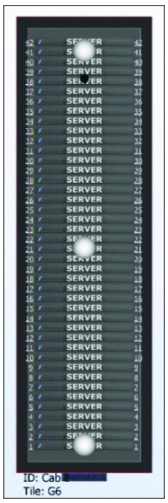

Figure 2: Rack with 42, 1U servers and 3 equally spaced temperature sensors (white sphere)

The outflow pressure curve denotes the pressure difference across the ITE during its operation at various modes or workloads. It maintains an indirect relation with the cooling system performance. ITE power is time dependent and is set to fluctuate based on the workload distribution and migration.

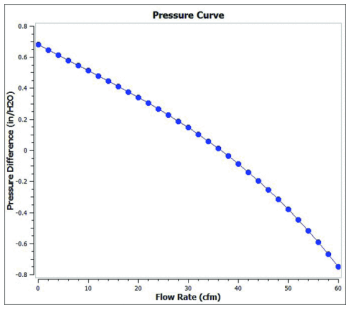

Figure 3: Outflow pressure difference Vs. air flow rate at the servers

3.4.5 AIR COOLING UNIT CONTROL STRATEGIES

ACU uses chilled water-cooling system where the primary coolant is the water supplied from the chiller. The reference air i.e. Return air from the ITE is passed through the cooling coils to cool down to the required temperature. Supply temperature and flowrate variation is determined based on the thermal energy consumption

equation embedded in the CFD software. Theoretically, the mass flow rate of air required to remove the heat generated by the ITEs can be calculated using the equation:

$$Q = \dot{m} C_p \Delta T$$

The Blackbox model of the servers are designed based on complex energy balance equations in CFD software that calculates parameters like temperature, pressure, velocity, humidity etc. The conventional construction of control network based on best practices for a small scale datacenter room are; Supply temperature of the air from the ACUs are controlled based on the temperature of air at the cold aisle, meaning, the work done/energy consumed by the heat exchanger depends on the server inlet air temperature. Supply air-flowrate is determined by the average pressure difference across the ITE in the datacenter, meaning, Variable Frequency drives are set to changing frequencies to operate the blower at different speeds to provide the desired air flowrate.

In this study, to understand the ACU's influence on provisioning the ITE's, we have setup the control network in such a manner that can be Average ITE outlet temperature sensor values based on % of influence are taken as T_{Return}. Similarly, supply temperature T_{Supply} setpoint is set to 22^{o}C such that the ACUs respond when any of the inlet temperature sensors read a value of more than 22^{0}C. The blower speed for the ACU fans are controlled using VFDs and the values are updated for every iteration to capture different scenarios using same boundary conditions.

CRAC unit dimensions and specifications are modeled according to Liebert CW 114, ACU built by Vertiv cooling technologies.

Major ACU design parameters are listed below:

Total sensible cooling capacity: 114 KW

Max. coolant flow rate: 6 GPM

Supply air flowrate range: 0 – 17,300 CFM

Two CFD analysis were carried out, one to visualize the zone of influence of the CRAC units in provisioning the ITEs and the second to calculate the total power consumed by the CRAC units in various scenarios also to generate datasets for ANN training.

3.4.6 ZONE OF INFLUENCE ANALYSIS

ACUs supply air to the room through underfloor plenum and reaches the racks in a random fashion. To visualize and understand the influence of an ACU supply over the racks we simulate a steady state analysis with set boundary conditions given below.

Boundary conditions:

ACU Blower Speed: 90 % (15,570 CFM)

ACU Supply temperature: 22^0C

ITE Power/workload: 180 W

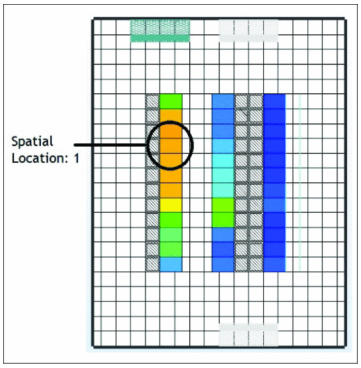

Figure 4: Zone of Influence of ACU-1

Once the spatial locations of the racks are found having maximum influence (75–100%) of every ACU, they are assigned as targeted ITEs. Power given to the targeted ITE is chosen such that it mimics the actual workload based on consumer usage. To address the fluctuating load on ITE, the ACU which has the highest influence on the respective servers start to respond. In a typical datacenter, all the ACUs respond together for minimal change in the workload but here, we forcibly allow the corresponding ACU to respond to the workload. From steady state

analysis, ACU-1 has the highest influence on the racks at spatial location: 1. These racks are targeted and given fluctuating workload for a certain interval and ACU-1 is forced to respond while the other ACUs are constantly working on providing cooling to other racks. By running such simulations, we can find the energy consumed by ACU-1 to provision the targeted rack. Similarly, the model is analyzed for similar scenarios according to the influence of ACUs. To capture the variability, several combinations of hotspot scenarios were created to generate training datasets for the Artificial neural network model. Using temperature dependent control for the ACU for varying IT load is one such strategy practiced in data centers. Datasets are generated by collecting data from a set of simulations using PAC study in 6SigmaRoom.

3.4.7 PARAMETRIC STUDY

The objective function of this study is to capture the nonlinearity of the physical phenomenon in the data center. A methodology for choosing the input parameter space out of 'N' number of measurable parameters is carried out using Latin hypercube sampling (LHS), a statistical technique where the domain of interest is filled with samples portraying the variability shown in original data.

The multi-dimensional parameter space should be space filling and non-collapsing to ensure a good variability in simulations [9]. CFD simulations are deterministic in nature therefore, it is important that the input parameter space is determined using a LHS technique to avoid any bias and introduce required variability in the training data [5]. Latin hypercube sampling (LHS), a statistical method for generating a near-random sample of parameter values from a multidimensional distribution, ensures that the ensemble of random numbers is representative of the real variability [10].

Using Latin Hypercube Sampling from a range of parameters, the input parameter space is generated to provide the maximum variability in the CFD simulation thus yielding datasets having good number of features. The CFD model is run for different combinations of inputs to generate training datasets. Python is used to generate the

LHS from a list of input parameters to have a space filling design. From known parameter values and resolutions, the input parameter space is defined for different combinations for 27 CFD simulations.

Inputs for the CFD simulations given are: Time based ITE Load, Spatial Location of targeted ITE, power ratio for the ITE.

Time varying Outputs from the CFD simulations obtained are total cooling power consumption of all three ACUs in different scenarios and ACU blower speed.

Table 2: Input parameters space

Input Variables	Bounds	Constraints
ACU Blower speed	50 – 90 %	Interval of 20 (50%, 70%,90%)
Total ITE Workload / rack	4 – 8 KW	Interval of 2 (4,6,8)
Spatial Location	1 - 3	Interval of 1 (1,2,3)
Temperature rise of the IT load	5 – 10^0C	Interval of 1 (5,6,7,…10)

The two functions that govern the control parameters being captured and learnt mathematically by the ANN model are as follows:

1. ACU Blower Speed = *f*(ACU number , Spatial Location, Outlet Temperature, IT Load)
2. ACU Cooling power = *f*(ACU number , Spatial Location, Supply temperature, IT Load)

3.4.8 ARTIFICIAL NEURAL NETWORK

The sheer number of possible equipment combinations and their setpoint values makes it difficult to determine where the optimal efficiency lies [11]. Using standard formulas for predictive modeling often produces large errors because they fail to capture such complex interdependencies. Data driven models are the best methods that can completely represent a non-linear physics-based scenario in mathematical form so that we can train neural network models to learn and predict the desired parameters. Neural networks are a class of machine learning algorithms that mimic cognitive behavior via interactions between artificial neurons [12].

3.4.9 ANN TRAINING AND VALIDATION

Using datasets from the CFD simulations, ANN model is trained, validated, and tested to predict the desired outputs that can allow us to frame a control strategy for the provisioning the ITE running under various workload scenarios. 70% of the dataset is used for training the neural network, the remaining 30% used for validation and testing. Data pre-processing such as sampling and data filtration is done using Python (PyCharm by JetBrains) in conjunction with the NumPy module and visualization using matplotlib module. MATLAB R2019a has predefined ANN structures to model train, validate, test and post-process.

In our study, the input parameters for the ANN are chosen in such a way that they can be measured directly from the data center facility. The probability of error becomes negligible. The list of input parameters for the ANN model are listed as follows:

1. ACU number
2. Spatial location of the targeted rack
3. Temperature at the cold aisle (^{0}C)
4. Rack IT Load (W)

The output parameters of the ANN model are considered in a way such that it can be used to frame a control strategy for every ACU.

The output parameters are as follows:

1. Blower Speed (cfm) for all 3 ACUs
2. Sensible cooling load on (Power consumed – KW) all 3 ACUs

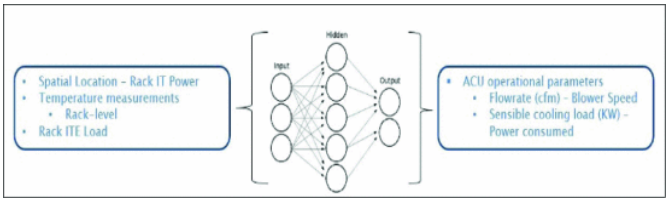

Figure 5: ANN Model

Number of neurons required to achieve minimal error in training the ANN is calculated with a set of values defined by the thumb rule [11].

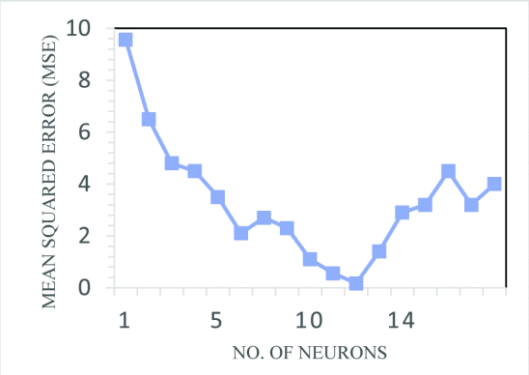

Figure 6: ANN training error vs No. of neurons used in the hidden layer

In this case 11 neurons in the hidden layer were used for the ANN to predict results with minimal error. If we have neurons more or less than 11, we may have predicted results with large error values also called as underfitting/overfitting of data.

The model selected was a three-layer model having one input, one output and one hidden layer. The dataset was trained using Levenberg-Marquardt Algorithm (LMA) to minimize the error as well as to overcome the flaws in using gradient descent method. Empirical relations are available to determine the suitable number of neurons for the hidden layer based on the number of parameters in the input and output layers [13][14][15]–[16]. The model is tested from a sample data that is not in the training dataset to evaluate the accuracy of the prediction. The Mean Squared Error (MSE) refers to the difference in original value and the predicted value, the lesser the value the more accurate is the prediction. Accuracy is improved by generating training dataset having higher resolution by increasing the number of scenarios using the CFD model.

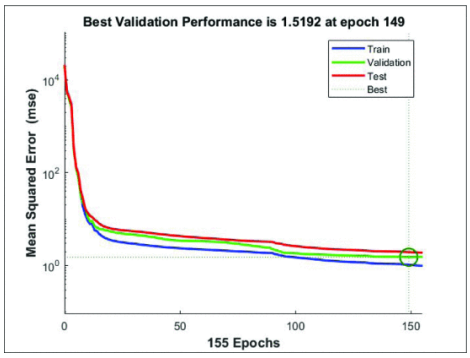

Figure 7: ANN Training Performance

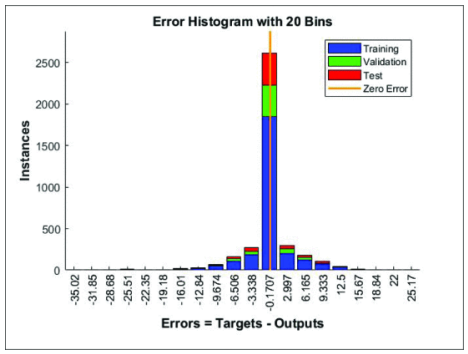

Figure 8: ANN Training Error

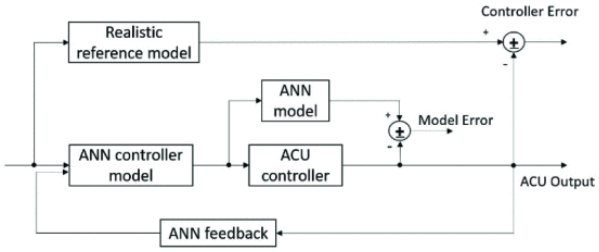

Figure 9: ANN – DC Controller Network

From these results we can observe that ANN model can predict the parameters for ACU control with MSE in the order of 10^{-1} showing the model is a good fit to the data. All these parameters are fed into the ANN controller module that is integrated with the DC facility. The above network shows a one of the implementation techniques

to have a control framework based on the ANN model thereby merging it with the datacenter facility. The feedback loop improves the ANN controller model for better prediction. Model error and controller error obtained from the comparison is used for further analysis and training of the system control design.

3.4.10 SUMMARY AND CONCLUSIONS

This paper encapsulates an approach to address energy saving by using multiple ACUs in a datacenter using predictive modeling with training datasets collected using CFD simulations. Summarizing ANN test prediction results in an average error <3KW of energy consumed by the cooling units and 0.2% of the air flow using a part of the training data as test data.

The predictions are then used to design a framework that allows the operation of multiple ACUs to optimally provision the ITE load. ANN model resulted in a good agreement with the CFD model having error at the order of 10^{-1} when tested using a part of the training data can be used to frame a control strategy based on the hotspot in a typical raised floor data center with chilled water-cooling system. This ANN model can be implemented in a realistic data center provided; it is trained based on in-house sensor values. Cooling strategy can be essentially based on the ANN predicted results thereby reducing power consumed by the cooling units.

Following up this research could be, having high resolution CFD models and a greater number of hotspot scenarios to address excessive cooling provisioning, increasing the resolution of input parameter space to get more variability in the dataset also, cooling unit failure analysis can be included in predicting ACU operational parameters. Step ahead prediction of parameters is one such method where we will be able to have a better response from the cooling unit and suitable for real-time implementation as well.

3.4.11 NOMENCLATURE

Q	Energy consumed by Air-cooling unit, J
M	mass flowrate of air, cfm
Cp	specific heat capacity of air, J/kg-K

N	number of iterations
TReturn	Temperature at the hot aisle, 0C
TSupply	Temperature at the cold aisle, 0C
dT	change in temperature of air (TReturn – TSupply), 0C

3.4.12 SUBSCRIPTS

Return	Return air at the ACU
Supply	Supply air provided by the ACU

3.4.13 ABBREVIATIONS

CFD	Computational Fluid Dynamics
ANN	Artificial Neural Network
ACU	Air-Cooling Unit
ITE	Information Technology Equipment
CRAC	Computer Room Air Conditioning
LMA	Levenberg-Marquardt Algorithm
CA	Cold Aisle
HA	Hot Aisle
LHS	Latin Hypercube Sampling
MSE	Mean Squared Error

3.4.14 REFERENCES

[1] J Scaramella, "Next-Generation Power and Cooling for Blade Environments", *IDC Framingham MA Technical Report 215675*, 2008.

[2] Jonathan Koomey, "Growth in data center electricity use 2005 to 2010", *A report by Analytical Press completed at the request of The New York Times*, vol. 9, pp. 161, 2011, [online] Available: http://www.analyticspress.com/datacenters.html.

[3] *ENERGY STAR Rating for Data Centers: Frequently Asked Questions [Online]*, [online] Available: https://www.energystar.gov/ia/partners/prod_development/downloads/DataCenterFAQs.pdf?acac-cbed.

[4] Steve Greenberg et al., "Best practices for data centers: Lessons learned from benchmarking 22 data centers", *Proceedings of the ACEEE Summer Study on Energy Efficiency in Buildings in Asilomar CA. ACEEE August*, vol. 3, pp. 76-87, 2006.

[5] Jayati Athavale, Yogendra Joshi and Minami Yoda, "Artificial neural network-based prediction of temperature and flow profile in data centers", *2018 17th IEEE Intersociety Conference on Thermal and Thermomechanical Phenomena in Electronic Systems (ITherm)*, 2018.

[6] Feyisola Adejokun, Ashwin Siddarth, Abhishek Guhe and Dereje Agonafer, "Weather Analysis Using Neural Networks for Modular Data Centers", *Proceedings of the ASME 2018 International Technical Conference and Exhibition on Packaging and Integration of Electronic and Photonic Microsystems. ASME 2018 International Technical Conference and Exhibition on Packaging and Integration of Electronic and Photonic Microsystems*, [online] Available: https://doi.org/10.1115/IPACK2018-8253.

[7] Abhishek Walekar et al., "Neural Network Based Bin Analysis for Indirect/Direct Evaporative Cooling of Modular Data Centers" in ASME 2018 International Mechanical Engineering Congress and Exposition, American Society of Mechanical Engineers Digital Collection, 2018.

[8] Betsegaw Kebede Gebrehiwot, "Maximizing use of airside economization direct and indirect evaporative cooling for energy efficient data centers", *Diss*, 2016.

[9] Douglas C. Montgomery, Design and analysis of experiments, John wiley & sons, 2017.

[10] Michael Stein, "Large sample properties of simulations using Latin hypercube sampling", *Technometrics*, vol. 29, no. 2, pp. 143-151, 1987.

[11] Jim Gao, *Machine learning applications for data center optimization*, 2014.

[12] Andrew Ng, "Neural Networks: Representation (Week 4)", *Machine Learning*, [online] Available: https://class.coursera.org/ml2012002.2012.Lecture.

[13] Kishan Mehrotra, Chilukuri K. Mohan and Sanjay Ranka, Elements of artificial neural networks, MIT press, 1997.

[14] Richard Lippmann, "An introduction to computing with neural nets", *IEEE Assp magazine*, vol. 4, no. 2, pp. 4-22, 1987.

[15] Lin Zhang et al., "Multivariate nonlinear modelling of fluorescence data by neural network with hidden node pruning algorithm", *Analytica Chimica Acta*, vol. 344, no. 1-2, pp. 29-39, 1997.

[16] Gao Daqi and Wu Shouyi, "An optimization method for the topological structures of feed-forward multi-layer neural networks", *Pattern recognition*, vol. 31, no. 9, pp. 1337-1342, 1998.

Chapter 4

Summary and Discussion

In utilizing data-driven modeling techniques with operational data acquired from a data center with appropriate sensors installed, non-linearities developed in the data center due to the interdependence of mechanical, electrical and control systems and hence give a more realistic results compared to psychrometric bin analysis. Logged field data from a modular data center was used to train the ANN model which was then used to predict the conditions inside the cold aisle. The results presented in Chapter 2, section 2.1, show that ANN can be utilized to predict the performance of the cooling systems which can be then used to set up control algorithms for the data centers. Firstly, the ANN model predicted the cold aisle conditions achieved when only one cooling mode is used over a typical year. For each cooling mode operated over a typical year, a CA envelope was visualized on a psychrometric chart. These results can be used to understand the variations in the cold aisle with respect to the cooling mode in different weather zones. Furthermore, OA envelopes were visualized on a psychrometric chart to determine the variability of the outside air conditions over which a cooling mode can be effectively used to attain ASHRAE recommended CA conditions.

Understanding the available cooling processes when configuring a cooling unit with multiple cooling modes is a key design choice that is a function of the location, top-up cooling mode switching, control strategies and other sizing choices. In Section 2.2, The general methods for the thermal design that have been identified developed and established are reliable and have been validated as shown in the results. It was observed that with increase in the inlet temperatures, the water and power consumption increased. The water consumption model developed here is complete and useful for evaluating water usage effectiveness. The tool that has been developed here is ready to be shipped as a standalone application. As observed from results, the PUE is best at 20℃ for both the cooling systems for each city. This temperature is well within the ASHRAE recommended region. Finally, it can

be concluded that the tool which is based on the established methods gives reliable results and it was observed that DEC is more efficient than IEC.

In Section 2.3, it was shown that by vertically splitting the wet cooling media pads and accommodating each vertical section with a dedicated pump, we can achieve incremental humidification along with staging control of cooling. However, it was also observed that the existence of multiple staged sections can result in stratification of hot and cold air and thus necessitates mixing downstream of the media pad wall. The vertically staging of DEC media has been successfully tested experimentally. The change in relative humidity and the temperature drop has been carefully reviewed and interesting results are found experimentally and theoretically by using the psychometric chart and adiabatic saturation equations. While operating the two unequal stage with similar assumed conditions these two stages can be turned on /off with mixing both the streams of air and bringing the mixed air inside the ASHRAE recommended and allowable envelops for both 66% and 33% wet running stages. The comparison of two configurations showed the un-equal configuration has better control on relative humidity than the single stage configuration. This clearly shows when the vertical split configuration is implemented for any number of staging, it would be beneficial, if the sections are un-equal.

This control on relative humidity and temperature greatly helps the data center environment to be run inside the ASHRAE's allowable range of relative humidity and temperature upon implementing the vertical split distribution system. This ultimately increases the reliability of the IT equipment and minimizes the cost associated with it. It also helps saving water utilization and power consumption.

In section 2.5, the design of an air handling unit to house an air-to-air heat exchanger that can be wetted on the secondary side to enhance the total heat exchange between primary and secondary air across the heat exchanger surface was presented.

Operations and maintenance requirements are a key topic when studying cooling units for a mission critical facility like a data center. For direct evaporative cooling, the media pad was subjected an accelerated

degradation test to study the impact of Calcium scaling on the performance of the media pad. The accelerated degradation testing performed by rapid wetting and drying clearly proved that it leads to scale deposition on the pads. However, the performance of the media pad i.e. the efficiency of the media pad does not drop drastically with scale deposition. This ADT leads to better understanding of maintaining a media pad based on water quality. Based on the conductivity of water in the sump, water can be replenished accordingly. By this way water is treated as a commodity and use of water can be controlled. In section 3.3, different approaches for efficient airflow management is discussed. Depending on the data center capacity and architecture different airflow provisioning can be deployed to meet the efficiency criteria. To study the effect of different airflow provisioning strategies research modular data center that uses direct and indirect evaporative cooling unit has been used. In actual data center facility, pressure inside CA is very low due to maldistribution of airflow. Also, with the increase in IT load, the amount of volume flow rate that needs to leave from HA increases but due to insufficient outlet vent area airflow gets trapped inside HA which results in high pressure in HA. This kind of imbalance of pressure in CA and HA results in negative pressure gradient across the rack and increases the risk of backflow.

Estimation of power consumption in IT pod earlier research study results was considered. Airflow bench test to obtain active flow curve to determine the airflow requirement. Using practical data detail CFD model was created to get pressure and temperature distribution inside the IT pod for different airflow provisioning. Results suggest that to reduce the risk of backflow and to maintain positive pressure gradient across the rack instead of fixed airflow provisioning, pressure differential-controlled airflow provisioning should be deployed. To estimate the correct amount of airflow requirement for IT pod additional efforts should be applied to determine pressure loss due to various factors like recirculation, Venturi effect, and losses due to friction presented by airflow path. Different cooling architecture has its own benefits and drawbacks. The second part of the study is focused to determine the effectiveness and comparison of different data center cooling architecture. Rack inlet temperature highly depends on the airflow management. Configurations presented with various assumptions like inlet louvers

angle, server fan operating speed, leakage ratio, and distribution, perforated tile design et cetera, depending on the performance requirements, configurations need to be changed. As per the results for efficient thermal performance of modular data center with small capacity ducted supply/return configuration, overhead supply/return system is suitable configuration. For data centers with large capacity and floor area raised floor data center is ideal due to liberty in rack arrangement. Finally, in section 3.4 the concept of dynamic control was investigated by an approach where predictive modeling using data-driven models is developed by using training data solely from CFD simulations.

Thus, a comprehensive body of knowledge related to various aspects of designing, implementing, and operating direct and indirect evaporative cooled air handling unit has been presented in this research report. The evaporative cooling market was valued at USD 4.9 billion in 2017 and is projected to reach USD 7.1 billion by the end of 2023. The main driver for the evaporative coolers market is their adoption in data centers. This study serves as an unbiased guide to several key aspects related to the evaporative cooled air handling units that are to be used for increasing energy efficiency in data center thermal management.

Biographical Information

Ashwin Siddarth received his Bachelor's degree in Mechanical Engineering from Visvesvaraya Technological University, India in June 2013. He received his Master's degree in Mechanical Engineering from University of Texas at Arlington in December 2015. His research focused on energy efficient operation of cooling systems in data centers. Ashwin served as a graduate research assistant (GRA) in Electronics, MEMS and Nanoelectronics Packaging Center and worked on various industry-funded projects as a graduate student researcher in NSF funded Industry University Cooperative Research Center called Center of Energy-Smart Electronic Systems (ES2).